



City Research Online

City, University of London Institutional Repository

Citation: Brown, N. H. (2023). The Multiple Scales Method for Non-parallel Three-Dimensional Stability Analysis in Boundary Layers. (Unpublished Doctoral thesis, City, University of London)

This is the accepted version of the paper.

This version of the publication may differ from the final published version.

Permanent repository link: <https://openaccess.city.ac.uk/id/eprint/30862/>

Link to published version:

Copyright: City Research Online aims to make research outputs of City, University of London available to a wider audience. Copyright and Moral Rights remain with the author(s) and/or copyright holders. URLs from City Research Online may be freely distributed and linked to.

Reuse: Copies of full items can be used for personal research or study, educational, or not-for-profit purposes without prior permission or charge. Provided that the authors, title and full bibliographic details are credited, a hyperlink and/or URL is given for the original metadata page and the content is not changed in any way.

City Research Online:

<http://openaccess.city.ac.uk/>

publications@city.ac.uk



THE MULTIPLE SCALES METHOD FOR
NON-PARALLEL THREE-DIMENSIONAL
STABILITY ANALYSIS IN BOUNDARY LAYERS

M.Phil. Thesis

Nicholas H. Brown

Thesis submitted for the fulfilment of the degree of
Master of Philosophy in Aeronautics

City, University of London

June 2023

For Rose Brown and Annie Munnis

Contents

Contents	i
List of Figures	v
List of Tables	vii
Symbols	x
Acknowledgements	xi
Declaration	xiii
Abstract	xv
Motivation	xvii
1 Introduction	1
2 Linear Stability Theory and Transition Analysis for Parallel Flows	7
2.1 Paths to transition	8
2.2 Linear stability theory	10
2.2.1 The Orr-Sommerfeld equation	10
2.2.2 Squire's transformation	12
2.2.3 Linear stability in primitive variables	12
2.2.4 Equivalence between Orr-Sommerfeld and primitive variables	14
2.3 Applying linear stability theory	15
2.3.1 Eigenvalue problems	15
2.3.2 The growth rate of waves	16
2.3.3 Transition prediction	16
2.4 Linear stability calculations	17
2.4.1 Single eigenvalue search results	17
2.4.2 Eigenfunction calculation results	19
2.4.3 Stability curves	21
3 Adjoint Equations	23
3.1 Definition of the adjoint	24
3.2 Adjoint of a square matrix	24
3.3 Adjoint of the differential operator	25
3.4 Adjoint of a combined matrix and differential	27
3.5 Adjoint Orr-Sommerfeld equation	29
3.6 Adjoint primitive variable linear stability system	31
3.7 Equivalence between adjoints systems	31
3.8 Adjoint calculations	34

3.8.1	Single eigenvalue search results	34
3.8.2	Adjoint eigenfunctions	36
3.9	Adjoint Sensitivity	39
3.10	Categorising adjoint problems	41
4	Non-parallel Stability Theory and Transition Analysis	43
4.1	The Method of multiple scales	44
4.1.1	Derivation	44
4.1.1.1	Eigenfunction derivatives	49
4.1.2	Comparison with Gaster's formulation	50
4.1.3	Definition of the growth rate	55
4.1.3.1	The value of ϵ	56
4.1.3.2	The problems in determining an amplitude metric	57
4.1.3.3	Selecting a part of \hat{q}	59
4.1.3.4	Reducing \hat{q} to a single value	59
4.1.3.5	Eigenfunction normalisation	59
4.1.3.6	The solution to determining an amplitude metric	60
4.1.4	Multiple scales calculations	61
4.1.4.1	Single eigenvalue validation	61
4.1.4.2	Stability curve validation	61
4.2	Surface curvature	63
4.2.1	Calculations	63
5	Numerical Methods	67
5.1	Root finding	68
5.1.1	The method of bisection	68
5.1.2	The Newton-Raphson method	68
5.2	Numerical solutions of ODEs	69
5.2.1	Shooting methods	69
5.2.1.1	The Euler method	69
5.2.1.2	The improved Euler method	70
5.2.1.3	Runge-Kutta (RK) methods	70
5.2.2	Matrix methods	71
5.2.2.1	Finite differences	71
5.2.2.2	Compact differences	71
5.2.2.3	Squaring a rectangular matrix	72
5.3	Solution of linear systems	72
5.3.1	Direct matrix inversion	73
5.3.2	Gaussian elimination	73
5.3.2.1	Pivoting	74
5.3.2.2	Gauss-Jordan elimination	74
5.3.3	Matrix decompositions	75
5.3.3.1	Cholesky decomposition	75
5.3.3.2	Crout decomposition	75
5.3.3.3	Doolittle decomposition	75
5.4	Numerical methods used in the present analysis	76
6	Code Development	77
6.1	Parameter space	78
6.2	Navigating the $Re - \omega$ plane	80
6.2.1	Space filling curves	80
6.2.1.1	The Archimedean spiral	80
6.2.1.2	Squaring the spiral	80
6.2.1.3	Fitting the curve to the problem	81

6.2.1.4	Correcting the point distribution	82
6.2.1.5	Correcting the spiral pitch	82
6.2.2	Intelligent navigation	85
6.2.2.1	Initial points	85
6.2.2.2	Subsequent points	86
6.3	Outside the $Re - \omega$ plane	86
6.4	Data structures	87
6.4.1	Base flow data	87
6.4.1.1	A point in space	87
6.4.1.2	A velocity profile	87
6.4.1.3	A 2D boundary layer	87
6.4.1.4	A 3D boundary layer	87
6.4.2	Disturbance data	88
6.4.3	Linear stability	88
6.4.4	Adjoint linear stability	88
6.4.5	Non-parallel correction	88
6.4.6	Interaction between classes	88
6.4.7	Growth rate data	89
6.5	Safety	89
6.5.1	Linear stability	89
6.5.2	Adjoint linear stability	90
6.5.3	Multiple scales	90
6.5.4	Coding practices	90
7	Conclusions and Recommendations for Further Work	91
7.1	Objectives	92
7.2	Technical Outcomes	93
7.3	Insights into the field	94
7.3.1	Understanding adjoints	94
7.3.2	Historical disagreements	94
7.4	Recommendations for further work	95
A	Expanded Derivations	I
A.1	The method of multiple scales	II
A.1.1	Continuity	II
A.1.2	Momentum (u)	IV
A.1.3	Momentum (v)	VII
A.1.4	Momentum (w)	X
	Bibliography	XII

List of Figures

2.1	Paths to transition	8
2.2	Eigenfunction validation of \hat{u}_r for a Blasius velocity profile with $Re_{\delta^*} = 725$, $\omega = 0.13$	19
2.3	Eigenfunction validation of \hat{u}_r for a Blasius velocity profile with $Re_{\delta^*} = 1000$, $\omega = 0.125$	19
2.4	Eigenfunction validation of \hat{u}_r for a Blasius velocity profile with $Re_{\delta^*} = 1200$, $\omega = 0.11$	20
2.5	Eigenfunction validation of \hat{u}_r for a Blasius velocity profile with $Re_{\delta^*} = 2500$, $\omega = 0.09$	20
2.6	Curves of neutral stability in a Blasius boundary layer	21
3.1	Adjoint eigenfunction validation of $ \hat{p}^\dagger $ for a Blasius profile with $Re = 725$, $\omega = 0.13$	36
3.2	Adjoint eigenfunction validation of $ \hat{p}^\dagger $ for a Blasius profile with $Re = 1000$, $\omega = 0.125$	36
3.3	Adjoint eigenfunction validation of $ \hat{p}^\dagger $ for a Blasius profile with $Re = 1200$, $\omega = 0.11$	37
3.4	Adjoint eigenfunction validation of $ \hat{p}^\dagger $ for a Blasius profile with $Re = 2500$, $\omega = 0.09$	37
3.5	Adjoint eigenfunction validation of \hat{p}_r^\dagger for a Blasius profile with $Re = 725$, $\omega = 0.13$	38
3.6	The taxonomy of adjoint problems	41
4.1	Eigenfunction at $Re = 725$, $\omega = 0.13$	59
4.2	Neutral curve comparison with Gaster[12]	62
4.3	Amplification - RAE5243 30° sweep - 200 ms ⁻¹ at sea level, F = 5.2kHz, SWN = 3500m ⁻¹ , Re _C = 13692140	65
4.4	N-Factor - RAE5243 30° sweep - 200 ms ⁻¹ at sea level, F = 5200Hz, SWN = 3500m ⁻¹ , Re _C = 13692140	65
6.1	Parameter Space in 2D	78
6.2	Parameter Space in full 3D	79
6.3	Archimedean spiral	81
6.4	Corner scaling function	82
6.5	Squared spiral	83
6.6	Rescaled squared spiral	83
6.7	Rescaled squared spiral with corrected point distribution	84
6.8	Rescaled squared spiral with corrected point distribution and corrected pitch	84

List of Tables

2.1	Temporal eigenvalue comparison with Davey	17
2.2	Spatial eigenvalue comparison with Gaster	18
3.1	Spatial and adjoint spatial comparison with Gaster	34
3.2	Oblique spatial comparison, $\beta = 0.1$	34
3.3	Oblique waves in a 3D boundary layer	35
3.4	Amplified oblique wave in a 3D boundary layer	35
4.1	Legacy mode shape change metrics	57
4.2	Non-parallel comparison with El Hady	61

Symbols

Fluid Properties	
ρ	Density
μ	Dynamic viscosity
ν	Kinematic viscosity
λ	Bulk viscosity
c_v	Specific heat capacity (constant volume)
c_p	Specific heat capacity (constant pressure)
γ	Ratio of specific heats
\mathcal{R}	Gas constant
κ	Thermal conductivity
Pr	Prandtl number
Flow Parameters	
x, y, z	Chordwise, wall-normal, and spanwise directions respectively
U, V, W	Base flow velocities in x, y, z
U'	Prime used to denote gradient with respect to y
U_e	Subscript e denotes value at the boundary layer edge
U_∞	Subscript ∞ denotes value in the free stream
T	Temperature
Re	Reynolds number
M	Mach number
Perturbation Parameters	
$\tilde{u}, \tilde{v}, \tilde{w}$	Instantaneous perturbations
$\hat{u}, \hat{v}, \hat{w}$	Perturbation amplitudes

ψ	Perturbation stream function
ϕ	Perturbation stream function amplitude
α	Chordwise disturbance wavenumber
β	Spanwise disturbance wavenumber
ω	Disturbance frequency
σ	Disturbance amplification rate
Mathematical Formatting and Notation	
a	Scalar
\mathbf{a}	Vector
A	Matrix
A_{ij}	Element of a matrix
a_i	Element of a vector
\bar{a}	Complex conjugate of a
c_r	Real part of c
c_i	Imaginary part of c
$\langle a, b \rangle$	Inner product of a and b
\dagger	Adjoint of an operator or adjoint state variable
A^H	Conjugate transpose of A
ϵ	Small parameter
u_0, u_1, u_2, \dots	Zeroth, first, second, and so on order expansions of u

Acknowledgements

Thanks to my supervisor, Prof. Chris Atkin, and to all the staff at City. Dr. Chetan Jagadeesh, Prof. Jamshid Nouri, and Dr. Youyou Yan have all been tirelessly supportive. Special thanks to Prof. Michael Gaster for such insightful conversations.

Thanks also to the other aerodynamics research group members, and especially to Dr. Tobias Backer Dirks for always answering my novice level coding queries with good humour.

Thanks to my parents, Bernard and Sharon Brown, for the advice, support, encouragement, and for my education.

Thanks finally to my partner, Robyn Smith. I'm especially grateful for your support, kindness, and patience during my write-up. When you read this, please count one final chicken.

I wish the very best of luck to any other engineers who choose to swim in turbulent flow. It's a famously bumpy ride.

Declaration

I, Nicholas Hugh Brown declare that this thesis entitled “The Multiple Scales Method for Non-parallel Three-Dimensional Stability Analysis In Boundary Layers” is my own work, generated as a result of my own original research. It has been completed wholly while in candidature for a research degree at City, University of London. Work from others, where it has been used, has been clearly cited. I grant powers of discretion to the Director of Library Services to allow this thesis to be copied in whole or in part without further reference to the author, for study purposes, and subject to normal conditions of acknowledgement.

Abstract

Linear stability has been an important method of industrial transition prediction for many years. In this time there have been a number of improvements made, and in almost all cases an increase in physical accuracy is bought by sacrificing a level of simplicity. This document presents the multiple scales method to incorporate some of the physics which has traditionally been neglected. This too comes with a complexity penalty, but in this case the additional complexity is in the mathematics, and not the code. This means that the end user should not feel its presence at all.

The mathematical prerequisites (linear stability analysis, and adjoint linear stability analysis) for the multiple scales method are presented and explained. Validation cases are shown for each step, calculated using a novel simulation package.

Results with a multiple scales correction are generated across a variety of test cases, including oblique waves in a swept non-similar boundary layer. In some cases a significant impact on amplification is observed.

Motivation

The age of heavier-than-air human flight had its humble origins in 1903 when the Wright brothers first achieved sustained, controlled flight of their fixed wing machine. In 2016, the International Air Transport Association reported that the global air passenger transport industry turned over \$709 billion, carrying a total of 3.8 billion passengers[16]. This total does not include air freight, military aircraft, and private aviation, which are themselves significant industries. The pace of development in that time has been rapid; great advances in safety, efficiency, and all aspects of performance have been made.

The most significant concern of the industry is now, and always will be continuing to turn a profit, although the environmental consideration has recently become a close second place. Both of these concerns can be addressed in many ways. Larger aircraft can sell more tickets, more efficient engines burn less fuel, which not only saves cost, but can also extend aircraft range. Fuel efficiency can also be tackled by utilising better airframe design. Fuselage, wings, power plants, landing gear, and aerodynamic surfaces all have a cost not only in manufacturing time and capital, but also in aerodynamic drag. If this cost could be reduced, it would provide the same benefits as increased engine efficiency i.e. reduced fuel cost, increased aircraft range, and reduced emissions of environmental pollutants. To reduce drag, it must first be understood. Especially its origins and the factors which affect this. Only then can informed decisions on design modifications with expected beneficial outcomes be made.

In an attempt to achieve a small part that goal, this document presents a methodology for one piece of the drag reduction puzzle; prediction of the laminar-turbulent transition location in a boundary layer. Such information is important to engineers engaged in aerofoil design and analysis, and this project has the explicit goal of delivering better information on this subject in order to inform wing design. With such information engineers can design wings with a more beneficial transition location, and gain the benefits described.

Chapter 1

Introduction

Fluid flows exist in two main regimes; laminar and turbulent. Turbulent flows are characterised by unsteady, highly vortical, and intrinsically three-dimensional behaviour. Laminar flows are rather simple by comparison; these flows can be steady, are not highly vortical, and in some cases are adequately described by a simplified two-dimensional (or even occasionally, one-dimensional) problem.

Laminar-turbulent transition (or just transition), the subject of this thesis, is the set of processes by which a laminar flow becomes turbulent. As a field of study it is of immense interest since laminar flows, though often difficult to maintain, offer a significant skin friction drag benefit compared to their turbulent counterparts. Turbulent flows however, are more resilient to flow separation, and often offer a form drag benefit. This is demonstrated in a highly accessible way by the example of rough golf balls versus smooth. Achenbach and Heinecke [1] give a good explanation of this phenomenon. Given these facts, it would therefore be very useful to know precisely when a given flow is likely to transition, or better yet, to design structures that control it.

The field of turbulence originated in the late nineteenth century with the experiments of Osborne Reynolds, who famously demonstrated transition from “direct” (laminar) to “sinuous” (turbulent) flow using streams of dye in a water filled tube [28]. In this paper he showed that the onset of turbulence could be related to a certain dimensionless parameter composed of flow variables. This is now known as Reynolds Number. Rayleigh was another key figure in the early history of the field. He demonstrated analytically that for an inviscid flow, it is a necessary and sufficient condition for transition, that the flow velocity profile have at least one point of inflection [27]. His results were somewhat unintuitive, as there are well known flows whose profiles are not inflectional, but which do transition. In fact, Reynolds’ pipe flow was one of these. The instability of these flows was thereafter attributed to viscosity, previously thought to be an entirely stabilising factor. William McFadden Orr and Arnold Sommerfeld provided another significant insight by considering the stability of viscous flows [25, 36], deriving for the first time the equation which bears their names.

In 1915 Taylor hinted that viscous effects could indeed be the source of instability [38], and in 1921 Prandtl [26] agreed. These theories suggested that at a critical Reynolds number, the flow regime would almost instantaneously switch from laminar to turbulent. This was not observed. Papers by Tollmien and Schlichting in the late 1920s and 1930s [31, 39] set the framework for linear stability theory, predicting the instability of unstable convective waves which are named for

them (TS waves). It wasn't until the experiments of Schubauer and Skramstad [34] that the theory became widely accepted. They were able to show experimentally, for the first time, the growing TS waves.

In 1956 two papers were published; one by Van Ingen, and one by Smith and Gamberoni [40, 35] which quite independently developed the same method for utilising the results from linear stability theory (LST). LST gives an amplification rate of a particular wave at a particular location; what it does not give is the precise amplitude of said wave. In fact such waves cannot even be measured in real world situations since at the point of receptivity their amplitude is in general too small. If the initial amplitude was known, the amplitude anywhere could be determined using the growth rate, and this could be correlated with likelihood of transition. Van Ingen, Smith, and Gamberoni do not quite give us this answer, but one which for engineering purposes, is close enough. They realised that the integral of growth rate between two points along the path a wave travels will give the total amplification ratio between those same points. It was determined that TS waves would begin to transition where this value was around e^9 , and this method was aptly named the e^9 method. Of course it was not so simple, and by 1965 Van Ingen had published a database which made allowances for varying free stream turbulence levels. This made it possible to relate the free stream turbulence level to some new amplification ratio, e^N , where transition would now be expected. This method, now called the e^N or N-factor method is still widely in use, although many alternative databases of correlations have since been published.

Linear stability primarily consists of two complementary theories; the temporal theory, which deals with disturbances growing in time, and spatial theory, where the disturbances grow in space. Much of the early computational work dealt with the temporal theory, as it results in a slightly easier formulation to solve. However, spatial theory more accurately reflects the situation in real world applications, such as aerofoils. Gaster, in 1962 [11] published his often cited note on the relation between the two theories. The present work is concerned mostly with the spatial theory, although the solution methodology adopted can very easily be applied to temporal. Much of LST is summarised by Mack in AGARD-R-709 [20].

LST is effective at predicting the behaviour of TS waves in their region of linear amplification. However, this is not the only mechanism which can lead to transition. In swept wings, for example, crossflow (CF) [7, 5] vortices typically dominate, and quickly become non-linear. Even on unswept

wings, the non-linear interactions of TS waves cause the eventual breakdown. LST, as the name suggests, does not predict these cases accurately.

Of course as computational power has increased, more sophisticated approaches have become available. The parabolized stability equations (PSEs) which are summarised by Herbert [15] achieve better agreement with experimental data than LST. It can take into account non-parallel and non-linear effects. The penalty for accuracy, as ever, is cost; PSEs are solved as partial differential equations (PDEs), compared to LST, which uses ordinary differential equations (ODEs). Even more complex methods can be used: bi-global and tri-global stability or even DNS. Even though these represent more flow physics and achieve greater accuracy, their cost is so great that they are an unrealistic prospect for industrial use. PSEs therefore can be regarded as the state of the art, at least from the industrial point of view. PSEs however, are not wholly superior to LST. Apart from the additional complexity, there is also a certain restriction in the approach which comes with treating the problem as non-local. If more resolution is required, for example upstream near the point of neutral stability, the LST practitioner simply computes another base flow velocity profile at the point required, then calculates the stability. PSEs on the other hand would require the entire problem be recalculated with a finer grid.

It is the goal of this project to investigate the mathematics capable of driving a simulation tool with the approximate accuracy of PSE, but with the speed and flexibility of LST.

In Chapter 2 the field of linear stability is discussed and several key equations are derived. These are the Orr-Sommerfeld equation, which describes the 2D linear stability problem and the primitive variable equations, which describe the 3D linear stability problem. The equivalence is also shown between these two formulations, and their application is discussed. Some calculations are presented here and comparisons are drawn with the literature. These results give an eigenvalue/vector pair, which give the full growth rate in linear stability. It is intended that this chapter give a full overview of the typical transition toolchain, but it must be kept in mind that this analysis is also the first prerequisite for the multiple scales approach.

Non-parallel theory is discussed later in Chapter 4. In mathematical terms this gives the first order term in an infinite series solution (where linear theory gave the zeroth order term). Practically speaking it returns some physics to the problem which was simplified away in LST, specifically that the boundary layer grows moving downstream, and that the structure of the instability also

changes in space. This chapter also presents some calculations and comparisons using the newly upgraded toolchain.

There are certain mathematical techniques required to apply the method of multiple scales. Particular attention is given to adjoints, and these are discussed in Chapter 3. The adjoint formulations for several model problems are derived, these are used as stepping stones towards the adjoint formulation of the linear stability problem. The equivalence between the adjoint Orr-Sommerfeld equation, and the adjoint primitive variable system, is shown; a very important result for the purposes of code validation. Here again some results are presented, along with existing values from the literature. The adjoint eigenfunction combined with the LST eigenpair, comprise the eigentriplet necessary to calculate the multiple scales correction.

In Chapter 5 details are given on the various numerical methods used to solve the systems that have been developed. Solution methods for ordinary differential equations (ODE) are discussed, as are methods for working with linear systems.

In Chapter 6 some details of code development are discussed, including a brief overview of the data structures used, and the solutions to a few particular challenges:

- Making sense of a higher-dimensional parameter space
- Dealing with numerical methods with a limited radius of convergence
- Making sure that the final code is safe and where possible only presents the expected behaviours ¹

Chapter 7 summarises the findings of the work. Some next steps which could be taken in this field of study are also suggested. Comments are made here on the potential utility of these steps, and advice on how to tackle them is given.

¹As will be shown, occasionally it is necessary to turn these safety features off.

Chapter 2

Linear Stability Theory and Transition Analysis for Parallel Flows

2.1 Paths to transition

There are several processes which incite laminar boundary layer flows to become turbulent and each pathway may contain many steps. Morkovin [23] summarised:

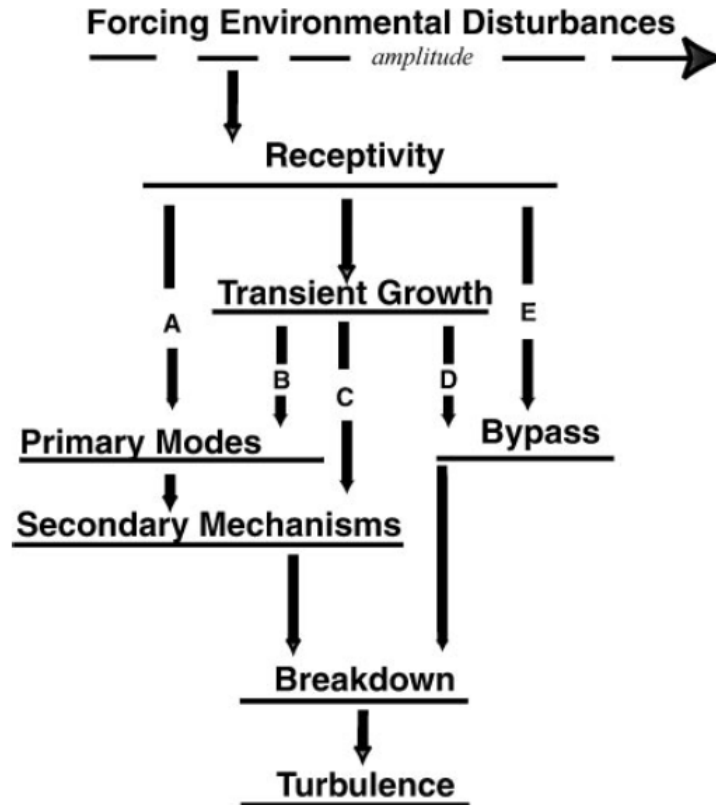


Figure 2.1: Paths to transition

His diagram attempts to map all the steps for every potential transition path. Moving from left to right, the intensity of the initial disturbance grows. Route A for example refers to very small amplitude disturbances such as the vortices in the upper atmosphere, whereas route E could deal with the impinging flow on a supersonic turbine blade tip. These have quite different mechanisms and physics involved, and also different applications; the vortices in the upper atmosphere, for example, have a strong influence on the flow regime over the wings of aircraft at cruise conditions. Receptivity refers to disturbances entering the boundary layer [22]. This is very sensitive to the wall roughness and also the free stream turbulence levels. Primary modes usually appear as TS waves on unswept wings, CF vortices on swept wings and Görtler vortices on concave surfaces. On a swept wing the spanwise pressure gradient bends the inviscid streamline resulting in a crossflow

component, whose profile is inflexional, which as shown by Rayleigh [27], makes it unstable. These primary modes tend to have very small magnitude initially, but may grow. In this case, the primary modes may begin to interact with each other, or be significant enough to influence the base flow. Turbulent spots can appear, which may in turn be elongated into streaks. Eventually, these will tend to dominate the overall flow, which will become fully turbulent. This thesis will focus mostly on route A, where small, already present disturbances grow linearly, although breakdown will be touched upon.

2.2 Linear stability theory

Linear stability theory seeks solutions to an equation or set of equations which describe a simplified version of reality, in which the following simplifications are made:

- Boundary layer growth can be neglected, at least when considering only local effects
- Transition is caused by phenomena which behave perfectly as waves
- The magnitude of the waves is small enough that the growth process can be considered linear

The wave will be described in terms of wavenumbers and frequency. α denotes streamwise wavenumber, β denotes spanwise wavenumber in 3D problems, and ω denotes frequency. These tell us how many complete waves fit into a certain space, or how many will complete in a certain time period. All of these are dimensionless, and may be complex. A complex ω signifies a temporal stability analysis. Complex α signifies a spatial stability analysis, where waves grow in the streamwise direction. Complex β signifies a spatial analysis where waves grow in the spanwise direction. A combination of these is possible, although that case will not be discussed due to its complexity, and rarity in real world applications. With the exception of a few temporal test cases, all of the work presented concerns complex α only.

2.2.1 The Orr-Sommerfeld equation

Fluid motion can usually be described by the Navier-Stokes equations. Here the dimensionless incompressible 2D form is used. Here u , v are velocities in two directions (x and y), p is pressure, t is time and Re is the Reynolds number ($Re = \rho U_e \delta^* / \mu$) based on boundary layer displacement thickness (δ^*), air density and viscosity (ρ, μ) and edge velocity (U_e):

$$\frac{\partial u}{\partial x} + \frac{\partial v}{\partial y} = 0 \quad (2.1a)$$

$$\frac{\partial u}{\partial t} + u \frac{\partial u}{\partial x} + v \frac{\partial u}{\partial y} = -\frac{\partial p}{\partial x} + \frac{1}{Re} \left(\frac{\partial^2 u}{\partial x^2} + \frac{\partial^2 u}{\partial y^2} \right) \quad (2.1b)$$

$$\frac{\partial v}{\partial t} + u \frac{\partial v}{\partial x} + v \frac{\partial v}{\partial y} = -\frac{\partial p}{\partial y} + \frac{1}{Re} \left(\frac{\partial^2 v}{\partial x^2} + \frac{\partial^2 v}{\partial y^2} \right) \quad (2.1c)$$

First the velocities are decomposed into base flow and fluctuating disturbance parts ($u = U + \tilde{u}$ etc.) Then they are linearised by subtracting the base flow equation, and neglecting products of the disturbances. Then by assuming parallel base flow ($V = 0, \partial U / \partial x = 0$), the perturbation

equations are derived:

$$\frac{\partial \tilde{u}}{\partial x} + \frac{\partial \tilde{v}}{\partial y} = 0 \quad (2.2a)$$

$$\frac{\partial \tilde{u}}{\partial t} + U \frac{\partial \tilde{u}}{\partial x} + \tilde{v} \frac{\partial U}{\partial y} = -\frac{\partial \tilde{p}}{\partial x} + \frac{1}{Re} \left(\frac{\partial^2 \tilde{u}}{\partial x^2} + \frac{\partial^2 \tilde{u}}{\partial y^2} \right) \quad (2.2b)$$

$$\frac{\partial \tilde{v}}{\partial t} + U \frac{\partial \tilde{v}}{\partial x} = -\frac{\partial \tilde{p}}{\partial y} + \frac{1}{Re} \left(\frac{\partial^2 \tilde{v}}{\partial x^2} + \frac{\partial^2 \tilde{v}}{\partial y^2} \right) \quad (2.2c)$$

Employing the stream function ($\tilde{u} = \partial\psi/\partial y$, $\tilde{v} = -\partial\psi/\partial x$) means continuity will become redundant, and the remaining disturbance equations become:

$$\frac{\partial}{\partial t} \frac{\partial \psi}{\partial y} + U \frac{\partial}{\partial x} \frac{\partial \psi}{\partial y} - \frac{\partial U}{\partial y} \frac{\partial \psi}{\partial x} = -\frac{\partial \tilde{p}}{\partial x} + \frac{1}{Re} \left(\frac{\partial^2}{\partial x^2} \frac{\partial \psi}{\partial y} + \frac{\partial^2}{\partial y^2} \frac{\partial \psi}{\partial y} \right) \quad (2.3a)$$

$$-\frac{\partial}{\partial t} \frac{\partial \psi}{\partial x} - U \frac{\partial}{\partial x} \frac{\partial \psi}{\partial x} = -\frac{\partial \tilde{p}}{\partial y} + \frac{1}{Re} \left(-\frac{\partial^2}{\partial x^2} \frac{\partial \psi}{\partial x} - \frac{\partial^2}{\partial y^2} \frac{\partial \psi}{\partial x} \right) \quad (2.3b)$$

Imposing the condition that the disturbances behave like waves in the x direction, but allowing structure in the y direction ($\hat{p} = \tilde{p}(y)e^{i(\alpha x - \omega t)}$, $\psi = \phi(y)e^{i(\alpha x - \omega t)}$), allows certain derivatives to be separated:

$$-i\omega\phi' + i\alpha U\phi' - i\alpha U'\phi = -i\alpha\hat{p} + \frac{1}{Re} (-\alpha^2 + \phi'') \quad (2.4a)$$

$$-i\omega\phi + \alpha^2 U\phi = -\hat{p}' + \frac{1}{Re} (i\alpha^3 - i\alpha\phi'') \quad (2.4b)$$

Taking the derivative of equation (2.4a) and substituting into equation (2.4b) permits the removal of any terms using pressure, and results in the Orr-Sommerfeld equation:

$$\phi'''' - 2\alpha^2\phi'' + \alpha^4\phi = iRe(\alpha U - \omega)(\phi'' - \alpha^2\phi) - iRe\alpha U''\phi \quad (2.5)$$

We apply boundary conditions to the equations which tell us that the disturbance disappears at the wall due to no slip, and that it also disappears as wall-normal distance tends to infinity i.e.:

$$\phi, \phi' \rightarrow 0 \quad \text{as } y \rightarrow \infty \quad (2.6a)$$

$$\phi = \phi' = 0 \quad \text{when } y = 0 \quad (2.6b)$$

This can then be solved with any suitable ODE solution algorithm. Shooting methods are a common choice (see § 5.2.1).

2.2.2 Squire's transformation

In his 1933 paper [37], Squire develops an expedient method for dealing with one part of the three-dimensional stability problem. For a problem with a three-dimensional disturbance but a one-dimensional base flow i.e.:

$$\begin{aligned}\tilde{u} &= \tilde{u}, & \tilde{v} &= \tilde{v}, & \tilde{w} &= \tilde{w} \\ U &= U, & V &= 0, & W &= 0\end{aligned}$$

He has shown that the Orr-Sommerfeld equation can be transformed to account for the three-dimensionality of the disturbance. In this case all that is required is to calculate an equivalent two-dimensional disturbance wavenumber, and equivalent Reynolds number. These are done as follows:

$$\alpha^2 + \beta^2 = \alpha_{Sq}^2 \tag{2.7a}$$

$$Re\alpha = Re_{Sq}\alpha_{Sq} \tag{2.7b}$$

Although this is a rather elegant formulation, its use cases are limited, and if the fully three-dimensional case is under investigation, the method presented in § 2.2.3 will be necessary.

2.2.3 Linear stability in primitive variables

Recall the dimensionless Navier-Stokes equations, now in 3D (the incompressible formulation is still used, although compressible flow can be treated in the same way):

$$\frac{\partial u}{\partial x} + \frac{\partial v}{\partial y} + \frac{\partial w}{\partial z} = 0 \tag{2.8a}$$

$$\frac{\partial u}{\partial t} + u\frac{\partial u}{\partial x} + v\frac{\partial u}{\partial y} + w\frac{\partial u}{\partial z} = -\frac{\partial p}{\partial x} + \frac{1}{Re}\left(\frac{\partial^2 u}{\partial x^2} + \frac{\partial^2 u}{\partial y^2} + \frac{\partial^2 u}{\partial z^2}\right) \tag{2.8b}$$

$$\frac{\partial v}{\partial t} + u\frac{\partial v}{\partial x} + v\frac{\partial v}{\partial y} + w\frac{\partial v}{\partial z} = -\frac{\partial p}{\partial y} + \frac{1}{Re}\left(\frac{\partial^2 v}{\partial x^2} + \frac{\partial^2 v}{\partial y^2} + \frac{\partial^2 v}{\partial z^2}\right) \tag{2.8c}$$

$$\frac{\partial w}{\partial t} + u\frac{\partial w}{\partial x} + v\frac{\partial w}{\partial y} + w\frac{\partial w}{\partial z} = -\frac{\partial p}{\partial z} + \frac{1}{Re}\left(\frac{\partial^2 w}{\partial x^2} + \frac{\partial^2 w}{\partial y^2} + \frac{\partial^2 w}{\partial z^2}\right) \tag{2.8d}$$

The disturbance equations are found in the same way as they were in § 2.2.1: by expressing the Navier-Stokes equations as the sum of a laminar base flow and a small disturbance ($u = U + \tilde{u}$ et.c.) and, subtracting the base flow solution, and neglecting the products of disturbances. The parallel flow assumption neglects wall-normal velocity, chordwise base flow derivatives, and spanwise base flow derivatives:

$$\frac{\partial \tilde{u}}{\partial x} + \frac{\partial \tilde{v}}{\partial y} + \frac{\partial \tilde{w}}{\partial z} = 0 \quad (2.9a)$$

$$\frac{\partial \tilde{u}}{\partial t} + U \frac{\partial \tilde{u}}{\partial x} + \tilde{v} \frac{\partial U}{\partial y} + W \frac{\partial \tilde{u}}{\partial z} = -\frac{\partial \tilde{p}}{\partial x} + \frac{1}{Re} \left(\frac{\partial^2 \tilde{u}}{\partial x^2} + \frac{\partial^2 \tilde{u}}{\partial y^2} + \frac{\partial^2 \tilde{u}}{\partial z^2} \right) \quad (2.9b)$$

$$\frac{\partial \tilde{v}}{\partial t} + U \frac{\partial \tilde{v}}{\partial x} + W \frac{\partial \tilde{v}}{\partial z} = -\frac{\partial \tilde{p}}{\partial y} + \frac{1}{Re} \left(\frac{\partial^2 \tilde{v}}{\partial x^2} + \frac{\partial^2 \tilde{v}}{\partial y^2} + \frac{\partial^2 \tilde{v}}{\partial z^2} \right) \quad (2.9c)$$

$$\frac{\partial \tilde{w}}{\partial t} + U \frac{\partial \tilde{w}}{\partial x} + \tilde{v} \frac{\partial W}{\partial y} + W \frac{\partial \tilde{w}}{\partial z} = -\frac{\partial \tilde{p}}{\partial z} + \frac{1}{Re} \left(\frac{\partial^2 \tilde{w}}{\partial x^2} + \frac{\partial^2 \tilde{w}}{\partial y^2} + \frac{\partial^2 \tilde{w}}{\partial z^2} \right) \quad (2.9d)$$

Assuming the disturbance behaves like a wave in the x and z directions, but allowing structure in y, the following substitution is made: $\tilde{u} = \hat{u}(y) e^{i(\alpha x + \beta z - \omega t)}$. The same substitution applies to v , and w . Separating the separable derivatives and division by $e^{i(\alpha x + \beta z - \omega t)}$ results in:

$$i\alpha \hat{u} + \hat{v}' + i\beta \hat{w} = 0 \quad (2.10a)$$

$$-i\omega \hat{u} + i\alpha U \hat{u} + U' \hat{v} + i\beta W \hat{u} + i\alpha \hat{p} - \frac{1}{Re} (-\alpha^2 \hat{u} + \hat{u}'' - \beta^2 \hat{u}) = 0 \quad (2.10b)$$

$$-i\omega \hat{v} + i\alpha U \hat{v} + i\beta W \hat{v} + \hat{p}' - \frac{1}{Re} (-\alpha^2 \hat{v} + \hat{v}'' - \beta^2 \hat{v}) = 0 \quad (2.10c)$$

$$-i\omega \hat{w} + i\alpha U \hat{w} + W' \hat{v} + i\beta W \hat{w} + i\beta \hat{p} - \frac{1}{Re} (-\alpha^2 \hat{w} + \hat{w}'' - \beta^2 \hat{w}) = 0 \quad (2.10d)$$

A system of first order ODEs can be created by introducing two new variables and substituting the wall-normal (y) derivative of equation (2.10a):

$$\hat{\tau}_u = \hat{u}' \quad (2.11a)$$

$$\hat{\tau}_w = \hat{w}' \quad (2.11b)$$

$$i\alpha \hat{u} + \hat{v}' + i\beta \hat{w} = 0 \quad (2.11c)$$

$$-i\omega \hat{u} + i\alpha U \hat{u} + U' \hat{v} + i\beta W \hat{u} + i\alpha \hat{p} - \frac{1}{Re} (-\alpha^2 \hat{u} + \hat{\tau}_u' - \beta^2 \hat{u}) = 0 \quad (2.11d)$$

$$-i\omega \hat{v} + i\alpha U \hat{v} + i\beta W \hat{v} + \hat{p}' - \frac{1}{Re} (-\alpha^2 \hat{v} - i\alpha \hat{\tau}_u - i\beta \hat{\tau}_w - \beta^2 \hat{v}) = 0 \quad (2.11e)$$

$$-i\omega \hat{w} + i\alpha U \hat{w} + W' \hat{v} + i\beta W \hat{w} + i\beta \hat{p} - \frac{1}{Re} (-\alpha^2 \hat{w} + \hat{\tau}_w' - \beta^2 \hat{w}) = 0 \quad (2.11f)$$

This system can be expressed in matrix form:

$$A\hat{q} - \hat{q}' = 0 \quad (2.12a)$$

$$A = \begin{bmatrix} 0 & a_{12} & 0 & 0 & ReU' & iRe\alpha \\ 1 & 0 & 0 & 0 & 0 & 0 \\ 0 & 0 & 0 & a_{12} & ReW' & iRe\beta \\ 0 & 0 & 1 & 0 & 0 & 0 \\ 0 & -i\alpha & 0 & -i\beta & 0 & 0 \\ -\frac{i\alpha}{Re} & 0 & -\frac{i\beta}{Re} & 0 & -\frac{a_{12}}{Re} & 0 \end{bmatrix} \quad (2.12b)$$

$$a_{12} = iRe(\alpha U + \beta W - \omega) + (\alpha^2 + \beta^2) \quad (2.12c)$$

$$\hat{q} = \begin{bmatrix} \hat{\tau}_u \\ \hat{u} \\ \hat{\tau}_w \\ \hat{w} \\ \hat{v} \\ \hat{p} \end{bmatrix} \quad (2.12d)$$

This system can then be solved with an appropriate numerical method. The present work uses a compact difference method (see § 5.2.2.2) to set up a large matrix system and then a lower-upper matrix decomposition (see § 5.3.3) to return the eigenfunction for validation.

2.2.4 Equivalence between Orr-Sommerfeld and primitive variables

The Orr-Sommerfeld equation describes the problems whose base flow are two-dimensional. The primitive variable problem can be used to describe those with three-dimensional base flows. First the primitive variable problem given in equations 2.10 is reduced to two dimensions, omitting any reference to the spanwise direction:

$$i\alpha\hat{u} + \hat{v}' = 0 \quad (2.13a)$$

$$-i\omega\hat{u} + i\alpha U\hat{u} + U'\hat{v} + i\alpha\hat{p} - \frac{1}{Re}(-\alpha^2\hat{u} + \hat{u}'') = 0 \quad (2.13b)$$

$$-i\omega\hat{v} + i\alpha U\hat{v} + \hat{p}' - \frac{1}{Re}(-\alpha^2\hat{v} + \hat{v}'') = 0 \quad (2.13c)$$

Next the stream function definition is employed:

$$\begin{aligned} \tilde{u} &= \frac{\partial \psi}{\partial y} & \tilde{v} &= -\frac{\partial \psi}{\partial x} \\ \hat{u}e^{i(\alpha x - \omega t)} &= \frac{\partial \phi e^{i(\alpha x - \omega t)}}{\partial y} & \hat{v}e^{i(\alpha x - \omega t)} &= -\frac{\partial \phi e^{i(\alpha x - \omega t)}}{\partial x} \\ \hat{u} &= \phi' & \hat{v} &= -i\alpha\phi \end{aligned}$$

These can be substituted into equation (2.13b), and equation (2.13c). Substituting these into equation (2.13a) renders it obsolete:

$$-i\omega\phi' + i\alpha U\phi' - i\alpha U'\phi + i\alpha\hat{p} - \frac{1}{Re}(-\alpha^2\phi' + \phi''') = 0 \quad (2.14a)$$

$$-\alpha\omega\phi + \alpha^2 U\phi + \hat{p}' - \frac{1}{Re}(+i\alpha^3\phi - i\alpha\phi'') = 0 \quad (2.14b)$$

By taking the derivative of equation (2.14a) it will now contain the term \hat{p}' , also in equation (2.14b).

This can be used to substitute one into the other giving:

$$\phi'''' - 2\alpha^2\phi'' + \alpha^4\phi + iRe\omega\phi'' - iRe\alpha U\phi'' + iRe\alpha U''\phi - iRe\alpha^2\omega\phi + iRe\alpha^3 U\phi = 0$$

And with a some manipulation it can be shown that this equation is exactly identical to the Orr-Sommerfeld equation:

$$\phi'''' - 2\alpha^2\phi'' + \alpha^4\phi = iRe(\alpha U - \omega)(\phi'' - \alpha^2\phi) - iRe\alpha U''\phi$$

2.3 Applying linear stability theory

2.3.1 Eigenvalue problems

For whichever formulation is chosen, the answer sought is still a particular value related to the overall structure of the problem, which is to say it is an eigenvalue problem. A spectral solution would return every eigenvalue, but in this type of problem we are typically only interested in the dominant one. A different type of solution will be used. In each case we shall supply a guess for what the eigenvalue is, then calculate the eigenvectors. These represent the shape of the wave, and their magnitude is of no consequence, however, physical knowledge of the problem can be used to

determine where certain values should be zero. This can then be used to check whether or not the supplied eigenvalue satisfies physics, and if it fails, it can be changed. This can be repeated until the correct eigenvalue is found.

2.3.2 The growth rate of waves

Interpreting the results of linear stability mostly depends on the relative growth rate of the wave. This is because often the actual amplitude is unknown, and also too small to physically measure. The relative growth rate (sometimes labelled σ) is given by:

$$\sigma = \left[\frac{1}{\tilde{q}} \frac{\partial \tilde{q}}{\partial x} \right]_r = \left[\frac{1}{\hat{q} e^{i\Phi}} \frac{\partial \hat{q} e^{i\Phi}}{\partial x} \right]_r = [i\alpha]_r = -\alpha_i \quad (2.15)$$

Where:

$$\Phi = \alpha x + \beta z - \omega t \quad (2.16)$$

Here subscripts i and r refer to the real and imaginary parts. Implied here is that \hat{q} is unchanged in the x direction. As will be seen in § 4.1.3.4, we will be amending this assumption; in fact the value of $1/\hat{q} \times \partial \hat{q} / \partial x$ can be very large, especially when \hat{q} itself is small, but its derivative is non-zero. This difference goes some way to explaining the discrepancies observed between theory and experiment. Nevertheless, knowing this tells us that when the imaginary part of α is zero, the wave is neutrally stable, neither growing nor decaying. By plotting the curve traced by this condition in the $Re - \omega$ plane, neutral curves are generated, whose perimeters bound the region in which waves grow. As will be shown in fig. 2.6 there is an area where no waves are amplified, and a critical Reynolds number, where the first wave begins to grow.

2.3.3 Transition prediction

A growing wave may be responsible for transition, although often this is not immediate, instead requiring the wave to develop as it travels downstream. Using the work of Smith, Gamberoni, and Van Ingen [40, 35] as a basis, it is known that the integral of the growth rate along the path of the wave will relate to the transition location. Integration of the growth rate between two points will give the total amplification ratio (N) across that distance. It can very reasonably be assumed that

waves will not cause transition upstream of their first point of neutral stability, and therefore this point (x_0) is taken to be the lower boundary of the integral. The upper boundary can be given by any point (x_N) where total amplification ratio is sought. i.e:

$$N = \int_{x_0}^{x_N} -\alpha_i dx \quad (2.17)$$

The total amplification ratio between any two points is known. The magnitude of the wave is still unknown. It is prohibitively difficult to measure the waves in real world applications. Instead databases have been compiled and published which correlate the expected transitional N to the free stream turbulence level. Therefore, if the free stream turbulence is known, a value of N where the boundary layer will transition can be determined. N can then be calculated all along the path of the wave, and the location where it reaches the critical value will be the predicted transition location. It is also possible to determine a range of N, where the boundary layer is transitional, and above which it is fully turbulent. This comprises the N-factor method, which is widely used.

2.4 Linear stability calculations

2.4.1 Single eigenvalue search results

As a step towards verification, several temporal stability cases are presented. As a base flow these use the boundary layer over a flat plate. They are compared with results calculated by Davey, and given in Gaster [13]. Davey's results are noteworthy since they were generated using an alternative asymptotic method and should therefore provide enhanced accuracy. The Reynolds number is calculated using $Re = \rho U_e \delta^* / \mu$. Good agreement is shown.

Re	α	ω	ω_{Davey}
500	0.3	0.119304 - 0.000280i	0.119304 - 0.000280i
1500	0.2	0.063123 + 0.003157i	0.063123 + 0.003157i
3000	0.15	0.040219 + 0.002781i	0.040219 + 0.002781i

Table 2.1: Temporal eigenvalue comparison with Davey

Spatial Blasius stability cases are compared with results provided by Gaster [10]. Once again good agreement is shown.

Re	ω	α	α_{Gaster}
725	0.13	0.336890 - 0.002064i	0.336891 - 0.002063i
1000	0.125	0.338399 - 0.002205i	0.338400 - 0.002205i
1200	0.11	0.310161 - 0.005616i	0.310163 - 0.005616i
2500	0.09	0.284744 - 0.004224i	0.284747 - 0.004219i
3000	0.08	0.263735 - 0.006507i	0.263739 - 0.006502i

Table 2.2: Spatial eigenvalue comparison with Gaster

2.4.2 Eigenfunction calculation results

Since the solution method used to find eigenvalues necessitates finding first an eigenfunction, several of these are presented in comparison with those given by Gaster [10]. η denotes the wall normal distance, non-dimensionalised using displacement thickness (y/δ^*). § 2.2.4 shows that the equivalent variables should be ϕ' in the OS, and \hat{u} for the primitive variables. There is good agreement in all cases.

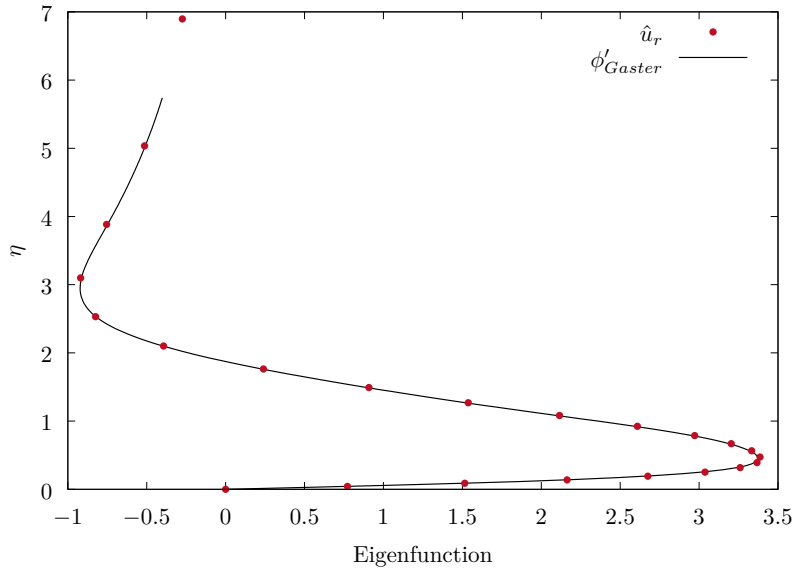


Figure 2.2: Eigenfunction validation of \hat{u}_r for a Blasius velocity profile with $Re_{\delta^*} = 725$, $\omega = 0.13$

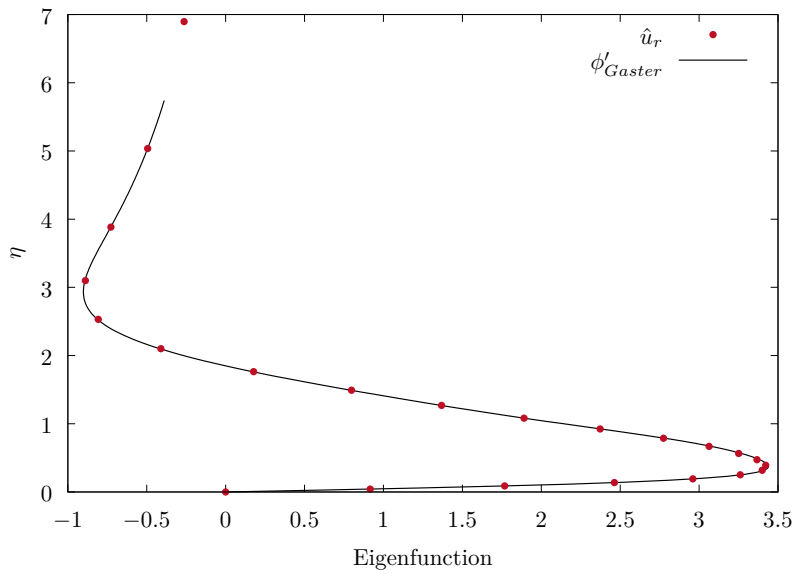


Figure 2.3: Eigenfunction validation of \hat{u}_r for a Blasius velocity profile with $Re_{\delta^*} = 1000$, $\omega = 0.125$

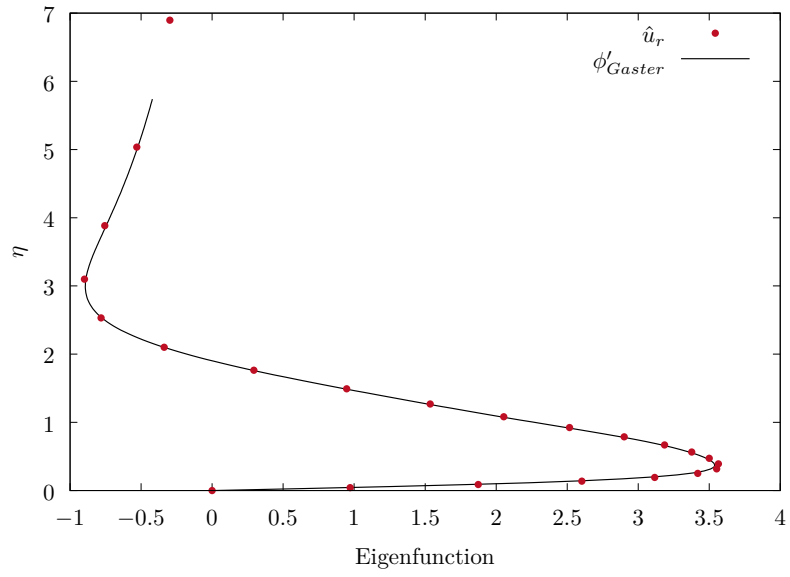


Figure 2.4: Eigenfunction validation of \hat{u}_r for a Blasius velocity profile with $Re_{\delta^*} = 1200$, $\omega = 0.11$

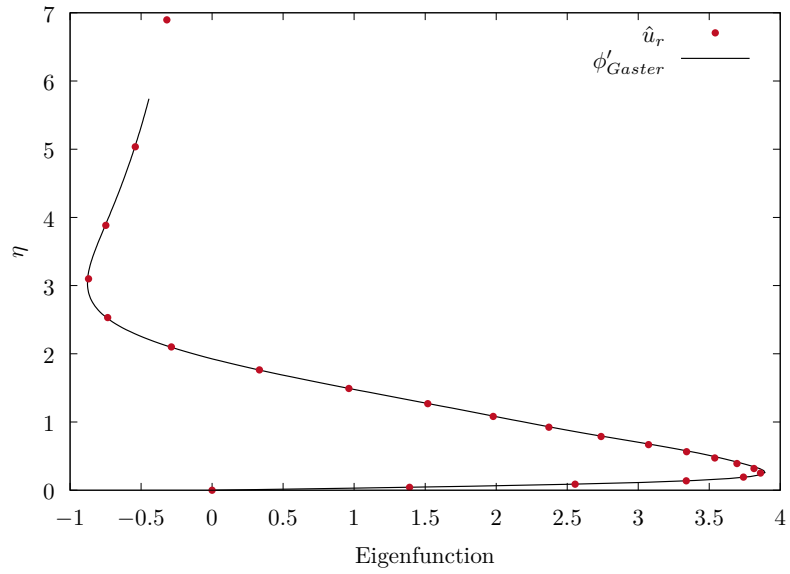


Figure 2.5: Eigenfunction validation of \hat{u}_r for a Blasius velocity profile with $Re_{\delta^*} = 2500$, $\omega = 0.09$

2.4.3 Stability curves

Calculating eigenvalues for a wide range of Reynolds numbers and frequencies allows the construction of stability curves. These can be given for any growth rate, but neutral stability is particularly useful as it shows at a single glance the boundary of the region where waves are amplified. Shown in fig. 2.6 is a curve of neutral stability in a Blasius boundary layer given by Gaster in [14] (in black). Superimposed is the same curve generated by the current code (shown in red). Good agreement is observed.

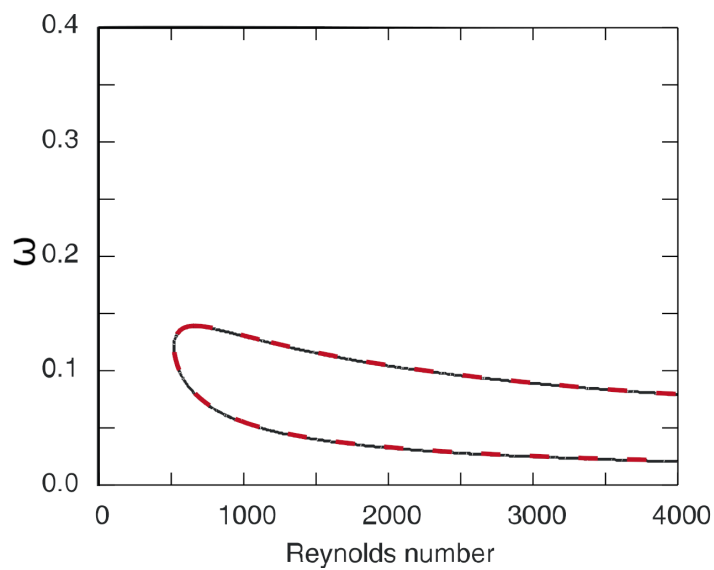


Figure 2.6: Curves of neutral stability in a Blasius boundary layer

Chapter 3

Adjoint Equations

In § 4.1.1 the adjoint equations will be invoked in order to generate a non-parallel correction term for the parallel linear stability equations. However it is trivial neither to formulate nor solve these. This section describes the procedure for finding adjoint equations of various kinds, and relates some important adjoint formulations to each other. Adjoint sensitivity is also briefly explored.

3.1 Definition of the adjoint

The adjoint of any operator \mathcal{L} is another operator \mathcal{L}^\dagger , such that:

$$\langle \mathcal{L}\mathbf{a}, \mathbf{b} \rangle = \langle \mathbf{a}, \mathcal{L}^\dagger \mathbf{b} \rangle \quad (3.1)$$

Where \mathbf{a} and \mathbf{b} are in the same domain, and $\langle \cdot, \cdot \rangle$ is an appropriately defined inner product. As this chapter proceeds, the specific definition will emerge, and by §3.4 will be fully apparent. The domain for the present work will be defined by the physical space between a wall and the far field, i.e. $[0; \infty)$. The direct problem under investigation in our case (see equation (2.12)) is of the form:

$$L\hat{q} - \frac{\partial \hat{q}}{\partial y} = 0 \quad (3.2)$$

Where \hat{q} is a six element vector and L is a six by six matrix. Therefore, it stands to reason that the adjoint equation will also be comprised of a matrix term and a differential term.

3.2 Adjoint of a square matrix

To begin, an appropriate inner product must be defined:

$$\langle \mathbf{a}, \mathbf{b} \rangle = \mathbf{a} \cdot \overline{\mathbf{b}} \quad (3.3)$$

The choice here is the conjugate dot product, rather than just the dot product. This is because the stability problem which will eventually be solved exists in a complex vector space, not a real one. The definition of the adjoint for an operator L becomes:

$$L\mathbf{a} \cdot \overline{\mathbf{b}} = \mathbf{a} \cdot \overline{L^\dagger \mathbf{b}} \quad (3.4)$$

For an n by n matrix this expands as:

$$\begin{bmatrix} l_{11} & l_{12} & \dots & l_{1n} \\ l_{21} & l_{22} & \dots & l_{2n} \\ \vdots & \vdots & \ddots & \vdots \\ l_{n1} & l_{n2} & \dots & l_{nn} \end{bmatrix} \begin{bmatrix} a_1 \\ a_2 \\ \vdots \\ a_n \end{bmatrix} \cdot \overline{\begin{bmatrix} b_1 \\ b_2 \\ \vdots \\ b_n \end{bmatrix}} = \begin{bmatrix} a_1 \\ a_2 \\ \vdots \\ a_n \end{bmatrix} \cdot \overline{L^\dagger \begin{bmatrix} b_1 \\ b_2 \\ \vdots \\ b_n \end{bmatrix}} \quad (3.5)$$

Clearly then, L^\dagger must also be a square matrix, specifically, the conjugate transpose of L . This is demonstrated below:

$$\begin{aligned} \langle L\mathbf{a}, \mathbf{b} \rangle &= \langle \mathbf{a}, L^\dagger \mathbf{b} \rangle \\ LHS &= \begin{bmatrix} l_{11} & l_{12} & \dots & l_{1n} \\ l_{21} & l_{22} & \dots & l_{2n} \\ \vdots & \vdots & \ddots & \vdots \\ l_{n1} & l_{n2} & \dots & l_{nn} \end{bmatrix} \begin{bmatrix} a_1 \\ a_2 \\ \vdots \\ a_n \end{bmatrix} \cdot \overline{\begin{bmatrix} b_1 \\ b_2 \\ \vdots \\ b_n \end{bmatrix}} \\ &= \overline{b_1} (l_{11}a_1 + l_{12}a_2 + \dots + l_{1n}a_n) + \\ &\quad \overline{b_2} (l_{21}a_1 + l_{22}a_2 + \dots + l_{2n}a_n) + \dots + \\ &\quad \overline{b_n} (l_{n1}a_1 + l_{n2}a_2 + \dots + l_{nn}a_n) + \\ RHS &= \begin{bmatrix} a_1 \\ a_2 \\ \vdots \\ a_n \end{bmatrix} \cdot \overline{\begin{bmatrix} \overline{l_{11}} & \overline{l_{21}} & \dots & \overline{l_{n1}} \\ \overline{l_{12}} & \overline{l_{22}} & \dots & \overline{l_{n2}} \\ \vdots & \vdots & \ddots & \vdots \\ \overline{l_{1n}} & \overline{l_{2n}} & \dots & \overline{l_{nn}} \end{bmatrix}} \begin{bmatrix} b_1 \\ b_2 \\ \vdots \\ b_n \end{bmatrix} \\ &= a_1 (l_{11}\overline{b_1} + l_{21}\overline{b_2} + \dots + l_{n1}\overline{b_n}) \\ &\quad a_2 (l_{12}\overline{b_1} + l_{22}\overline{b_2} + \dots + l_{n2}\overline{b_n}) + \dots + \\ &\quad a_n (l_{1n}\overline{b_1} + l_{2n}\overline{b_2} + \dots + l_{nn}\overline{b_n}) = LHS \end{aligned}$$

3.3 Adjoint of the differential operator

To find the adjoint of a continuous operator, a different inner product more suited for the task is needed. The choice is typically:

$$\langle a, b \rangle = \int_0^\infty (a \overline{b}) dy \quad (3.6)$$

This is analogous to that chosen in §3.2. Both can be seen as taking the sum of all products of two functions within the bounds of the problem. Now \mathcal{L}^\dagger is sought such that:

$$\begin{aligned}\left\langle \frac{\partial a}{\partial y}, b \right\rangle &= \langle a, \mathcal{L}^\dagger b \rangle \\ LHS &= \int_0^\infty \left(\frac{\partial a}{\partial y} \bar{b} \right) dy \\ RHS &= \int_0^\infty (a \overline{\mathcal{L}b}) dy\end{aligned}$$

Integrating the LHS by parts returns:

$$LHS = [a\bar{b}]_0^\infty - \int_0^\infty \left(a \frac{\partial \bar{b}}{\partial y} \right) dy$$

Which means that:

$$\mathcal{L}^\dagger = -\frac{\partial}{\partial y}$$

This holds with the restriction that the sum of the products of a and b at the domain boundaries is equal to zero ($[a\bar{b}]_0^\infty = 0$). This will inform the setting of boundary conditions when it comes time to solve this type of equation. In our case, derived from equation (2.12), this means that at the boundaries the dot products of the direct and adjoint solutions should be zero, this is guaranteed by checking which boundary values are finite in the direct solution, and setting their corresponding value in the adjoint form to zero.

3.4 Adjoint of a combined matrix and differential

The stability problem is formulated with a continuous and discrete part. From §3.2, and §3.3 the adjoints of each part are known from §3.2 and §3.3. The sum of the adjoints of two operators is the adjoint of their sum. However, it is not necessarily true that combining adjoints in such a fashion will leave the boundary restrictions unchanged. The inner product chosen for the combined operator takes elements from each of the two constituent parts:

$$\langle \mathbf{a}, \mathbf{b} \rangle = \int_0^\infty (\mathbf{a} \cdot \bar{\mathbf{b}}) dy \quad (3.7)$$

Once again the definition of the adjoint must be satisfied:

$$\begin{aligned} LHS &= \int_0^\infty \left(\left(L\mathbf{a} + \frac{\partial \mathbf{a}}{\partial y} \right) \cdot \bar{\mathbf{b}} \right) dy \\ &= \int_0^\infty \left(\left(\begin{bmatrix} l_{11} & l_{12} & \cdots & l_{1n} \\ l_{21} & l_{22} & \cdots & l_{2n} \\ \vdots & \vdots & \ddots & \vdots \\ l_{n1} & l_{n2} & \cdots & l_{nn} \end{bmatrix} \begin{bmatrix} a_1 \\ a_2 \\ \vdots \\ a_n \end{bmatrix} + \begin{bmatrix} a'_1 \\ a'_2 \\ \vdots \\ a'_n \end{bmatrix} \right) \cdot \begin{bmatrix} \bar{b}_1 \\ \bar{b}_2 \\ \vdots \\ \bar{b}_n \end{bmatrix} \right) dy \\ &= \int_0^\infty \bar{b}_1 (l_{11}a_1 + l_{12}a_2 + \cdots + l_{1n}a_n + a'_1) + \\ &\quad \bar{b}_2 (l_{21}a_1 + l_{22}a_2 + \cdots + l_{2n}a_n + a'_2) + \cdots + \\ &\quad \bar{b}_n (l_{n1}a_1 + l_{n2}a_2 + \cdots + l_{nn}a_n + a'_n) dy \\ &= \int_0^\infty \bar{b}_1 (l_{11}a_1 + l_{12}a_2 + \cdots + l_{1n}a_n) + \\ &\quad \bar{b}_2 (l_{21}a_1 + l_{22}a_2 + \cdots + l_{2n}a_n) + \cdots + \\ &\quad \bar{b}_n (l_{n1}a_1 + l_{n2}a_2 + \cdots + l_{nn}a_n) + \\ &\quad \bar{b}_1 a'_1 + \bar{b}_2 a'_2 + \cdots + \bar{b}_n a'_n dy \end{aligned}$$

$$\begin{aligned}
RHS &= \int_0^\infty \left(\mathbf{a} \cdot \left(L^H \bar{\mathbf{b}} - \frac{\partial \bar{\mathbf{b}}}{\partial y} \right) \right) dy \\
&= \int_0^\infty \left(\begin{bmatrix} a_1 \\ a_2 \\ \vdots \\ a_n \end{bmatrix} \cdot \left(\begin{bmatrix} \bar{l}_{11} & \bar{l}_{21} & \dots & \bar{l}_{n1} \\ \bar{l}_{12} & \bar{l}_{22} & \dots & \bar{l}_{n2} \\ \vdots & \vdots & \ddots & \vdots \\ \bar{l}_{1n} & \bar{l}_{2n} & \dots & \bar{l}_{nn} \end{bmatrix} \begin{bmatrix} \bar{b}_1 \\ \bar{b}_2 \\ \vdots \\ \bar{b}_n \end{bmatrix} - \begin{bmatrix} \bar{b}'_1 \\ \bar{b}'_2 \\ \vdots \\ \bar{b}'_n \end{bmatrix} \right) \right) dy \\
&= \int_0^\infty a_1 (l_{11}\bar{b}_1 + l_{21}\bar{b}_2 + \dots + l_{n1}\bar{b}_n) - a_1\bar{b}'_1 + \\
&\quad a_2 (l_{12}\bar{b}_1 + l_{22}\bar{b}_2 + \dots + l_{n2}\bar{b}_n) - a_2\bar{b}'_2 + \dots + \\
&\quad a_n (l_{1n}\bar{b}_1 + l_{2n}\bar{b}_2 + \dots + l_{nn}\bar{b}_n) - a_n\bar{b}'_n dy \\
&= \int_0^\infty a_1 (l_{11}\bar{b}_1 + l_{21}\bar{b}_2 + \dots + l_{n1}\bar{b}_n) + \\
&\quad a_2 (l_{12}\bar{b}_1 + l_{22}\bar{b}_2 + \dots + l_{n2}\bar{b}_n) + \dots + \\
&\quad a_n (l_{1n}\bar{b}_1 + l_{2n}\bar{b}_2 + \dots + l_{nn}\bar{b}_n) - \\
&\quad a_1\bar{b}'_1 - a_2\bar{b}'_2 - \dots - a_n\bar{b}'_n dy
\end{aligned}$$

By splitting the terms with differentials and integrating by parts:

$$\begin{aligned}
&= \int_0^\infty a_1 (l_{11}\bar{b}_1 + l_{21}\bar{b}_2 + \dots + l_{n1}\bar{b}_n) + \\
&\quad a_2 (l_{12}\bar{b}_1 + l_{22}\bar{b}_2 + \dots + l_{n2}\bar{b}_n) + \dots + \\
&\quad a_n (l_{1n}\bar{b}_1 + l_{2n}\bar{b}_2 + \dots + l_{nn}\bar{b}_n) dy + \\
&\quad [a_1\bar{b}_1 + a_2\bar{b}_2 + \dots + a_n\bar{b}_n]_0^\infty - \int_0^\infty -a'_1\bar{b}_1 - a'_2\bar{b}_2 - \dots - a'_n\bar{b}_n dy \\
&= \int_0^\infty a_1 (l_{11}\bar{b}_1 + l_{21}\bar{b}_2 + \dots + l_{n1}\bar{b}_n) + \\
&\quad a_2 (l_{12}\bar{b}_1 + l_{22}\bar{b}_2 + \dots + l_{n2}\bar{b}_n) + \dots + \\
&\quad a_n (l_{1n}\bar{b}_1 + l_{2n}\bar{b}_2 + \dots + l_{nn}\bar{b}_n) dy + \\
&\quad [\mathbf{a} \cdot \bar{\mathbf{b}}]_0^\infty + \int_0^\infty a'_1\bar{b}_1 + a'_2\bar{b}_2 + \dots + a'_n\bar{b}_n dy = LHS
\end{aligned}$$

This holds if and only if the dot product term at the domain boundaries is equal to zero. Once again, this information can be used to generate appropriate boundary conditions to use in the solution of the adjoint equation.

3.5 Adjoint Orr-Sommerfeld equation

The vast majority of the literature concerning adjoint stability uses the Orr-Sommerfeld formulation. Recall equation (2.5) the Orr-Sommerfeld equation:

$$\phi'''' - 2\alpha^2\phi'' + \alpha^4\phi = iRe(\alpha U - \omega)(\phi'' - \alpha^2\phi) - iRe\alpha U''\phi$$

This can be expressed as:

$$\begin{aligned} & [\partial^4 - 2\alpha^2\partial^2 + \alpha^4 - iRe(\alpha U - \omega)(\partial^2 - \alpha^2) + iRe\alpha U'']\phi = 0 \\ & [\partial^4 - 2\alpha^2\partial^2 + \alpha^4 - iRe\alpha U\partial^2 + iRe\alpha^3U + iRe\omega\partial^2 - iRe\omega\alpha^2 + iRe\alpha U'']\phi = 0 \\ & \mathcal{L}_{OS}\phi = 0 \end{aligned}$$

So the adjoint operator (\mathcal{L}_{OS}^\dagger) must satisfy:

$$\begin{aligned} \langle \mathcal{L}_{OS}\phi, \phi^\dagger \rangle &= \langle \phi, \mathcal{L}_{OS}^\dagger\phi^\dagger \rangle \\ &= \int_0^\infty (\partial^4 - 2\alpha^2\partial^2 + \alpha^4 - iRe\alpha U\partial^2 + iRe\alpha^3U + iRe\omega\partial^2 - iRe\omega\alpha^2 + iRe\alpha U'')\phi \cdot \overline{\phi^\dagger} dy \quad (3.8) \\ &= \int_0^\infty \phi \cdot \overline{(\mathcal{L}_{OS}^\dagger\phi^\dagger)} dy \end{aligned}$$

Taking the Left hand side of the equation:

$$\begin{aligned} LHS &= \int_0^\infty \underbrace{\phi'''' \cdot \overline{\phi^\dagger}}_{\boxed{1}} - \underbrace{2\alpha^2\phi'' \cdot \overline{\phi^\dagger}}_{\boxed{2}} + \underbrace{\alpha^4\phi \cdot \overline{\phi^\dagger}}_{\boxed{3}} - \underbrace{iRe\alpha U\phi'' \cdot \overline{\phi^\dagger}}_{\boxed{4}} \\ &\quad + \underbrace{iRe\alpha^3U\phi \cdot \overline{\phi^\dagger}}_{\boxed{5}} + \underbrace{iRe\omega\phi'' \cdot \overline{\phi^\dagger}}_{\boxed{6}} - \underbrace{iRe\omega\alpha^2\phi \cdot \overline{\phi^\dagger}}_{\boxed{7}} + \underbrace{iRe\alpha U''\phi \cdot \overline{\phi^\dagger}}_{\boxed{8}} dy \end{aligned}$$

Each term in \mathcal{L}_{OS} will have a corresponding term in \mathcal{L}_{OS}^\dagger , so these will be dealt with in order.

Term 1 requires integration by parts four times:

$$\boxed{1} = \int_0^\infty \phi'''' \cdot \overline{\phi^\dagger} dy = \left[\phi'''' \cdot \overline{\phi^\dagger} \right]_0^\infty - \left[\phi''' \cdot \overline{\phi^\dagger'} \right]_0^\infty + \left[\phi'' \cdot \overline{\phi^\dagger''} \right]_0^\infty - \left[\phi \cdot \overline{\phi^\dagger'''} \right]_0^\infty + \int_0^\infty \phi \cdot \overline{\phi^{\dagger''''}} dy$$

Term 2 only needs to be integrated by parts twice:

$$\boxed{2} = -2\alpha^2 \int_0^\infty \phi'' \cdot \bar{\phi}^\dagger dy = -2\alpha^2 \left(\left[\phi' \cdot \bar{\phi}^\dagger \right]_0^\infty - \left[\phi \cdot \bar{\phi}^{\dagger'} \right]_0^\infty + \int_0^\infty \phi \cdot \bar{\phi}^{\dagger''} dy \right)$$

Term 3 is in a suitable form already. Term 4 however is worthy of attention, since it has a factor of U , which is a function of y :

$$\begin{aligned} \boxed{4} &= -i\text{Re}\alpha \int_0^\infty U \phi'' \cdot \bar{\phi}^\dagger dy \\ &= -i\text{Re}\alpha \left(\left[\phi' \cdot U \bar{\phi}^\dagger \right]_0^\infty - \left[\phi \cdot (U \bar{\phi}^\dagger)' \right]_0^\infty + \int_0^\infty \phi \cdot (U \bar{\phi}^\dagger)'' dy \right) \\ &= -i\text{Re}\alpha \left(\left[\phi' \cdot U \bar{\phi}^\dagger \right]_0^\infty - \left[\phi \cdot (U' \bar{\phi}^\dagger + U \bar{\phi}^{\dagger'}) \right]_0^\infty + \int_0^\infty \phi \cdot (U'' \bar{\phi}^\dagger + 2U' \bar{\phi}^{\dagger'} + U \bar{\phi}^{\dagger''}) dy \right) \end{aligned}$$

Like term 4, term 5 already has a factor of U , however, like term 3, it is already in a suitable form.

Term 6 is treated similarly to term 2:

$$\boxed{6} = i\text{Re}w \int_0^\infty \phi'' \cdot \bar{\phi}^\dagger dy = i\text{Re}w \left(\left[\phi' \cdot \bar{\phi}^\dagger \right]_0^\infty - \left[\phi \cdot \bar{\phi}^{\dagger'} \right]_0^\infty + \int_0^\infty \phi \cdot \bar{\phi}^{\dagger''} dy \right)$$

And finally terms 7 and 8, which are in the correct form without manipulation as well. Of the square brackets, most become zero due to boundary conditions on U , ϕ , or ϕ' . Those which do not must be made zero in another way. By setting boundary values for each daggered variable to be equal to their undaggered counterpart, the remaining square brackets cancel each other out. The terms can then be reassembled into :

$$\begin{aligned} &\int_0^\infty \underbrace{\phi \cdot \bar{\phi}^{\dagger''''}}_{\boxed{1}} + \underbrace{-2\alpha^2 \phi \cdot \bar{\phi}^{\dagger''}}_{\boxed{2}} + \underbrace{\alpha^4 \phi \cdot \bar{\phi}^\dagger}_{\boxed{3}} - \underbrace{i\text{Re}\alpha \phi \cdot (U'' \bar{\phi}^\dagger + 2U' \bar{\phi}^{\dagger'} + U \bar{\phi}^{\dagger''})}_{\boxed{4}} \\ &\quad + \underbrace{i\text{Re}\alpha^3 U \phi \cdot \bar{\phi}^\dagger}_{\boxed{5}} + \underbrace{i\text{Re}w \phi \cdot \bar{\phi}^{\dagger''}}_{\boxed{6}} - \underbrace{i\text{Re}w \alpha^2 \phi \cdot \bar{\phi}^\dagger}_{\boxed{7}} + \underbrace{i\text{Re}\alpha U'' \phi \cdot \bar{\phi}^\dagger}_{\boxed{8}} dy = 0 \end{aligned}$$

which reduces to:

$$\begin{aligned} &\int_0^\infty \phi \cdot \bar{\phi}^{\dagger''''} + -2\alpha^2 \phi \cdot \bar{\phi}^{\dagger''} + \alpha^4 \phi \cdot \bar{\phi}^\dagger - 2i\text{Re}U' \alpha \phi \cdot \bar{\phi}^{\dagger'} - iU\text{Re}\alpha \phi \cdot \bar{\phi}^{\dagger''} \\ &\quad + i\text{Re}\alpha^3 U \phi \cdot \bar{\phi}^\dagger + i\text{Re}w \phi \cdot \bar{\phi}^{\dagger''} - i\text{Re}w \alpha^2 \phi \cdot \bar{\phi}^\dagger dy = 0 \end{aligned}$$

This will equal the RHS if and only if:

$$\mathcal{L}_{OS}^\dagger = \partial^4 - 2\alpha^2\partial^2 + \alpha^4 - 2iRe\alpha U'\partial - iRe\alpha U\partial'' + iRe\alpha^3 U + iRe\omega\partial^2 - iRe\alpha^2\omega \quad (3.9)$$

This gives the adjoint Orr-Sommerfeld operator as used by Gaster [10] and others.

3.6 Adjoint primitive variable linear stability system

Since the primitive variable operator (equation (2.12a)) comes in the form of a matrix and a simple derivative, the adjoint equation should not be difficult to find. The matrix should be replaced by its complex conjugate, and the derivative should be made negative, or since the right hand side of the equation is zero, the matrix can be made negative instead:

$$\begin{bmatrix} 0 & 1 & 0 & 0 & 0 & -\frac{i\alpha}{Re} \\ a_{12} & 0 & 0 & 0 & -i\alpha & 0 \\ 0 & 0 & 0 & 1 & 0 & -\frac{i\beta}{Re} \\ 0 & 0 & a_{12} & 0 & -i\beta & 0 \\ ReU' & 0 & ReW' & 0 & 0 & -\frac{a_{12}}{Re} \\ iRe\alpha & 0 & iRe\beta & 0 & 0 & 0 \end{bmatrix} \begin{bmatrix} q_1^\dagger \\ q_2^\dagger \\ q_3^\dagger \\ q_4^\dagger \\ q_5^\dagger \\ q_6^\dagger \end{bmatrix} + \begin{bmatrix} q_1^\dagger \\ q_2^\dagger \\ q_3^\dagger \\ q_4^\dagger \\ q_5^\dagger \\ q_6^\dagger \end{bmatrix}' = 0 \quad (3.10a)$$

$$-\begin{bmatrix} 0 & 1 & 0 & 0 & 0 & -\frac{i\alpha}{Re} \\ a_{12} & 0 & 0 & 0 & -i\alpha & 0 \\ 0 & 0 & 0 & 1 & 0 & -\frac{i\beta}{Re} \\ 0 & 0 & a_{12} & 0 & -i\beta & 0 \\ ReU' & 0 & ReW' & 0 & 0 & -\frac{a_{12}}{Re} \\ iRe\alpha & 0 & iRe\beta & 0 & 0 & 0 \end{bmatrix} \begin{bmatrix} q_1^\dagger \\ q_2^\dagger \\ q_3^\dagger \\ q_4^\dagger \\ q_5^\dagger \\ q_6^\dagger \end{bmatrix} - \begin{bmatrix} q_1^\dagger \\ q_2^\dagger \\ q_3^\dagger \\ q_4^\dagger \\ q_5^\dagger \\ q_6^\dagger \end{bmatrix}' = 0 \quad (3.10b)$$

3.7 Equivalence between adjoints systems

In order to show equivalence between the adjoint Orr-Sommerfeld and adjoint in primitive variables formulations; first the adjoint primitive system is first reduced to 2D:

$$\begin{bmatrix} 0 & 1 & 0 & -\frac{i\alpha}{Re} \\ a_{12} & 0 & -i\alpha & 0 \\ ReU' & 0 & 0 & -\frac{a_{12}}{Re} \\ iRe\alpha & 0 & 0 & 0 \end{bmatrix} \begin{bmatrix} q_1^\dagger \\ q_2^\dagger \\ q_3^\dagger \\ q_4^\dagger \end{bmatrix} + \begin{bmatrix} q_1^\dagger \\ q_2^\dagger \\ q_3^\dagger \\ q_4^\dagger \end{bmatrix}' = 0 \quad (3.11)$$

This can be split into four equations (here, where matrix elements have not been conjugated, it is because they are real only):

$$q_2^\dagger - \frac{i\bar{\alpha}}{Re} q_4^\dagger + q_1^{\dagger'} = 0 \quad (3.12a)$$

$$\bar{a}_{12} q_1^\dagger - i\bar{\alpha} q_3^\dagger + q_2^{\dagger'} = 0 \quad (3.12b)$$

$$ReU' q_1^\dagger - \frac{\bar{a}_{12}}{Re} q_4^\dagger + q_3^{\dagger'} = 0 \quad (3.12c)$$

$$-iRe\bar{\alpha} q_1^\dagger + q_4^{\dagger'} = 0 \quad (3.12d)$$

Now equation (3.12d) can be manipulated:

$$\begin{aligned} -iRe\bar{\alpha} q_1^\dagger + q_4^{\dagger'} &= 0 \\ q_1^\dagger &= \frac{i}{Re\bar{\alpha}} q_4^{\dagger'} \end{aligned}$$

Now equation (3.12a) can be manipulated:

$$\begin{aligned} q_2^\dagger - \frac{i\bar{\alpha}}{Re} q_4^\dagger + q_1^{\dagger'} &= 0 \\ q_2^\dagger &= \frac{i\bar{\alpha}}{Re} q_4^\dagger - \frac{i}{Re\bar{\alpha}} q_4^{\dagger''} \end{aligned}$$

And equation (3.12b):

$$\begin{aligned} \bar{a}_{12} q_1^\dagger - i\bar{\alpha} q_3^\dagger + q_2^{\dagger'} &= 0 \\ i\bar{\alpha} q_3^\dagger &= \bar{a}_{12} \left(\frac{i}{Re\bar{\alpha}} q_4^{\dagger'} \right) + \left(\frac{i\bar{\alpha}}{Re} q_4^\dagger - \frac{i}{Re\bar{\alpha}} q_4^{\dagger''} \right)' \\ q_3^\dagger &= \frac{\bar{a}_{12}}{Re\bar{\alpha}^2} q_4^{\dagger'} + \frac{1}{Re} q_4^{\dagger''} - \frac{1}{Re\bar{\alpha}^2} q_4^{\dagger'''} \end{aligned}$$

And finally equation (3.12c):

$$\begin{aligned} ReU' q_1^\dagger - \frac{\bar{a}_{12}}{Re} q_4^\dagger + q_3^{\dagger'} &= 0 \\ ReU' \left(\frac{i}{Re\bar{\alpha}} q_4^{\dagger'} \right) - \frac{\bar{a}_{12}}{Re} q_4^\dagger + \left(\frac{\bar{a}_{12}}{Re\bar{\alpha}^2} q_4^{\dagger'} + \frac{1}{Re} q_4^{\dagger''} - \frac{1}{Re\bar{\alpha}^2} q_4^{\dagger'''} \right)' &= 0 \\ \frac{iU'}{\bar{\alpha}} q_4^{\dagger'} - \frac{\bar{a}_{12}}{Re} q_4^\dagger + \frac{\bar{a}_{12}}{Re\bar{\alpha}^2} q_4^{\dagger''} + \frac{\bar{a}_{12}'}{Re\bar{\alpha}^2} q_4^{\dagger'} + \frac{1}{Re} q_4^{\dagger''} - \frac{1}{Re\bar{\alpha}^2} q_4^{\dagger'''} &= 0 \end{aligned}$$

$$iRe\bar{\alpha}U'q_4^\dagger - \bar{\alpha}^2\bar{a}_{12}q_4^\dagger + \bar{a}_{12}q_4^{\dagger''} + \bar{a}_{12}'q_4^{\dagger'} + \bar{\alpha}^2q_4^{\dagger''} - q_4^{\dagger''''} = 0$$

Now using the definition of a_{12} from equation (2.12c) modified to make it two-dimensional:

$$iRe(\omega - \bar{\alpha}U) + \bar{\alpha}^2 = \bar{a}_{12} \quad (3.13a)$$

$$-iRe\bar{\alpha}U' = \bar{a}_{12}' \quad (3.13b)$$

These are substituted in where appropriate:

$$\begin{aligned} iRe\bar{\alpha}U'q_4^{\dagger'} - \bar{\alpha}^2(iRe(\bar{\alpha}U - \omega) + \bar{\alpha}^2)q_4^\dagger + (iRe(\bar{\alpha}U - \omega) + \bar{\alpha}^2)q_4^{\dagger''} + iRe\bar{\alpha}U'q_4^{\dagger'} + \bar{\alpha}^2q_4^{\dagger''} - q_4^{\dagger''''} &= 0 \\ -q_4^{\dagger''''} + 2\bar{\alpha}^2q_4^{\dagger''} - \bar{\alpha}^4q_4^\dagger + 2iRe\bar{\alpha}U'q_4^{\dagger'} + iRe\bar{\alpha}Uq_4^{\dagger''} - iRe\bar{\alpha}^3Uq_4^\dagger - iRe\omega q_4^{\dagger''} + iRe\bar{\alpha}\omega q_4^\dagger &= 0 \\ q_4^{\dagger''''} - 2\bar{\alpha}^2q_4^{\dagger''} + \bar{\alpha}^4q_4^\dagger - 2iRe\bar{\alpha}U'q_4^{\dagger'} - iRe\bar{\alpha}Uq_4^{\dagger''} + iRe\bar{\alpha}^3Uq_4^\dagger + iRe\omega q_4^{\dagger''} - iRe\bar{\alpha}\omega q_4^\dagger &= 0 \\ (\partial^4 - 2\bar{\alpha}^2\partial^2 + \bar{\alpha}^4 - 2iRe\bar{\alpha}U'\partial - iRe\bar{\alpha}U\partial^2 + iRe\bar{\alpha}^3U + iRe\omega\partial^2 - iRe\bar{\alpha}\omega)q_4^\dagger &= 0 \end{aligned} \quad (3.14)$$

Compare this to the adjoint Orr-Sommerfeld operator given in equation (3.9) it can be seen that q_4^\dagger is exactly analagous to ϕ^\dagger , therefore:

$$\mathcal{L}_{OS}^\dagger q_4^\dagger = 0 \quad (3.15a)$$

$$\alpha^\dagger = \bar{\alpha} \quad (3.15b)$$

\hat{q}_4 in the direct system corresponds to pressure (\hat{p}) therefore as a shorthand, \hat{q}_4^\dagger is referred to as ‘adjoint pressure’.

3.8 Adjoint calculations

3.8.1 Single eigenvalue search results

The simplest use case for the adjoint is as a replacement for its forward counterpart. Solving the forward and adjoint systems results in different eigenfunctions, however the eigenvalues should be identical. Compared now are the same two-dimensional spatial stability cases provided by Gaster [10] shown in Chapter 2. Each of these has a Blasius velocity profile, and Reynolds number is calculated using $Re = \rho U_e \delta^* / \mu$. Forward and adjoint solutions are now included. All cases show good agreement.

Re	ω	α	α_{Adj}	α_{Gaster}	$\alpha_{GasterAdj}$
725	0.13	0.336890 - 0.002064i	0.336889 - 0.002064i	0.336891 - 0.002063i	0.336889 - 0.002065i
1000	0.125	0.338399 - 0.002205i	0.338398 - 0.002206i	0.338400 - 0.002205i	0.338399 - 0.002207i
1200	0.11	0.310161 - 0.005616i	0.310161 - 0.005616i	0.310163 - 0.005616i	0.310161 - 0.005618i
2500	0.09	0.284744 - 0.004224i	0.284743 - 0.004224i	0.284747 - 0.004219i	0.284748 - 0.004228i
3000	0.08	0.263735 - 0.006507i	0.263735 - 0.006508i	0.263739 - 0.006502i	0.263739 - 0.006512i

Table 3.1: Spatial and adjoint spatial comparison with Gaster

Good agreement between forward and adjoint methods is also seen for Blasius cases with oblique disturbances, in these cases $\beta = 0.1$. Both calculations are completed using the novel code.

Re	ω	α	α_{Adj}
725	0.13	0.333086 - 0.000783i	0.333086 - 0.000783i
1000	0.125	0.334539 - 0.000621i	0.334538 - 0.000621i
1200	0.11	0.305910 - 0.004109i	0.305910 - 0.004109i
2500	0.09	0.279692 - 0.001992i	0.279692 - 0.001992i
3000	0.08	0.258261 - 0.004311i	0.258260 - 0.004312i

Table 3.2: Oblique spatial comparison, $\beta = 0.1$

Most importantly, the method can be applied to oblique disturbances in 3D boundary layers. Shown are stability results for a Falkner-Skan-Cooke profile with $\beta = 0.1$, $\theta_{wedge} = 10^\circ$, and $\theta_{sweep} = 30^\circ$.

Re	ω	α	α_{Adj}
725	0.13	0.344552 + 0.121012i	0.344538 + 0.121019i
1000	0.125	0.352349 + 0.101671i	0.352328 + 0.101685i
1200	0.11	0.323755 + 0.093360i	0.323733 + 0.093376i
2500	0.09	0.303033 + 0.063527i	0.302994 + 0.063566i
3000	0.08	0.280772 + 0.058731i	0.280731 + 0.058772i

Table 3.3: Oblique waves in a 3D boundary layer

And by forcing the calculation into some rather extreme conditions, even amplified oblique waves in three dimensional boundary layers can be identified. In the same swept wedge as before:

Re	β	ω	α	α_{Adj}
2000	0.8	0.05	0.120970 + 0.032103i	0.120957 + 0.032091i
4000	0.8	0.05	0.130371 + 0.012338i	0.130351 + 0.012331i
6000	0.8	0.05	0.134942 + 0.002624i	0.134916 + 0.002621i
8000	0.8	0.05	0.138380 - 0.003655i	0.138348 - 0.003654i
10000	0.8	0.05	0.141306 - 0.008157i	0.141269 - 0.008153i
12000	0.8	0.05	0.143909 - 0.011564i	0.143865 - 0.011558i
14000	0.8	0.05	0.146272 - 0.014231i	0.146221 - 0.014224i
16000	0.8	0.05	0.148440 - 0.016364i	0.148382 - 0.016356i

Table 3.4: Amplified oblique wave in a 3D boundary layer

3.8.2 Adjoint eigenfunctions

As with the direct approach, the adjoint problem yields an eigenfunction. The equivalence of the adjoint primitive variable system and adjoint Orr-Sommerfeld system is shown in §3.7; this informs which values should be compared. Results from Gaster [10] using the traditional adjoint OS equation are plotted along with the “adjoint pressure” from the present analysis. Good agreement is observed in all cases.

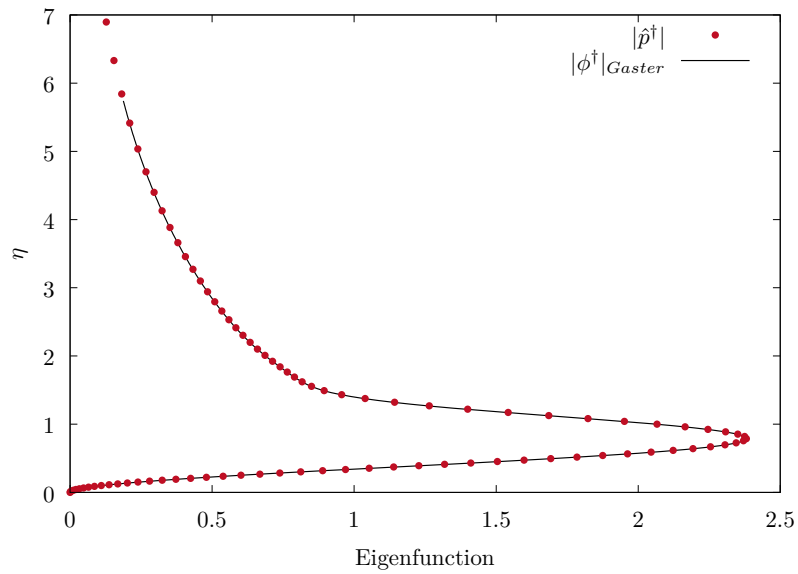


Figure 3.1: Adjoint eigenfunction validation of $|\hat{p}^\dagger|$ for a Blasius profile with $\text{Re} = 725$, $\omega = 0.13$

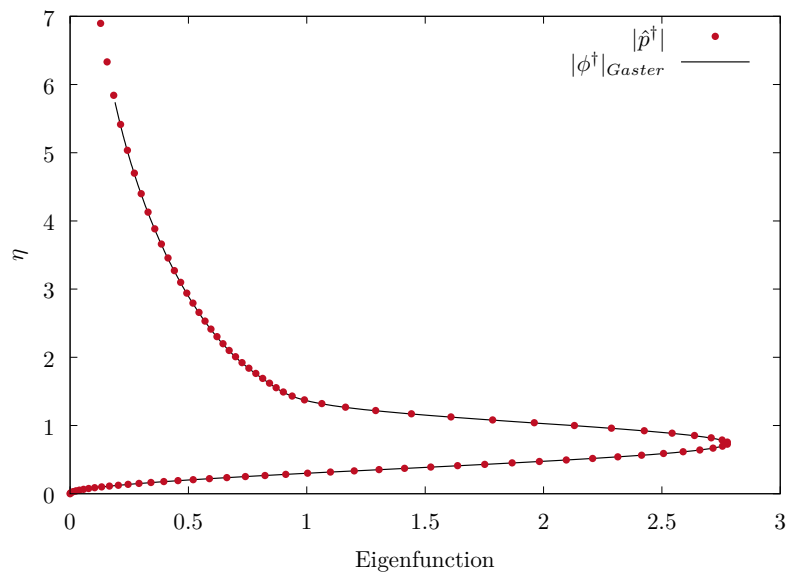


Figure 3.2: Adjoint eigenfunction validation of $|\hat{p}^\dagger|$ for a Blasius profile with $\text{Re} = 1000$, $\omega = 0.125$

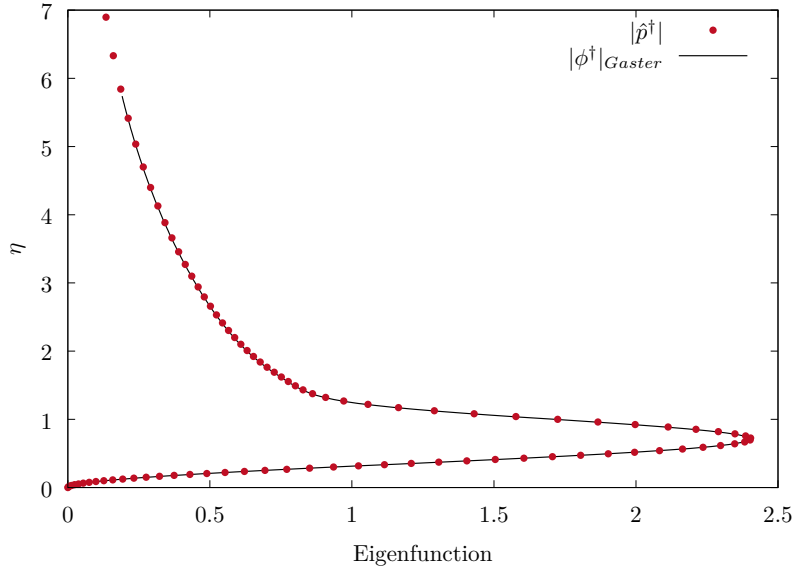


Figure 3.3: Adjoint eigenfunction validation of $|\hat{p}^\dagger|$ for a Blasius profile with $\text{Re} = 1200$, $\omega = 0.11$

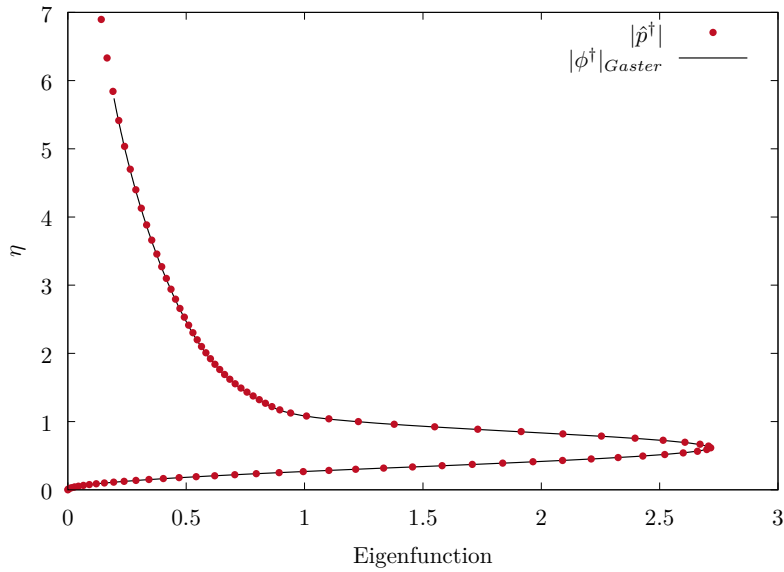


Figure 3.4: Adjoint eigenfunction validation of $|\hat{p}^\dagger|$ for a Blasius profile with $\text{Re} = 2500$, $\omega = 0.09$

Absolute values of the eigenfunctions are used from fig. 3.1–fig. 3.4, since it is possible that the results of the two analyses differ by a constant complex coefficient. The reader may be unconvinced that absolute values do indeed represent the truth of the matter, or omit important phase information; to nullify such doubts, a case is presented where the complex coefficient has been deduced, and used to rescale one eigenfunction. The real part is shown. Good agreement is observed. This

further validates the methodology for generating adjoint eigenfunctions, and should increase our confidence that the choice of inner product shown in equation (3.7) was sound.

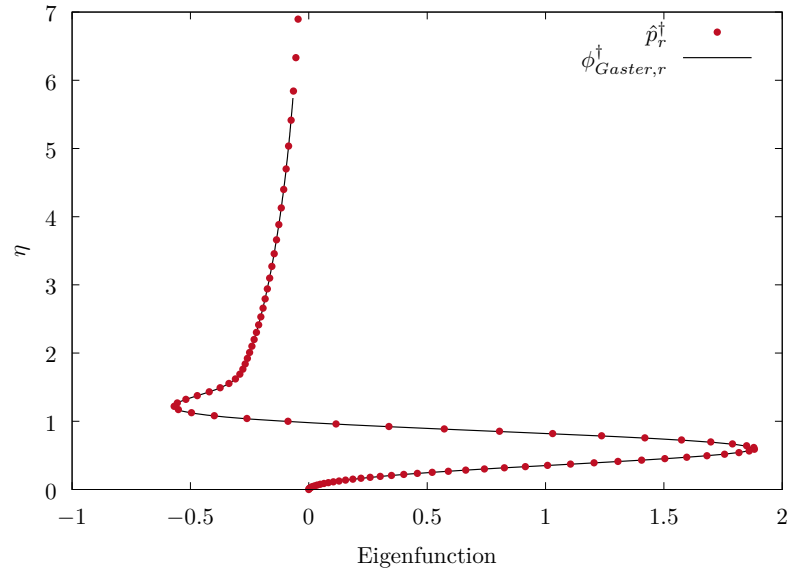


Figure 3.5: Adjoint eigenfunction validation of \hat{p}_r^\dagger for a Blasius profile with $\text{Re} = 725$, $\omega = 0.13$

3.9 Adjoint Sensitivity

Adjoint sensitivity has a second function distinct from simply finding eigenvalues. As Juniper shows in [18], if the right and left eigenfunctions are known, then the eigenvalue drift (or sensitivity to structural change) from a change to the input parameters can be computed at reduced computational effort. Luchini and Bottaro [19] give a thorough overview of these sensitivity fields in their 2013 paper. Consider a square matrix A , which can be decomposed into the following:

$$A = BCB^{-1} \quad (3.16)$$

where C is a diagonal matrix. It follows:

$$AB = BCB^{-1}B = BC \quad (3.17)$$

$$B^{-1}A = B^{-1}BCB^{-1} = CB^{-1} \quad (3.18)$$

This implies that the rows of B are the right eigenvectors of A , the columns of B^{-1} are the left eigenvectors, and the values in C are the corresponding eigenvalues. Stability eigenvalue problems tend to have the form $M\hat{v} - \hat{v}' = 0$ so the trial solution will take the form:

$$\begin{aligned} \hat{v} &= \chi e^{\lambda y} \\ \rightarrow \hat{v}' &= \lambda \chi e^{\lambda y} \\ \therefore A\hat{v} - \hat{v}' &= 0 \rightarrow A\chi = \lambda\chi \end{aligned}$$

Where χ is a right eigenvector of A , and λ is the corresponding eigenvalue. Now consider the case where a small change is made to A :

$$A \rightarrow A + \delta A \quad (3.19a)$$

$$\lambda \rightarrow \lambda + \delta\lambda \quad (3.19b)$$

$$\chi \rightarrow \chi + \delta\chi \quad (3.19c)$$

$$\chi^\dagger \rightarrow \chi^\dagger + \delta\chi^\dagger \quad (3.19d)$$

Here the left eigenvector χ^\dagger has been introduced, which arises from:

$$\chi^\dagger A = \chi \lambda \quad (3.20)$$

The system given in equation (3.19) satisfies:

$$(A + \delta A) (\chi + \delta \chi) = (\lambda + \delta \lambda) (\chi + \delta \chi)$$

For terms of the order δ :

$$\begin{aligned} ((\lambda - A) + (\lambda + \delta \lambda)) (\chi + \delta \chi) &= 0 \\ \rightarrow (\lambda - A) \delta \chi + (\delta \lambda - \delta A) \chi &= 0 \end{aligned}$$

Multiplying by the left eigenvector gives:

$$\chi^\dagger (\lambda - A) \delta \chi + \chi^\dagger (\delta \lambda - \delta A) \chi = 0$$

Which reduces the first term to zero because as seen in equation (3.20), $\chi^\dagger (\lambda - A) = 0$. This leaves:

$$\begin{aligned} \chi^\dagger (\delta \lambda - \delta A) \chi &= 0 \\ \chi^\dagger \delta \lambda \chi - \chi^\dagger \delta A \chi &= 0 \end{aligned}$$

And eigenvalue drift is given by:

$$\delta \lambda = \frac{\chi^\dagger \delta A \chi}{\chi^\dagger \chi} \quad (3.21)$$

So if a very small change to the structure of the problem is required the corresponding change in solution can be found using equation (3.21) at a significantly reduced computational cost. In fact this method promises as many eigenvalues as necessary¹, at the cost of solving only two matrix systems. This method is not implemented in Chapter 4, but is nevertheless an important part of the literature, and this example is useful in illustrating the terminological overlap in the field.

¹Assuming these secondary eigenvalues are only a small change away from the original one.

3.10 Categorising adjoint problems

This chapter has outlined two classes of problems where the adjoint formulation shows it has distinct uses. In Chapter 4 a third class of problems is discussed. In these the adjoint will be used to ensure that a certain set of equations has a non-trivial solution; the method of multiple scales is in this class. Taken together these classes of problems form a taxonomy, linked by the adjoint, but applied quite differently. This new way of more precisely describing the relationships between these classes of problems could be useful, especially as an introduction to the field.

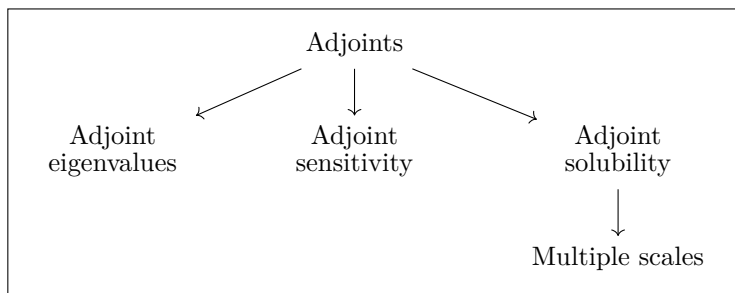


Figure 3.6: The taxonomy of adjoint problems

Chapter 4

Non-parallel Stability Theory and Transition Analysis

4.1 The Method of multiple scales

4.1.1 Derivation

This section presents the derivation of the multiple scales method, which provides a correction term to the result generated by linear stability. For brevity, many of the more tedious steps are omitted. A much more detailed derivation is included in Appendix A. Recall the dimensionless Navier-Stokes equations as stated in equations 2.8 (the incompressible formulation is used here, although compressible can be treated in the same way):

$$\frac{\partial u}{\partial x} + \frac{\partial v}{\partial y} + \frac{\partial w}{\partial z} = 0 \quad (4.1a)$$

$$\frac{\partial u}{\partial t} + u \frac{\partial u}{\partial x} + v \frac{\partial u}{\partial y} + w \frac{\partial u}{\partial z} = -\frac{\partial p}{\partial x} + \frac{1}{Re} \left(\frac{\partial^2 u}{\partial x^2} + \frac{\partial^2 u}{\partial y^2} + \frac{\partial^2 u}{\partial z^2} \right) \quad (4.1b)$$

$$\frac{\partial v}{\partial t} + u \frac{\partial v}{\partial x} + v \frac{\partial v}{\partial y} + w \frac{\partial v}{\partial z} = -\frac{\partial p}{\partial y} + \frac{1}{Re} \left(\frac{\partial^2 v}{\partial x^2} + \frac{\partial^2 v}{\partial y^2} + \frac{\partial^2 v}{\partial z^2} \right) \quad (4.1c)$$

$$\frac{\partial w}{\partial t} + u \frac{\partial w}{\partial x} + v \frac{\partial w}{\partial y} + w \frac{\partial w}{\partial z} = -\frac{\partial p}{\partial z} + \frac{1}{Re} \left(\frac{\partial^2 w}{\partial x^2} + \frac{\partial^2 w}{\partial y^2} + \frac{\partial^2 w}{\partial z^2} \right) \quad (4.1d)$$

Disturbance equations would usually be found by expressing the Navier-Stokes equations as the sum of a laminar base flow and a small disturbance ($u = U + \tilde{u}$ etc.) and linearising in disturbances. The parallel flow assumption usually equates wall-normal velocity, chordwise base flow derivatives, and spanwise base flow derivatives to zero. In this case however they are allowed to remain, but substituting V with ϵV , and inserting an ϵ next to the base flow derivatives in x and z . This ϵ accounts for the new assumption that these values are not zero, but change slowly enough that the separation of scales is possible. It can be thought of as a ratio of two important length scales, specifically the length scale over which wave behaviour varies significantly, and the length scale over which the boundary layer itself varies significantly. The actual value ϵ takes will therefore be some measure of the non-parallelism of the flow; it will be important for § 4.1.3 and is discussed in greater detail in § 4.1.3.1.

$$\frac{\partial \tilde{u}}{\partial x} + \frac{\partial \tilde{v}}{\partial y} + \frac{\partial \tilde{w}}{\partial z} = 0 \quad (4.2a)$$

$$\begin{aligned} \frac{\partial \tilde{u}}{\partial t} + U \frac{\partial \tilde{u}}{\partial x} + \epsilon \tilde{u} \frac{\partial U}{\partial x} + \epsilon V \frac{\partial \tilde{u}}{\partial y} + \tilde{v} \frac{\partial U}{\partial y} + W \frac{\partial \tilde{u}}{\partial z} + \epsilon \tilde{w} \frac{\partial U}{\partial z} = \\ -\frac{\partial \tilde{p}}{\partial x} + \frac{1}{Re} \left(\frac{\partial^2 \tilde{u}}{\partial x^2} + \frac{\partial^2 \tilde{u}}{\partial y^2} + \frac{\partial^2 \tilde{u}}{\partial z^2} \right) \end{aligned} \quad (4.2b)$$

$$\begin{aligned} \frac{\partial \tilde{v}}{\partial t} + U \frac{\partial \tilde{v}}{\partial x} + \epsilon^2 \tilde{u} \frac{\partial V}{\partial x} + \epsilon V \frac{\partial \tilde{v}}{\partial y} + \epsilon \tilde{v} \frac{\partial V}{\partial y} + W \frac{\partial \tilde{v}}{\partial z} + \epsilon^2 \tilde{w} \frac{\partial V}{\partial z} = \\ - \frac{\partial \tilde{p}}{\partial y} + \frac{1}{Re} \left(\frac{\partial^2 \tilde{v}}{\partial x^2} + \frac{\partial^2 \tilde{v}}{\partial y^2} + \frac{\partial^2 \tilde{v}}{\partial z^2} \right) \end{aligned} \quad (4.2c)$$

$$\begin{aligned} \frac{\partial \tilde{w}}{\partial t} + U \frac{\partial \tilde{w}}{\partial x} + \epsilon \tilde{u} \frac{\partial W}{\partial x} + \epsilon V \frac{\partial \tilde{w}}{\partial y} + \tilde{v} \frac{\partial W}{\partial y} + W \frac{\partial \tilde{w}}{\partial z} + \epsilon \tilde{w} \frac{\partial W}{\partial z} = \\ - \frac{\partial \tilde{p}}{\partial z} + \frac{1}{Re} \left(\frac{\partial^2 \tilde{w}}{\partial x^2} + \frac{\partial^2 \tilde{w}}{\partial y^2} + \frac{\partial^2 \tilde{w}}{\partial z^2} \right) \end{aligned} \quad (4.2d)$$

Using the expansion $\tilde{u} = \tilde{u}_0 + \epsilon \tilde{u}_1 + \epsilon^2 \tilde{u}_2 + \dots$ (and the same for \tilde{v} and \tilde{w}), the equations are expanded in the chordwise and spanwise directions, then split by similar powers of ϵ (it is also necessary to use derivative expansion as Nayfeh suggests [24]):

$$\frac{\partial \tilde{u}_0}{\partial x_0} + \frac{\partial \tilde{v}_0}{\partial y} + \frac{\partial \tilde{w}_0}{\partial z_0} = 0 \quad (4.3a)$$

$$\begin{aligned} \frac{\partial \tilde{u}_1}{\partial x_0} + \frac{\partial \tilde{v}_1}{\partial y} + \frac{\partial \tilde{w}_0}{\partial z_1} = \\ - \frac{\partial \tilde{u}_0}{\partial x_1} - \frac{\partial \tilde{w}_0}{\partial z_1} \end{aligned} \quad (4.3b)$$

$$\frac{\partial \tilde{u}_0}{\partial t} + U \frac{\partial \tilde{u}_0}{\partial x_0} + \tilde{v}_0 \frac{\partial U}{\partial y} + W \frac{\partial \tilde{u}_0}{\partial z_0} + \frac{\partial \tilde{p}_0}{\partial x_0} - \frac{1}{Re} \left(\frac{\partial^2 \tilde{u}_0}{\partial x_0^2} + \frac{\partial^2 \tilde{u}_0}{\partial y^2} + \frac{\partial^2 \tilde{u}_0}{\partial z_0^2} \right) = 0 \quad (4.3c)$$

$$\begin{aligned} \frac{\partial \tilde{u}_1}{\partial t} + U \frac{\partial \tilde{u}_1}{\partial x_0} + \tilde{v}_1 \frac{\partial U}{\partial y} + W \frac{\partial \tilde{u}_1}{\partial z_0} + \frac{\partial \tilde{p}_1}{\partial x_0} - \frac{1}{Re} \left(\frac{\partial^2 \tilde{u}_1}{\partial x_0^2} + \frac{\partial^2 \tilde{u}_1}{\partial y^2} + \frac{\partial^2 \tilde{u}_1}{\partial z_0^2} \right) = \\ \frac{1}{Re} \left(2 \frac{\partial^2 \tilde{u}_0}{\partial x_0 \partial x_1} + 2 \frac{\partial^2 \tilde{u}_0}{\partial z_0 \partial z_1} \right) - U \frac{\partial \tilde{u}_0}{\partial x_1} - \tilde{u}_0 \frac{\partial U}{\partial x_0} - V \frac{\partial \tilde{u}_0}{\partial y} - W \frac{\partial \tilde{u}_0}{\partial z_1} - \tilde{w}_0 \frac{\partial U}{\partial z_0} - \frac{\partial \tilde{p}_0}{\partial x_1} \end{aligned} \quad (4.3d)$$

$$\frac{\partial \tilde{v}_0}{\partial t} + U \frac{\partial \tilde{v}_0}{\partial x_0} + W \frac{\partial \tilde{v}_0}{\partial z_0} + \frac{\partial \tilde{p}_0}{\partial y} - \frac{1}{Re} \left(\frac{\partial^2 \tilde{v}_0}{\partial x_0^2} + \frac{\partial^2 \tilde{v}_0}{\partial y^2} + \frac{\partial^2 \tilde{v}_0}{\partial z_0^2} \right) = 0 \quad (4.3e)$$

$$\frac{\partial \tilde{v}_0}{\partial t} + U \frac{\partial \tilde{v}_0}{\partial x_0} + W \frac{\partial \tilde{v}_0}{\partial z_0} + \frac{\partial \tilde{p}_0}{\partial y} - \frac{1}{Re} \left(\frac{\partial^2 \tilde{v}_0}{\partial x_0^2} + \frac{\partial^2 \tilde{v}_0}{\partial y^2} + \frac{\partial^2 \tilde{v}_0}{\partial z_0^2} \right) = \quad (4.3f)$$

$$\frac{1}{Re} \left(2 \frac{\partial^2 \tilde{v}_0}{\partial x_0 \partial x_1} + 2 \frac{\partial^2 \tilde{v}_0}{\partial z_0 \partial z_1} \right) - U \frac{\partial \tilde{v}_0}{\partial x_1} - v_0 \frac{\partial V}{\partial y} - V \frac{\partial \tilde{v}_0}{\partial y} - W \frac{\partial \tilde{v}_0}{\partial z_1}$$

$$\frac{\partial \tilde{w}_0}{\partial t} + U \frac{\partial \tilde{w}_0}{\partial x_0} + \tilde{v}_0 \frac{\partial W}{\partial y} + W \frac{\partial \tilde{w}_0}{\partial z_0} + \frac{\partial \tilde{p}_0}{\partial z_0} - \frac{1}{Re} \left(\frac{\partial^2 \tilde{w}_0}{\partial x_0^2} + \frac{\partial^2 \tilde{w}_0}{\partial y^2} + \frac{\partial^2 \tilde{w}_0}{\partial z_0^2} \right) = 0 \quad (4.3g)$$

$$\begin{aligned} \frac{\partial \tilde{w}_1}{\partial t} + U \frac{\partial \tilde{w}_1}{\partial x_0} + \tilde{v}_1 \frac{\partial W}{\partial y} + W \frac{\partial \tilde{w}_1}{\partial z_0} + \frac{\partial \tilde{p}_1}{\partial z_0} - \frac{1}{Re} \left(\frac{\partial^2 \tilde{w}_1}{\partial x_0^2} + \frac{\partial^2 \tilde{w}_1}{\partial y^2} + \frac{\partial^2 \tilde{w}_1}{\partial z_0^2} \right) = \\ \frac{1}{Re} \left(2 \frac{\partial^2 \tilde{w}_0}{\partial x_0 \partial x_1} + 2 \frac{\partial^2 \tilde{w}_0}{\partial z_0 \partial z_1} \right) - U \frac{\partial \tilde{w}_0}{\partial x_1} - \tilde{w}_0 \frac{\partial W}{\partial x_0} - V \frac{\partial \tilde{w}_0}{\partial y} - W \frac{\partial \tilde{w}_0}{\partial z_1} - \tilde{w}_0 \frac{\partial W}{\partial z_0} - \frac{\partial \tilde{p}_0}{\partial z_1} \end{aligned} \quad (4.3h)$$

Assuming the disturbance behaves like a wave in the x_0 and z_0 directions, but allowing structure in x_1 , y , and z_1 , the following substitution is made: $\tilde{u} = \hat{u}(x_1, y, z_1) e^{i(\alpha x_0 + \beta z_0 - \omega t)}$. Resolving the derivatives and division through by $e^{i(\alpha x_0 + \beta z_0 - \omega t)}$ results in:

$$i\alpha\hat{u}_0 + \hat{v}'_0 + i\beta\hat{w}_0 = 0 \quad (4.4a)$$

$$i\alpha\hat{u}_1 + \hat{v}'_1 + i\beta\hat{w}_1 = -\frac{\partial\hat{u}_0}{\partial x_1} - \frac{\partial\hat{w}_0}{\partial z_1} \quad (4.4b)$$

$$-i\omega\hat{u}_0 + i\alpha U\hat{u}_0 + U'\hat{v}_0 + i\beta W\hat{u}_0 + i\alpha\hat{p}_0 - \frac{1}{Re}(-\alpha^2\hat{u}_0 + \hat{u}''_0 - \beta^2\hat{u}_0) = 0 \quad (4.4c)$$

$$-i\omega\hat{u}_1 + i\alpha U\hat{u}_1 + U'\hat{v}_1 + i\beta W\hat{u}_1 + i\alpha\hat{p}_1 - \frac{1}{Re}(-\alpha^2\hat{u}_1 + \hat{u}''_1 - \beta^2\hat{u}_1) = \frac{1}{Re}\left(2i\alpha\frac{\partial\hat{u}_0}{\partial x_1} + 2i\beta\frac{\partial\hat{u}_0}{\partial z_1}\right) - U\frac{\partial\hat{u}_0}{\partial x_1} - \frac{\partial U}{\partial x_0}\hat{u}_0 - V\hat{u}'_0 - W\frac{\partial\hat{u}_0}{\partial x_1} - \frac{\partial U}{\partial z_0}\hat{w}_0 - \frac{\partial\hat{p}_0}{\partial x_1} \quad (4.4d)$$

$$-i\omega\hat{v}_0 + i\alpha U\hat{v}_0 + i\beta W\hat{v}_0 + \hat{p}'_0 - \frac{1}{Re}(-\alpha^2\hat{v}_0 + \hat{v}''_0 - \beta^2\hat{v}_0) = 0 \quad (4.4e)$$

$$-i\omega\hat{v}_1 + i\alpha U\hat{v}_1 + i\beta W\hat{v}_1 + \hat{p}'_1 - \frac{1}{Re}(-\alpha^2\hat{v}_1 + \hat{v}''_1 - \beta^2\hat{v}_1) = \frac{1}{Re}\left(2i\alpha\frac{\partial\hat{v}_0}{\partial x_1} + 2i\beta\frac{\partial\hat{v}_0}{\partial z_1}\right) - U\frac{\partial\hat{v}_0}{\partial x_1} - W\frac{\partial\hat{v}_0}{\partial z_1} - V'\hat{v}_0 - V\hat{v}'_0 \quad (4.4f)$$

$$-i\omega\hat{w}_0 + i\alpha U\hat{w}_0 + W'\hat{v}_0 + i\beta W\hat{w}_0 + i\beta\hat{p}_0 - \frac{1}{Re}(-\alpha^2\hat{w}_0 + \hat{w}''_0 - \beta^2\hat{w}_0) = 0 \quad (4.4g)$$

$$-i\omega\hat{w}_1 + i\alpha U\hat{w}_1 + W'\hat{v}_1 + i\beta W\hat{w}_1 + i\beta\hat{p}_1 - \frac{1}{Re}(-\alpha^2\hat{w}_1 + \hat{w}''_1 - \beta^2\hat{w}_1) = \frac{1}{Re}\left(2i\alpha\frac{\partial\hat{v}_0}{\partial x_1} + 2i\beta\frac{\partial\hat{v}_0}{\partial z_1}\right) - U\frac{\partial\hat{w}_0}{\partial x_1} - \hat{u}_0\frac{\partial W}{\partial x_0} - V\frac{\partial\hat{w}_0}{\partial y} - W\frac{\partial\hat{w}_0}{\partial x_1} - \hat{w}_0\frac{\partial W}{\partial z_0} - \frac{\partial\hat{p}_0}{\partial z_1} \quad (4.4h)$$

Two systems of ODEs can be created by introducing new variables $\hat{\tau}_u$, and $\hat{\tau}_w$, then substituting the wall-normal derivatives of equation (4.4a) and equation (4.4b):

$$\hat{\tau}_{u0} = \hat{u}'_0 \quad (4.5a)$$

$$\hat{\tau}_{u1} = \hat{u}'_1 \quad (4.5b)$$

$$\hat{\tau}_{w0} = \hat{w}'_0 \quad (4.5c)$$

$$\hat{\tau}_{w1} = \hat{w}'_1 \quad (4.5d)$$

$$i\alpha\hat{u}_0 + \hat{\tau}_{u0} + i\beta\hat{w}_0 = 0 \quad (4.5e)$$

$$i\alpha\hat{u}_1 + \hat{\tau}_{u1} + i\beta\hat{w}_1 = -\frac{\partial\hat{u}_0}{\partial x_1} - \frac{\partial\hat{w}_0}{\partial z_1} \quad (4.5f)$$

$$-i\omega\hat{u}_0 + i\alpha U\hat{u}_0 + U'\hat{v}_0 + i\beta W\hat{u}_0 + i\alpha\hat{p}_0 - \frac{1}{Re}(-\alpha^2\hat{u}_0 + \hat{\tau}'_{u0} - \beta^2\hat{u}_0) = 0 \quad (4.5g)$$

$$\begin{aligned} & -i\omega\hat{u}_1 + i\alpha U\hat{u}_1 + U'\hat{v}_1 + i\beta W\hat{u}_1 + i\alpha\hat{p}_1 - \frac{1}{Re}(-\alpha^2\hat{u}_1 + \hat{\tau}'_{u1} - \beta^2\hat{u}_1) = \\ & \frac{1}{Re} \left(2i\alpha \frac{\partial\hat{u}_0}{\partial x_1} + 2i\beta \frac{\partial\hat{u}_0}{\partial z_1} \right) - U \frac{\partial\hat{u}_0}{\partial x_1} - \frac{\partial U}{\partial x_0} \hat{u}_0 - V\hat{\tau}_{u0} - W \frac{\partial\hat{u}_0}{\partial z_1} - \frac{\partial U}{\partial z_0} \hat{w}_0 - \frac{\partial\hat{p}_0}{\partial x_1} \end{aligned} \quad (4.5h)$$

$$-i\omega\hat{v}_0 + i\alpha U\hat{v}_0 + i\beta W\hat{v}_0 + \hat{p}'_0 - \frac{1}{Re}(-\alpha^2\hat{v}_0 - i\alpha\hat{\tau}_{u0} - i\beta\hat{\tau}_{w0} - \beta^2\hat{v}_0) = 0 \quad (4.5i)$$

$$\begin{aligned} & -i\omega\hat{v}_1 + i\alpha U\hat{v}_1 + i\beta W\hat{v}_1 + \hat{p}'_1 - \frac{1}{Re}(-\alpha^2\hat{v}_1 - i\alpha\hat{\tau}_{u1} - i\beta\hat{\tau}_{w1} - \beta^2\hat{v}_1) = \\ & \frac{1}{Re} \left(2i\alpha \frac{\partial\hat{v}_0}{\partial x_1} + 2i\beta \frac{\partial\hat{v}_0}{\partial z_1} + \frac{\partial\hat{u}_0}{\partial x_1} + \frac{\partial\hat{w}_0}{\partial z_1} \right) - U \frac{\partial\hat{v}_0}{\partial x_1} - W \frac{\partial\hat{v}_0}{\partial z_1} - V'\hat{v}_0 + i\alpha V u_0 + i\beta V w_0 \end{aligned} \quad (4.5j)$$

$$-i\omega\hat{w}_0 + i\alpha U\hat{w}_0 + W'\hat{v}_0 + i\beta W\hat{w}_0 + i\beta\hat{p}_0 - \frac{1}{Re}(-\alpha^2\hat{w}_0 + \hat{\tau}'_{w0} - \beta^2\hat{w}_0) = 0 \quad (4.5k)$$

$$\begin{aligned} & -i\omega\hat{w}_1 + i\alpha U\hat{w}_1 + W'\hat{v}_1 + i\beta W\hat{w}_1 + i\beta\hat{p}_1 - \frac{1}{Re}(-\alpha^2\hat{w}_1 + \hat{\tau}'_{w1} - \beta^2\hat{w}_1) = \\ & \frac{1}{Re} \left(2i\alpha \frac{\partial\hat{v}_0}{\partial x_1} + 2i\beta \frac{\partial\hat{v}_0}{\partial z_1} \right) - U \frac{\partial\hat{w}_0}{\partial x_1} - \hat{u}_0 \frac{\partial W}{\partial x_0} - V\hat{\tau}_{w0} - W \frac{\partial\hat{w}_0}{\partial z_1} - \hat{w}_0 \frac{\partial W}{\partial z_0} - \frac{\partial\hat{p}_0}{\partial z_1} \end{aligned} \quad (4.5l)$$

Which can be expressed as matrices:

$$A = \begin{bmatrix} 0 & a_{12} & 0 & 0 & ReU' & iRe\alpha \\ 1 & 0 & 0 & 0 & 0 & 0 \\ 0 & 0 & 0 & a_{12} & ReW' & iRe\beta \\ 0 & 0 & 1 & 0 & 0 & 0 \\ 0 & -i\alpha & 0 & -i\beta & 0 & 0 \\ -\frac{i\alpha}{Re} & 0 & -\frac{i\beta}{Re} & 0 & \frac{a_{12}}{Re} & 0 \end{bmatrix} \quad (4.6a)$$

$$a_{12} = iRe(\alpha U + \beta W - \omega) + (\alpha^2 + \beta^2) \quad (4.6b)$$

$$b = \begin{bmatrix} 2i\alpha \frac{\partial\hat{u}_0}{\partial x_1} + 2i\beta \frac{\partial\hat{u}_0}{\partial z_1} + Re \left(-U \frac{\partial\hat{u}_0}{\partial x_1} - \frac{\partial U}{\partial x_0} \hat{u}_0 - V\hat{\tau}_{u0} - W \frac{\partial\hat{u}_0}{\partial z_1} - \frac{\partial U}{\partial z_0} \hat{w}_0 - \frac{\partial\hat{p}_0}{\partial x_1} \right) \\ 2i\alpha \frac{\partial\hat{v}_0}{\partial x_1} + 2i\beta \frac{\partial\hat{v}_0}{\partial z_1} + Re \left(-U \frac{\partial\hat{v}_0}{\partial x_1} - \hat{u}_0 \frac{\partial W}{\partial x_0} - V\hat{\tau}_{w0} - W \frac{\partial\hat{v}_0}{\partial z_1} - \hat{w}_0 \frac{\partial W}{\partial z_0} - \frac{\partial\hat{p}_0}{\partial z_1} \right) \\ 0 \\ -\frac{1}{Re} \left(2i\alpha \frac{\partial\hat{v}_0}{\partial x_1} + 2i\beta \frac{\partial\hat{v}_0}{\partial z_1} + \frac{\partial\hat{u}_0}{\partial x_1} + \frac{\partial\hat{w}_0}{\partial z_1} \right) + U \frac{\partial\hat{v}_0}{\partial x_1} + W \frac{\partial\hat{v}_0}{\partial z_1} + V'\hat{v}_0 - i\alpha V u_0 - i\beta V w_0 \end{bmatrix} \quad (4.6c)$$

$$\hat{q}_{0,1} = \begin{bmatrix} \hat{\tau}_u \\ \hat{u} \\ \hat{\tau}_w \\ \hat{w} \\ \hat{v} \\ \hat{p} \end{bmatrix}_{0,1} \quad (4.6d)$$

$$A\hat{q}_0 - \hat{q}'_0 = 0 \quad (4.7a)$$

$$A\hat{q}_1 - \hat{q}'_1 = b \quad (4.7b)$$

The vector b can be rewritten by collecting derivatives of \hat{q}_0 in x_1 and z_1 :

$$b = b_1 + b_2 + b_3 \quad (4.8)$$

$$b_1 = \begin{bmatrix} 2i\alpha \frac{\partial \hat{u}_0}{\partial x_1} + Re \left(-U \frac{\partial \hat{u}_0}{\partial x_1} - \frac{\partial \hat{p}_0}{\partial x_1} \right) \\ 0 \\ 2i\alpha \frac{\partial \hat{v}_0}{\partial x_1} - ReU \frac{\partial \hat{w}_0}{\partial x_1} \\ 0 \\ \frac{\partial \hat{u}_0}{\partial x_1} \\ -\frac{1}{Re} \left(2i\alpha \frac{\partial \hat{v}_0}{\partial x_1} + \frac{\partial \hat{u}_0}{\partial x_1} \right) + U \frac{\partial \hat{v}_0}{\partial x_1} \end{bmatrix} = \begin{bmatrix} 0 & 2i\alpha - ReU & 0 & 0 & 0 & -Re \\ 0 & 0 & 0 & 0 & 0 & 0 \\ 0 & 0 & 0 & 2i\alpha - ReU & 0 & 0 \\ 0 & 0 & 0 & 0 & 0 & 0 \\ 0 & 1 & 0 & 0 & 0 & 0 \\ \frac{1}{Re} & 0 & 0 & 0 & U - \frac{2i\alpha}{Re} & 0 \end{bmatrix} \frac{\partial \hat{q}_0}{\partial x_1} \quad (4.9)$$

$$b_2 = \begin{bmatrix} 2i\beta \frac{\partial \hat{u}_0}{\partial z_1} - ReW \frac{\partial \hat{u}_0}{\partial z_1} \\ 0 \\ 2i\beta \frac{\partial \hat{v}_0}{\partial z_1} + Re \left(-W \frac{\partial \hat{w}_0}{\partial z_1} - \frac{\partial \hat{p}_0}{\partial z_1} \right) \\ 0 \\ \frac{\partial \hat{u}_0}{\partial z_1} \\ -\frac{1}{Re} \left(2i\beta \frac{\partial \hat{v}_0}{\partial z_1} + \frac{\partial \hat{w}_0}{\partial z_1} \right) + W \frac{\partial \hat{v}_0}{\partial z_1} \end{bmatrix} = \begin{bmatrix} 0 & 2i\beta - ReW & 0 & 0 & 0 & 0 \\ 0 & 0 & 0 & 0 & 0 & 0 \\ 0 & 0 & 0 & 2i\beta - ReW & 0 & -Re \\ 0 & 0 & 0 & 0 & 0 & 0 \\ 0 & 0 & 0 & 1 & 0 & 0 \\ 0 & 0 & \frac{1}{Re} & 0 & W - \frac{2i\beta}{Re} & 0 \end{bmatrix} \frac{\partial \hat{q}_0}{\partial z_1} \quad (4.10)$$

$$b_3 = \begin{bmatrix} +Re \left(-\frac{\partial U}{\partial x_0} \hat{u}_0 - V \hat{\tau}_{u0} - \frac{\partial U}{\partial z_0} \hat{w}_0 \right) \\ 0 \\ +Re \left(-\frac{\partial W}{\partial x_0} \hat{u}_0 - V \hat{\tau}_{w0} - \frac{\partial W}{\partial z_0} \hat{w}_0 \right) \\ 0 \\ 0 \\ V' \hat{v}_0 - i\alpha V u_0 - i\beta V w_0 \end{bmatrix} = \begin{bmatrix} -ReV & -Re \frac{\partial U}{\partial x_0} & 0 & -Re \frac{\partial U}{\partial z_0} & 0 & 0 \\ 0 & 0 & 0 & 0 & 0 & 0 \\ 0 & -Re \frac{\partial W}{\partial x_0} & -ReV & -Re \frac{\partial W}{\partial z_0} & 0 & 0 \\ 0 & 0 & 0 & 0 & 0 & 0 \\ 0 & 0 & 0 & 0 & 0 & 0 \\ 0 & -i\alpha V & 0 & -i\beta V & V' & 0 \end{bmatrix} \hat{q}_0 \quad (4.11)$$

Solving equation (4.7a) results in an eigenfunction, whose shape is significant but with normalised magnitude. Since it is not the true \hat{q}_0 , it is renamed \hat{q}_n . It can however be related to the magnitude of the actual zero order disturbance by a complex magnitude distribution: $\hat{q}_0 = Q(x_1, z_1)\hat{q}_n(x_1, y, z_1)$. In order for equation (4.7b) to have a non-trivial solution, the non-homogeneous terms must be orthogonal to the solution of the adjoint equation [33]. This defines the third class of adjoint problem discussed in §3.10, and gives the solubility condition ($\int_0^\infty b \cdot \hat{q}^\dagger d\eta = 0$). The adjoint eigenfunction is labelled as \hat{q}^\dagger , and is also discussed in Chapter 3. Assuming that the

correct magnitude of the wave is now known i.e. substituting the new \hat{q}_0 into the equations leads to the equation:

$$\int_0^\infty b \cdot \hat{q}^\dagger dy = \int_0^\infty b_3 Q \hat{q}_n \cdot \hat{q}^\dagger + b_1 \frac{\partial Q \hat{q}_n}{\partial x_1} \cdot \hat{q}^\dagger + b_2 \frac{\partial Q \hat{q}_n}{\partial z_1} \cdot \hat{q}^\dagger dy = 0 \quad (4.12)$$

This is a PDE for Q in x_1 , and z_1 . By using the product rule can it be expressed:

$$\begin{aligned} Q \int_0^\infty b_3 \hat{q}_n \cdot \hat{q}^\dagger dy + Q \int_0^\infty b_1 \frac{\partial \hat{q}_n}{\partial x_1} \cdot \hat{q}^\dagger dy + \frac{\partial Q}{\partial x_1} \int_0^\infty b_1 \hat{q}_n \cdot \hat{q}^\dagger dy \\ + Q \int_0^\infty b_2 \frac{\partial \hat{q}_n}{\partial z_1} \cdot \hat{q}^\dagger dy + \frac{\partial Q}{\partial z_1} \int_0^\infty b_2 \hat{q}_n \cdot \hat{q}^\dagger dy = 0 \end{aligned} \quad (4.13)$$

or as:

$$LQ + M \frac{\partial Q}{\partial x_1} + N \frac{\partial Q}{\partial z_1} = 0 \quad (4.14)$$

where:

$$\begin{aligned} L &= \int_0^\infty b_3 \hat{q}_n \cdot \hat{q}^\dagger dy + \int_0^\infty b_1 \frac{\partial \hat{q}_n}{\partial x_1} \cdot \hat{q}^\dagger dy + \int_0^\infty b_2 \frac{\partial \hat{q}_n}{\partial z_1} \cdot \hat{q}^\dagger dy \\ M &= \int_0^\infty b_1 \hat{q}_n \cdot \hat{q}^\dagger dy \\ N &= \int_0^\infty b_2 \hat{q}_n \cdot \hat{q}^\dagger dy \end{aligned}$$

whose solution is simply:

$$Q = Q_0 e^{-\frac{1}{2} \left(\frac{L}{M} x_1 + \frac{L}{N} z_1 \right)} \quad (4.15)$$

4.1.1.1 Eigenfunction derivatives

Solving equation (4.15) requires knowledge of not only the eigenfunction, but also of its derivatives in the streamwise and spanwise directions. In the LST procedure these will be generated at a number of streamwise locations. On first appearances it may seem that using a finite difference between two locations would give an appropriate solution for $\partial \hat{q} / \partial x$, however this is not the case. Each solution is scaled locally, and there are no assurances that the scalings correspond to each other at all, in fact it should be surprising if they did. Instead to calculate the derivatives the

following formulation is derived:

$$\begin{aligned}
(A - \partial_y) \hat{q} &= 0 \\
\partial_x (A - \partial_y) \hat{q} &= 0 \\
\partial_x (A\hat{q} - \partial_y \hat{q}) &= 0 \\
\partial_x (A\hat{q}) - \partial_x \partial_y \hat{q} &= 0 \\
A\partial_x \hat{q} + \hat{q}\partial_x A - \partial_x \partial_y \hat{q} &= 0 \\
(A - \partial_y) \partial_x \hat{q} &= -\partial_x A\hat{q}
\end{aligned} \tag{4.16}$$

This formulation allows us to calculate derivatives using a non homogeneous version of the linear stability equations, using only information which is already known, and which is all locally scaled.

4.1.2 Comparison with Gaster's formulation

In order to compare results with Gaster, it must first be shown that the two formulations are equivalent. The initial step is to show the terms used in the present analysis in the form used by Gaster in [12]. Beginning with the linearised Navier-Stokes equations in 2D:

$$\frac{\partial \tilde{u}}{\partial x} + \frac{\partial \tilde{v}}{\partial y} = 0 \tag{4.17a}$$

$$\frac{\partial \tilde{u}}{\partial t} + U \frac{\partial \tilde{u}}{\partial x} + \tilde{u} \frac{\partial U}{\partial x} + V \frac{\partial \tilde{u}}{\partial y} + \tilde{v} \frac{\partial U}{\partial y} = -\frac{\partial \tilde{p}}{\partial x} + \frac{1}{Re} \left(\frac{\partial^2 \tilde{u}}{\partial x^2} + \frac{\partial^2 \tilde{u}}{\partial y^2} \right) \tag{4.17b}$$

$$\frac{\partial \tilde{v}}{\partial t} + U \frac{\partial \tilde{v}}{\partial x} + \tilde{u} \frac{\partial V}{\partial x} + V \frac{\partial \tilde{v}}{\partial y} + \tilde{v} \frac{\partial V}{\partial y} = -\frac{\partial \tilde{p}}{\partial y} + \frac{1}{Re} \left(\frac{\partial^2 \tilde{v}}{\partial x^2} + \frac{\partial^2 \tilde{v}}{\partial y^2} \right) \tag{4.17c}$$

These are then assumed to follow a quasi-parallel behaviour, and certain terms are deemed small:

$$\frac{\partial \tilde{u}}{\partial x} + \frac{\partial \tilde{v}}{\partial y} = 0 \tag{4.18a}$$

$$\frac{\partial \tilde{u}}{\partial t} + U \frac{\partial \tilde{u}}{\partial x} + \epsilon \tilde{u} \frac{\partial U}{\partial x} + \epsilon V \frac{\partial \tilde{u}}{\partial y} + \tilde{v} \frac{\partial U}{\partial y} = -\frac{\partial \tilde{p}}{\partial x} + \frac{1}{Re} \left(\frac{\partial^2 \tilde{u}}{\partial x^2} + \frac{\partial^2 \tilde{u}}{\partial y^2} \right) \tag{4.18b}$$

$$\frac{\partial \tilde{v}}{\partial t} + U \frac{\partial \tilde{v}}{\partial x} + \epsilon^2 \tilde{u} \frac{\partial V}{\partial x} + \epsilon V \frac{\partial \tilde{v}}{\partial y} + \epsilon \tilde{v} \frac{\partial V}{\partial y} = -\frac{\partial \tilde{p}}{\partial y} + \frac{1}{Re} \left(\frac{\partial^2 \tilde{v}}{\partial x^2} + \frac{\partial^2 \tilde{v}}{\partial y^2} \right) \tag{4.18c}$$

The stream function ($\tilde{u} = \partial\psi/\partial y$, $\tilde{v} = -\partial\psi/\partial x$) is used:

$$\frac{\partial^2\psi}{\partial y\partial t} + U\frac{\partial^2\psi}{\partial x\partial y} + \epsilon\frac{\partial\psi}{\partial y}\frac{\partial U}{\partial x} + \epsilon V\frac{\partial^2\psi}{\partial y^2} - \frac{\partial\psi}{\partial x}\frac{\partial U}{\partial y} = -\frac{\partial\tilde{p}}{\partial x} + \frac{1}{Re}\left(\frac{\partial^3\psi}{x^2y} + \frac{\partial^3\psi}{y^3}\right) \quad (4.19a)$$

$$-\frac{\partial^2\psi}{\partial x\partial t} - U\frac{\partial^2\psi}{\partial x^2} + \epsilon^2\frac{\partial\psi}{\partial y}\frac{\partial V}{\partial x} - \epsilon V\frac{\partial^2\psi}{\partial x\partial y} - \epsilon\frac{\partial\psi}{\partial x}\frac{\partial V}{\partial y} = -\frac{\partial\tilde{p}}{\partial y} - \frac{1}{Re}\left(\frac{\partial^3\psi}{x^3} + \frac{\partial^3\psi}{xy^2}\right) \quad (4.19b)$$

These equations are cross-differentiated to force pressure terms into equality and subtracted to eliminate them altogether:

$$\begin{aligned} & \frac{\partial^3\psi}{\partial y^2t} + \frac{\partial^3\psi}{\partial x^2t} - \frac{\partial^2U}{\partial y^2}\frac{\partial\psi}{\partial x} + U\frac{\partial^3\psi}{\partial xy^2} \\ & + U\frac{\partial^3\psi}{\partial x^3} + \epsilon\frac{\partial U}{\partial x}\frac{\partial^2\psi}{\partial x^2} + \epsilon\frac{\partial^2U}{\partial xy}\frac{\partial\psi}{\partial y} + \epsilon\frac{\partial U}{\partial x}\frac{\partial^2\psi}{\partial y^2} \\ & + \epsilon V\frac{\partial^3\psi}{\partial y^3} + \epsilon V\frac{\partial^3\psi}{\partial x^2y} + \epsilon\frac{\partial V}{\partial y}\frac{\partial^2\psi}{\partial y^2} + \epsilon\frac{\partial V}{\partial y}\frac{\partial^2\psi}{\partial x^2} \\ & - \frac{1}{Re}\left(2\frac{\partial^4\psi}{\partial x^2y^2} + \frac{\partial^4\psi}{\partial x^4} + \frac{\partial^4\psi}{\partial y^4}\right) = 0 \end{aligned} \quad (4.20)$$

and then expanded into multiple scales:

$$\begin{aligned} & \frac{\partial^3\psi_0}{\partial y^2t} + \epsilon\frac{\partial^3\psi_1}{\partial y^2t} + \frac{\partial^3\psi_0}{\partial x_0^2t} + \epsilon\frac{\partial^3\psi_1}{\partial x_0^2t} \\ & + 2\epsilon\frac{\partial^3\psi_0}{\partial x_0x_1t} - \frac{\partial^2U}{\partial y^2}\frac{\partial\psi_0}{\partial x_0} - \epsilon\frac{\partial^2U}{\partial y^2}\frac{\partial\psi_1}{\partial x_0} - \epsilon\frac{\partial^2U}{\partial y^2}\frac{\partial\psi_0}{\partial x_1} \\ & + U\frac{\partial^3\psi_0}{\partial x_0y^2} + \epsilon U\frac{\partial^3\psi_1}{\partial x_0y^2} + \epsilon U\frac{\partial^3\psi_0}{\partial x_1y^2} + U\frac{\partial^3\psi_0}{\partial x_0^3} \\ & + \epsilon U\frac{\partial^3\psi_1}{\partial x_0^3} + 3\epsilon U\frac{\partial^3\psi_0}{\partial x_0^2x_1} + \epsilon\frac{\partial U}{\partial x_0}\frac{\partial^2\psi_0}{\partial x_0^2} + \epsilon\frac{\partial^2U}{\partial x_0y}\frac{\partial\psi_0}{\partial y} \\ & + \epsilon\frac{\partial U}{\partial x_0}\frac{\partial^2\psi_0}{\partial y^2} + \epsilon V\frac{\partial^3\psi_0}{\partial y^3} + \epsilon V\frac{\partial^3\psi_0}{\partial x_0^2y} + \epsilon\frac{\partial V}{\partial y}\frac{\partial^2\psi_0}{\partial y^2} + \epsilon\frac{\partial V}{\partial y}\frac{\partial^2\psi_0}{\partial x_0^2} \\ & - \frac{1}{Re}\left(2\frac{\partial^4\psi_0}{\partial x_0^2y^2} + 2\epsilon\frac{\partial^4\psi_1}{\partial x_0^2y^2} + 4\epsilon\frac{\partial^4\psi_0}{\partial x_0x_1y^2} + \frac{\partial^4\psi_0}{\partial x_0^4} + \epsilon\frac{\partial^4\psi_1}{\partial x_0^4} + 4\epsilon\frac{\partial^4\psi_0}{\partial x_0^3x_1} + \frac{\partial^4\psi_0}{\partial y^4} + \epsilon\frac{\partial^4\psi_1}{\partial y^4}\right) = 0 \end{aligned} \quad (4.21)$$

and by separating the scales (similar powers of ϵ):

$$\frac{\partial^3\psi_0}{\partial y^2t} + \frac{\partial^3\psi_0}{\partial x_0^2t} - \frac{\partial^2U}{\partial y^2}\frac{\partial\psi_0}{\partial x_0} + U\frac{\partial^3\psi_0}{\partial x_0y^2} + U\frac{\partial^3\psi_0}{\partial x_0^3} - \frac{1}{Re}\left(2\frac{\partial^4\psi_0}{\partial x_0^2y^2} + \frac{\partial^4\psi_0}{\partial x_0^4} + \frac{\partial^4\psi_0}{\partial y^4}\right) = 0 \quad (4.22a)$$

$$\begin{aligned}
& \frac{\partial^3 \psi_1}{\partial y^2 t} + \frac{\partial^3 \psi_1}{\partial x_0^2 t} - \frac{\partial^2 U}{\partial y^2} \frac{\partial \psi_1}{\partial x_0} + U \frac{\partial^3 \psi_1}{\partial x_0 y^2} + U \frac{\partial^3 \psi_1}{\partial x_0^3} - \frac{1}{Re} \left(2 \frac{\partial^4 \psi_1}{\partial x_0^2 y^2} + \frac{\partial^4 \psi_1}{\partial x_0^4} + \frac{\partial^4 \psi_1}{\partial y^4} \right) \\
& + 2 \frac{\partial^3 \psi_0}{\partial x_0 x_1 t} - \frac{\partial^2 U}{\partial y^2} \frac{\partial \psi_0}{\partial x_1} + U \frac{\partial^3 \psi_0}{\partial x_1 y^2} + 3U \frac{\partial^3 \psi_0}{\partial x_0^2 x_1} \\
& + \frac{\partial U}{\partial x_0} \frac{\partial^2 \psi_0}{\partial x_0^2} + \frac{\partial^2 U}{\partial x_0 y} \frac{\partial \psi_0}{\partial y} + \frac{\partial U}{\partial x_0} \frac{\partial^2 \psi_0}{\partial y^2} \\
& + V \frac{\partial^3 \psi_0}{\partial y^3} + V \frac{\partial^3 \psi_0}{\partial x_0^2 y} + \frac{\partial V}{\partial y} \frac{\partial^2 \psi_0}{\partial y^2} + \frac{\partial V}{\partial y} \frac{\partial^2 \psi_0}{\partial x_0^2} \\
& - \frac{1}{Re} \left(+4 \frac{\partial^4 \psi_0}{\partial x_0 x_1 y^2} + 4 \frac{\partial^4 \psi_0}{\partial x_0^3 x_1} \right) = 0
\end{aligned} \tag{4.22b}$$

or:

$$-iRe\omega\phi_0'' + iRe\alpha^2\omega\phi_0 - iReU''\alpha\phi_0 + iReU\alpha\phi_0'' - iReU\alpha^3\phi_0 - 2\alpha^2\phi_0'' + \alpha^4\phi_0 + \phi_0'''' = 0 \tag{4.23a}$$

$$\begin{aligned}
& -iRe\omega\phi_1'' + iRe\alpha^2\omega\phi_1 - iReU''\alpha\phi_1 + iReU\alpha\phi_1'' - iReU\alpha^3\phi_1 - 2\alpha^2\phi_1'' + \alpha^4\phi_1 + \phi_1'''' \\
& + ReV\phi_0'''' + Re\frac{\partial U}{\partial x_0}\phi_0'' + ReV'\phi_0'' + Re\frac{\partial U'}{\partial x_0}\phi_0' - ReV\alpha^2\phi_0' - Re\frac{\partial U}{\partial x_0}\alpha^2\phi_0 - ReV'\alpha^2\phi_0 \\
& + ReU\frac{\partial\phi_0''}{\partial x_1} - 4i\alpha\frac{\partial\phi_0''}{\partial x_1} + 2Re\alpha\omega\frac{\partial\phi_0}{\partial x_1} - ReU''\frac{\partial\phi_0}{\partial x_1} - 3ReU\alpha^2\frac{\partial\phi_0}{\partial x_1} + 4i\alpha^3\frac{\partial\phi_0}{\partial x_1} = 0
\end{aligned} \tag{4.23b}$$

A similar procedure can be carried out on the Orr-Sommerfeld equation (equation (2.5)) to show equivalence. The Orr-Sommerfeld equation states:

$$\phi'''' - 2\alpha^2\phi'' + \alpha^4\phi = iRe(\alpha U - \omega)(\phi'' - \alpha^2\phi) - iRe\alpha U''\phi \tag{4.24}$$

In order to expand correctly the following must be included:

$$\phi \longrightarrow \phi_0 + \epsilon\phi_1 \tag{4.25}$$

$$\frac{\partial}{\partial x} \longrightarrow \frac{\partial}{\partial x_0} + \epsilon\frac{\partial}{\partial x_1} \tag{4.26}$$

Expanding ϕ is simple, however, no derivatives in x remain, since they were all separated utilising the wavelike properties of the disturbance. In their place stand powers of $i\alpha$ equivalent to the orders of the x derivatives which were there beforehand. This allows construction of a map to

generate the expanded terms:

$$\begin{aligned}
i\alpha &\longrightarrow \frac{\partial}{\partial x} \longrightarrow \frac{\partial}{\partial x_0} + \epsilon \frac{\partial}{\partial x_1} \longrightarrow i\alpha + \epsilon \frac{\partial}{\partial x_1} \\
i^2\alpha^2 &\longrightarrow \frac{\partial^2}{\partial x^2} \longrightarrow \frac{\partial^2}{\partial x_0^2} + 2\epsilon \frac{\partial}{\partial x_0 x_1} \longrightarrow -\alpha^2 + 2i\alpha\epsilon \frac{\partial}{\partial x_1} \\
i^3\alpha^3 &\longrightarrow \frac{\partial^3}{\partial x^3} \longrightarrow \frac{\partial^3}{\partial x_0^3} + 3\epsilon \frac{\partial}{\partial x_0^2 x_1} \longrightarrow -i\alpha^3 + 3i\alpha^2\epsilon \frac{\partial}{\partial x_1} \\
i^4\alpha^4 &\longrightarrow \frac{\partial^4}{\partial x^4} \longrightarrow \frac{\partial^4}{\partial x_0^4} + 4\epsilon \frac{\partial}{\partial x_0^3 x_1} \longrightarrow \alpha^4 + 4i\alpha^3\epsilon \frac{\partial}{\partial x_1}
\end{aligned}$$

Now the OSE (equation 4.24) is expanded:

$$\phi'''' - 2\alpha^2\phi'' + \alpha^4\phi = i\alpha ReU\phi'' - iRe\omega\phi'' - i\alpha^3 ReU\phi + i\alpha^2\omega Re\phi - iRe\alpha U''\phi \quad (4.27)$$

Using the aforementioned map, both ϕ , and $\frac{\partial}{\partial x}$ are expanded into multiple scales:

$$\begin{aligned}
&\phi_0'''' + \epsilon\phi_1'''' \\
&-2\alpha^2\phi_0'' + \epsilon 4i\alpha \frac{\partial\phi_0''}{\partial x_1} - \epsilon 2\alpha^2\phi_1'' \\
&+ \alpha^4\phi_0 + \epsilon 4i\alpha^3 \frac{\partial\phi_0}{\partial x_1} + \epsilon\alpha^4\phi_1 = \\
&ReU i\alpha\phi_0'' + \epsilon ReU \frac{\partial\phi_0''}{\partial x_1} + \epsilon ReU i\alpha\phi_1'' \\
&-iRe\omega\phi_0'' - \epsilon iRe\omega\phi_1'' \\
&-i\alpha^3 ReU\phi_0 - \epsilon 3\alpha^2 ReU \frac{\partial\phi_0}{\partial x_1} - i\epsilon\alpha^3 ReU\phi_1 \\
&+ i\omega Re\alpha^2\phi_0 + \epsilon 2\omega Re\alpha \frac{\partial\phi_0}{\partial x_1} + i\epsilon\omega Re\alpha^2\phi_1 \\
&-iRe\alpha U''\phi_0 - \epsilon ReU'' \frac{\partial\phi_0}{\partial x_1} - i\epsilon Re\alpha U''\phi_1
\end{aligned} \quad (4.28)$$

And by splitting similar powers of ϵ :

$$\phi_0'''' - 2\alpha^2\phi_0'' + \alpha^4\phi_0 - ReU i\alpha\phi_0'' + Re i\omega\phi_0'' + ReU i\alpha^3\phi_0 - Re i\alpha^2\omega\phi_0 + ReU'' i\alpha\phi_0 = 0 \quad (4.29)$$

$$\begin{aligned}
&\phi_1'''' - 2\alpha^2\phi_1'' + \alpha^4\phi_1 + iReU\alpha\phi_1'' - iRe\omega\phi_1'' - iReU\alpha^3\phi_1 + iRe\alpha^2\omega\phi_1 - iReU''\alpha\phi_1 \\
&+ 4i\alpha \frac{\partial\phi_0''}{\partial x_1} + 4i\alpha^3 \frac{\partial\phi_0}{\partial x_1} + ReU \frac{\partial\phi_0''}{\partial x_1} - 3ReU\alpha^2 \frac{\partial\phi_0}{\partial x_1} + 2Re\alpha\omega \frac{\partial\phi_0}{\partial x_1} - ReU'' \frac{\partial\phi_0}{\partial x_1} = 0
\end{aligned} \quad (4.30)$$

This does not quite give the completed formulation: no account has yet been taken for the terms involving a streamwise derivative of a base flow, which will have been considered negligible in the

parallel case. Recall that the x and y momentum equations contained respectively:

$$\epsilon \tilde{u} \frac{\partial U}{\partial x} + \epsilon V \frac{\partial \tilde{u}}{\partial y} + \dots = \dots \quad (4.31)$$

$$U \frac{\partial \tilde{v}}{\partial x} + \epsilon V \frac{\partial \tilde{v}}{\partial y} + \epsilon \tilde{v} \frac{\partial V}{\partial y} + \dots = \dots \quad (4.32)$$

These too must be cross differentiated and the terms from the y momentum equation subtracted:

$$\epsilon \frac{\partial^2 U}{\partial x \partial y} \tilde{u} + \epsilon \frac{\partial U}{\partial x} \frac{\partial \tilde{u}}{\partial y} + \epsilon V \frac{\partial^2 \tilde{u}}{\partial y^2} + \epsilon \frac{\partial V}{\partial y} \frac{\partial \tilde{u}}{\partial y} + \dots = \dots \quad (4.33)$$

$$-\epsilon \frac{\partial U}{\partial x} \frac{\partial \tilde{v}}{\partial x} - U \frac{\partial^2 \tilde{v}}{\partial x^2} - \epsilon V \frac{\partial^2 \tilde{v}}{\partial x \partial y} - \epsilon \frac{\partial V}{\partial x} \frac{\partial \tilde{v}}{\partial y} - \epsilon \frac{\partial^2 V}{\partial x \partial y} \tilde{v} - \epsilon \frac{\partial V}{\partial y} \frac{\partial \tilde{v}}{\partial x} - \dots = \dots \quad (4.34)$$

Then this is expanded into multiple scales, keeping only those terms with a factor of ϵ^1 :

$$\epsilon \frac{\partial^2 U}{\partial x_0 \partial y} \tilde{u}_0 + \epsilon \frac{\partial U}{\partial x_0} \frac{\partial \tilde{u}_0}{\partial y} + \epsilon V \frac{\partial^2 \tilde{u}_0}{\partial y^2} + \epsilon \frac{\partial V}{\partial y} \frac{\partial \tilde{u}_0}{\partial y} + \dots = \dots \quad (4.35)$$

$$-\epsilon \frac{\partial U}{\partial x_0} \frac{\partial \tilde{v}_0}{\partial x_0} - \epsilon V \frac{\partial^2 \tilde{v}_0}{\partial x_0 \partial y} - \epsilon^2 \frac{\partial V}{\partial x_0} \frac{\partial \tilde{v}_0}{\partial y} - \epsilon^2 \frac{\partial^2 V}{\partial x_0 \partial y} \tilde{v}_0 - \epsilon \frac{\partial V}{\partial y} \frac{\partial \tilde{v}_0}{\partial x_0} - \dots = \dots \quad (4.36)$$

And then the stream function is substituted in:

$$\epsilon \frac{\partial U'}{\partial x_0} \phi'_0 + \epsilon \frac{\partial U}{\partial x_0} \phi''_0 + \epsilon V \phi'''_0 + \epsilon V' \phi''_0 + \dots = \dots \quad (4.37)$$

$$-\epsilon \alpha^2 \frac{\partial U}{\partial x_0} \phi_0 - \epsilon \alpha^2 V \phi'_0 - \epsilon \alpha^2 V' \phi_0 - \dots = \dots \quad (4.38)$$

And simplified:

$$\epsilon V \phi'''_0 + \epsilon \frac{\partial U}{\partial x_0} \phi''_0 + \epsilon V' \phi''_0 + \epsilon \frac{\partial U'}{\partial x_0} \phi'_0 - \epsilon \alpha^2 V \phi'_0 - \epsilon \alpha^2 \frac{\partial U}{\partial x_0} \phi_0 - \epsilon \alpha^2 V' \phi_0 + \dots = \dots \quad (4.39)$$

And finally returned to the expanded OSE (with a factor of Re):

$$\phi_0'''' - 2\alpha^2 \phi_0'' + \alpha^4 \phi_0 - ReU i \alpha \phi_0'' + Re i \omega \phi_0'' + ReU i \alpha^3 \phi_0 - Re i \alpha^2 \omega \phi_0 + ReU'' i \alpha \phi_0 = 0 \quad (4.40)$$

$$\begin{aligned} & \phi_1'''' - 2\alpha^2 \phi_1'' + \alpha^4 \phi_1 + i ReU \alpha \phi_1'' - i Re \omega \phi_1'' - i ReU \alpha^3 \phi_1 + i Re \alpha^2 \omega \phi_1 - i ReU'' \alpha \phi_1 \\ & + 4i \alpha \frac{\partial \phi_0''}{\partial x_1} + ReU \frac{\partial \phi_0''}{\partial x_1} + 2Re \alpha \omega \frac{\partial \phi_0}{\partial x_1} - 3ReU \alpha^2 \frac{\partial \phi_0}{\partial x_1} - ReU'' \frac{\partial \phi_0}{\partial x_1} + 4i \alpha^3 \frac{\partial \phi_0}{\partial x_1} \end{aligned} \quad (4.41)$$

$$+ ReV \phi_0''' + Re \frac{\partial U}{\partial x_0} \phi_0'' + ReV' \phi_0'' + Re \frac{\partial U'}{\partial x_0} \phi_0' - ReV \alpha^2 \phi_0' - ReV' \alpha^2 \phi_0 - Re \frac{\partial U}{\partial x_0} \alpha^2 \phi_0 = 0$$

Which gives an identical formulation to equation (4.23), and demonstrates that the two methods are equivalent.

4.1.3 Definition of the growth rate

In equation (4.15) Q and Q_0 are unknown, but the useful engineering quantities are actually the relative growth rates in either direction which are given by:

$$\left[\frac{1}{\tilde{q}_0} \frac{\partial \tilde{q}_0}{\partial x} \right]_r \quad (4.42a)$$

$$\left[\frac{1}{\tilde{q}_0} \frac{\partial \tilde{q}_0}{\partial z} \right]_r \quad (4.42b)$$

This can now be rewritten:

$$\left[\frac{1}{Q\tilde{q}_n} \frac{\partial Q\tilde{q}_n}{\partial x} \right]_r \quad (4.43a)$$

$$\left[\frac{1}{Q\tilde{q}_n} \frac{\partial Q\tilde{q}_n}{\partial z} \right]_r \quad (4.43b)$$

and Expanded:

$$\left[\frac{1}{Q\tilde{q}_n} \left(Q \frac{\partial \tilde{q}_n}{\partial x} + \tilde{q}_n \frac{\partial Q}{\partial x} \right) \right]_r \quad (4.44a)$$

$$\left[\frac{1}{Q\tilde{q}_n} \left(Q \frac{\partial \tilde{q}_n}{\partial z} + \tilde{q}_n \frac{\partial Q}{\partial z} \right) \right]_r \quad (4.44b)$$

and simplified:

$$\left[\frac{1}{\tilde{q}_n} \frac{\partial \tilde{q}_n}{\partial x} + \frac{1}{Q} \frac{\partial Q}{\partial x} \right]_r \quad (4.45a)$$

$$\left[\frac{1}{\tilde{q}_n} \frac{\partial \tilde{q}_n}{\partial z} + \frac{1}{Q} \frac{\partial Q}{\partial z} \right]_r \quad (4.45b)$$

From equation (4.15) it can be deduced that:

$$\frac{1}{Q} \frac{\partial Q}{\partial x_1} = -\frac{L}{2M} \quad (4.46a)$$

$$\frac{1}{Q} \frac{\partial Q}{\partial z_1} = -\frac{L}{2N} \quad (4.46b)$$

This can be used to find $1/Q \partial Q/\partial x$ and $1/Q \partial Q/\partial z$:

$$\frac{1}{Q} \frac{\partial Q}{\partial x} = \frac{1}{Q} \frac{\partial Q}{\partial x_1} \frac{\partial x_1}{\partial x} = -\epsilon \frac{L}{2M} \quad (4.47a)$$

$$\frac{1}{Q} \frac{\partial Q}{\partial z} = \frac{1}{Q} \frac{\partial Q}{\partial z_1} \frac{\partial z_1}{\partial z} = -\epsilon \frac{L}{2N} \quad (4.47b)$$

And from equation (2.15) it is known that:

$$\left[\frac{1}{\tilde{q}_n} \frac{\partial \tilde{q}_n}{\partial x} \right]_r = -\alpha_i, \quad \left[\frac{1}{\tilde{q}_n} \frac{\partial \tilde{q}_n}{\partial z} \right]_r = -\beta_i$$

However, this formulation does not account for the wall-normal variation in the eigenfunction shape, which was considered negligible under the parallel flow assumption. Under the quasi-parallel assumption this becomes a first order consideration, and must be included. Accounting for it gives the modified form:

$$\left[\frac{1}{\tilde{q}_n} \frac{\partial \tilde{q}_n}{\partial x} \right]_r = -\alpha_i + \left[\frac{1}{\hat{q}_n} \frac{\partial \hat{q}_n}{\partial x} \right]_r \quad (4.48a)$$

$$\left[\frac{1}{\tilde{q}_n} \frac{\partial \tilde{q}_n}{\partial z} \right]_r = -\beta_i + \left[\frac{1}{\hat{q}_n} \frac{\partial \hat{q}_n}{\partial z} \right]_r \quad (4.48b)$$

These derivatives can be computed directly from the eigenfunctions which were generated and used in the linear stability calculation, and together with equation (4.47) give the corrected growth rate formulations:

$$\left[\frac{1}{\tilde{q}_0} \frac{\partial \tilde{q}_0}{\partial x} \right]_r = -\alpha_i + \left[\frac{1}{\hat{q}_n} \frac{\partial \hat{q}_n}{\partial x} - \epsilon \frac{L}{2M} \right]_r \quad (4.49a)$$

$$\left[\frac{1}{\tilde{q}_0} \frac{\partial \tilde{q}_0}{\partial z} \right]_r = -\beta_i + \left[\frac{1}{\hat{q}_n} \frac{\partial \hat{q}_n}{\partial z} - \epsilon \frac{L}{2N} \right]_r \quad (4.49b)$$

4.1.3.1 The value of ϵ

When it comes time to evaluate the growth rate using equation (4.49), the value of ϵ will be needed. This has yet to be defined, save for mentioning that it in some way measures the deviation from parallel of the boundary layer, and that it is small. Its value has been discussed by many, but it is Gaster [12] who makes the most convincing argument. He assumes nothing about the magnitude of ϵ and allows it to come out as part of his iterative solution. The value relates to the size of terms which were ignored in LST, which for Gaster were of order $O(Re_{x_0}^{-1/2})$, where x_0 is a location where

a wave is assumed to exist. El Hady identifies its value as $1/\sqrt{Re_x}$. The present analysis also uses this scaling and as will be shown, this facilitates good agreement with results in the literature. This value should not come as a particular surprise; this is a measure of how quickly the boundary layer changes, and of course the boundary layer growth is available in any good book on Boundary layers[32, 29]:

$$\delta_{99} \approx \frac{4.9x}{\sqrt{Re_x}} \quad (4.50)$$

So it might be reasonable to expect the $1/\sqrt{Re_x}$ term to be present.

4.1.3.2 The problems in determining an amplitude metric

Capturing some knowledge about the mode shape change and boundary layer growth is necessary to complete equation (4.49). However, quantifying this shape change is not trivial, since \tilde{q} is a vector representing velocities, velocity gradients, and pressure, all given as a function of wall-normal distance. Various amplitude metrics may be appropriate for different purposes. For example, a comparison between simulated and experimental results may be best served by choosing the largest value of \hat{u} at each station, since this is a readily measured quantity in a wind tunnel. This is not necessarily the best choice for comparison with other simulations, where some metric of energy may be better suited. It is quite possible that there is no ‘true’ metric at all. The normalisation of \hat{q} is also important, as might the part of \hat{q} (real, imaginary, absolute) chosen. A range of options must therefore be explored. The following table shows various combinations used in the literature:

Author	Metric	Normalisation	Wall-normal location of $\partial_x \hat{q} / \hat{q}$
Bouthier [6]	$\hat{u}^2 + \hat{v}^2$	-	one location with positive growth rate
Bouthier [6]	$\hat{u}^2 + \hat{v}^2$	-	all locations with positive growth rate
Gaster [12]	$\hat{u}^2 + \hat{v}^2$	-	integrated wall-normally
Gaster [12]	\hat{u}^2	-	integrated wall-normally
Gaster [12]	$ \hat{u} $	-	$ \hat{u} $ inner lobe maximum
Gaster [12]	$ \hat{u} $	-	$ \hat{u} $ outer lobe maximum
Saric & Nayfeh [30]	$2U\hat{u}$	$c(x) = 1^*$	effectively ignored
El Hady [8]	$\xi_9 = U + \hat{u}$	$ \xi_9 _{max} = 1$	$ \xi_9 _{max}$
El Hady [8]	$\xi_9 \bar{\xi}_9$	$ \xi_9 _{max} = 1$	integrated wall-normally

Table 4.1: Legacy mode shape change metrics

* $c(x_0) = \left[\frac{\partial q_0}{\partial y} \right]_0 / \left[\frac{\partial q_1}{\partial y} \right]_0$

As can be seen, the literature provides a wealth of options, but each of these comes with its own difficulties:

- Although Bouthier broke ground in this field, his metric is not quite what is needed; it does give a criterion which can be used to define a neutral curve, but converting this into something more practical like a modified N-factor is not feasible.
- As El Hady points out, the choice of wall-normal location is extremely consequential. If one with large magnitude of the metric was chosen, then $1/\hat{q}$ becomes small. If the magnitude at the chosen location was small then $1/\hat{q}$ becomes very large. Some, including Saric & Nayfeh, have asserted that by choosing a location with large enough magnitude, the contribution of the mode shape change becomes negligible. This is convenient, but ultimately unsatisfactory. To further complicate matters, the stability curves given in their 1975 paper use a “dimensionless frequency parameter” whose units appear to be s^2 . This makes comparison difficult.
- Wall-normal resolution is also of concern, as it will affect the accuracy of any integrals, and the detection of any maxima. The use of mixed base flow and fluctuating parts is also unsatisfactory, since the fluctuation returned by a parallel flow solution is an eigensolution and therefore arbitrary in magnitude. This makes it inappropriate to use in conjunction with a base flow, whose value is *not* arbitrary, to calculate relative growth rates in most cases.

It is also noteworthy that, perhaps unsurprisingly, none of these options give matching results consistently; and where they do this appears to be entirely accidental. To summarise, in each case from the literature there is either an unsatisfactory metric or an unclear normalisation, and no real consensus on any of these factors.

In order to proceed, some clarity is required on three broad questions:

1. Is there a better or worse part of \hat{q} to use, if so which part is which, and why? (§ 4.1.3.3)
2. Is there a better or worse way to reduce \hat{q} down to a single value at each station, if so, why? (§ 4.1.3.4)
3. Is there a better or worse eigenfunction normalisation to use, if so what is it, and why? (§ 4.1.3.5)

4.1.3.3 Selecting a part of \hat{q}

Something must be chosen to represent the mode shape change. The literature has spawned a number of different ideas on this issue. The present analysis will proceed by using the kinetic energy ($E = \hat{u}^2 + \hat{v}^2 + \hat{w}^2$). It gives good agreement with Schubauer and Skramstad[34], it is fairly intuitive to understand, and importantly, it gives a number which can be used to input into a modified N-factor algorithm.

4.1.3.4 Reducing \hat{q} to a single value

In order to sensibly define the growth rate, $1/\hat{q} \partial\hat{q}/\partial x$, a function in y is taken, and reduced down to a single value. Precisely how this is done can have a dramatic effect on its contribution. Recall in § 2.4.2 the shape of $\hat{q} = f(y)$ has been shown. For example, fig. 2.2 (which is duplicated as fig. 4.1) shows:

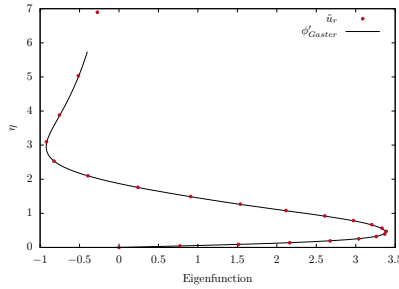


Figure 4.1: Eigenfunction at $\text{Re} = 725$, $\omega = 0.13$

The location of maximum \hat{q} could be selected; this would result in a vanishingly small contribution. Conversely a location could be intentionally selected where the growth is largest, likely where \hat{q} is smallest. Neither of these are satisfactory however. A method should not be chosen in order to satisfy some preconceived notion of what the behaviour should be. Instead a method should be chosen to best reflect what the behaviour actually is. This is why integral methods are used in the present work. By taking the integral of the eigenfunction in the wall-normal direction, this takes account not only of the extrema, but also of every point in between.

4.1.3.5 Eigenfunction normalisation

El Hady specifies an eigenfunction normalisation which makes his mass flow variable equal unity at its maximum; Saric and Nayfeh use a different function which is shown in table 4.1; others in

the literature don't specify a particular normalisation at all. What follows is an explanation for why the choice is irrelevant:

- The present normalisation comes from the chosen finite value of pressure at the wall
- Any factor applied to this value will be applied to the entire eigenfunction
- Recalling § 4.1.1.1 the derivatives of the eigenfunction are calculated using the eigenfunction itself
- Therefore the relative $(\partial_x \hat{q}/\hat{q})$ change is calculated, the normalisation factor cancels itself out

This logic applies to the term $\partial_x \hat{q}/\hat{q}$, but can also be applied to $\partial_x Q/Q$ since this works out as proportional L/M , and both L , and M are generated using the original eigenfunction. Therefore the scaling factor will cancel itself out here too. Calculations have been made with a number of different scaling factors, including pseudorandomly generated. No effect whatsoever on the results have been observed.

4.1.3.6 The solution to determining an amplitude metric

To summarise § 4.1.3.3-§ 4.1.3.5, the analysis which follows measures mode shape change by the integral of the kinetic energy $(\int_0^\infty \hat{u}^2 + \hat{v}^2 + \hat{w}^2 d\eta)$. The relative gradient is measured in such a way that the normalisation holds no relevance whatsoever.

4.1.4 Multiple scales calculations

4.1.4.1 Single eigenvalue validation

El Hady gives two results in [8] with a Mach number of zero and which can therefore be compared with the present analysis. But first the scaling he uses must be understood. The length, velocity, and time scales employed by El Hady are $L^* = \sqrt{\nu_0^* x^* / u_{0e}^*}$, u_{0e}^* , and L^* / u_{0e}^* respectively, giving a Reynolds number of $Re = u_{0e}^* L^* / \nu_0^* = \sqrt{Re_x}$. Results are given at $Re = 1000$, and $Re = 500$ which, at standard temperature and pressure, and using values free stream velocity of $10ms^{-1}$ give:

$$\begin{aligned}
 500 &= \sqrt{u_{0e}^* x / \nu_0^*} = \sqrt{\frac{10 \cdot 1.2273088}{1.7928066 \times 10^{-5}}} & 1000 &= \sqrt{u_{0e}^* x / \nu_0^*} = \sqrt{\frac{10 \cdot 1.2273088}{1.7928066 \times 10^{-5}}} \\
 x &= \frac{500^2 \cdot 1.7928066 \times 10^{-5}}{10 \cdot 1.2273088} & x &= \frac{1000^2 \cdot 1.7928066 \times 10^{-5}}{10 \cdot 1.2273088} \\
 &= 0.36519061m & &= 1.46076244m
 \end{aligned}$$

Growth rates are calculated at these points and used to verify the method. El Hady gives growth rates for the “most amplified non-parallel mode”, however the frequency of this mode is not precisely defined, nor is the resolution of the frequency domain. Results should therefore be taken in this context. Comparisons are made excluding mode shape change as El Hady uses a metric which is incompatible with the one used in the present analysis. Good agreement is observed.

Re	$-\alpha_{i,ElHady}$	$(-\alpha_i + f(Q))_{ElHady}$	$-\alpha_i$	$-\alpha_i + f(Q)$
1000	0.006237	0.006813	0.00625	0.00684
500	0.0035	0.0046	0.00357	0.00467

Table 4.2: Non-parallel comparison with El Hady

4.1.4.2 Stability curve validation

Nayfeh and Gaster both provide neutral stability curves, but these do not agree with each other. Nayfeh uses an erroneous “dimensionless” frequency, and his criterion is not satisfactory, therefore results will be presented against those given by Gaster, and using his criterion. Gaster’s curve is copied and a corresponding neutral curve from the present analysis is superimposed onto it for comparison. Present results are shown in red. Reasonable agreement is observed.

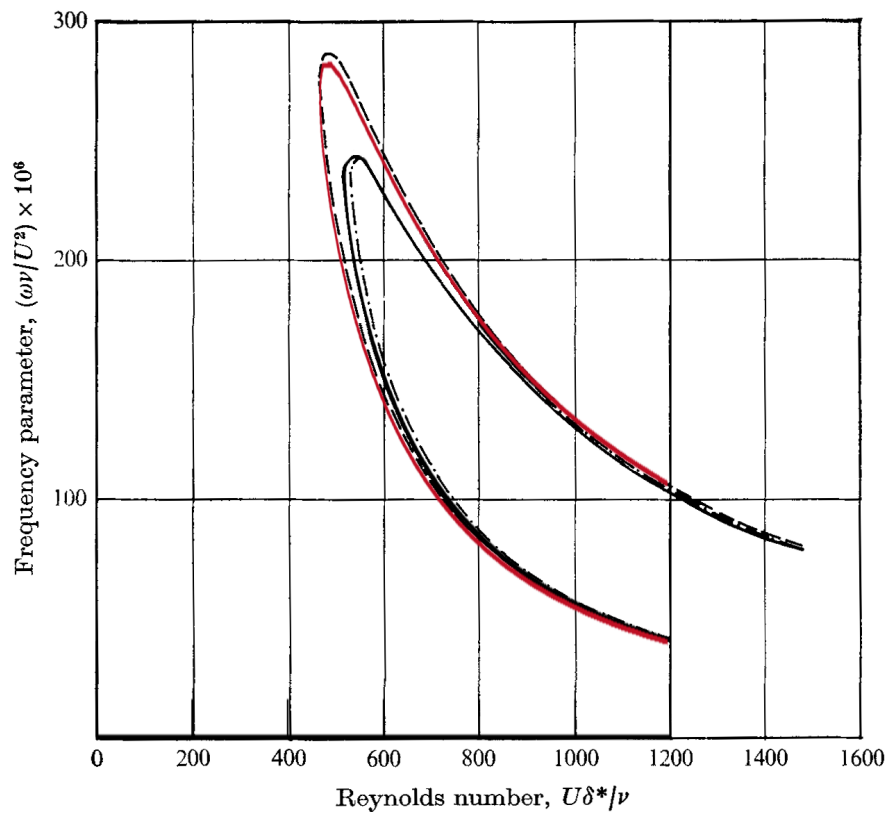


Figure 4.2: Neutral curve comparison with Gaster[12]

— Linear stability only, - - - Integral of kinetic energy criterion,
 - · - Integral of \bar{u}^2 criterion, — Present analysis

4.2 Surface curvature

Most surfaces of interest to engineers are not flat but instead, curved. This has a subtle, but noticeable effect on the stability, which should be included. The curvature modifies the governing equations by adding several terms. These can be found by considering the Navier-Stokes equations in a curvilinear coordinate system, a comprehensive derivation of which has been shown by Backer Dirks [4], however for this problem only surface curvature terms (κ_{xy} , κ_{zy}) are included. Additionally products of two curvatures are neglected, as are products of curvature and viscosity:

$$i\alpha\hat{u} + \hat{v}' + i\beta\hat{w} + \kappa_{xy}\hat{v} + \kappa_{zy}\hat{v} = 0 \quad (4.51)$$

$$-i\omega\hat{u} + i\alpha U\hat{u} + U'\hat{v} + i\beta W\hat{u} + i\alpha\hat{p} - \frac{1}{Re}(-\alpha^2\hat{u} + \hat{u}'' - \beta^2\hat{u}) + \kappa_{xy}U\hat{v} = 0 \quad (4.52)$$

$$-i\omega\hat{v} + i\alpha U\hat{v} + i\beta W\hat{v} + \hat{p}' - \frac{1}{Re}(-\alpha^2\hat{v} + \hat{v}'' - \beta^2\hat{v}) - 2\kappa_{xy}U\hat{u} - 2\kappa_{zy}W\hat{w} = 0 \quad (4.53)$$

$$-i\omega\hat{w} + i\alpha U\hat{w} + W'\hat{v} + i\beta W\hat{w} + i\beta\hat{p} - \frac{1}{Re}(-\alpha^2\hat{w} + \hat{w}'' - \beta^2\hat{w}) + \kappa_{zy}W\hat{v} = 0 \quad (4.54)$$

If the multiple scales approach is to be used, the flow is treated as locally parallel, but non-parallel over longer distances. Consequently, the additional terms due to curvature should be included along with boundary layer growth terms in the first order correction. Recall equation (4.7b), which will now instead become:

$$A\hat{q}_1 - \hat{q}_1' = b + b_\kappa \quad (4.55)$$

where b_κ contains the additional terms arising from curvature.

4.2.1 Calculations

To demonstrate the effects of surface curvature, the development of a crossflow vortex in a relatively fast flow is shown (fig. 4.3 & fig. 4.4). In both of these cases, the terms arising from surface curvature are built into the LST calculation, not the MSM correction. The result appears to be highly oscillatory close to the leading edge; this makes it very difficult to accurately determine where the N-factor integration should begin¹. Consequently, there is a disparity between them, even though the eigenvalues are mostly in agreement.

¹In fact for this case, safety features of the code were overridden in order to generate results.

As a mathematical exercise it is fairly simple to build the curvature terms into the MSM. In computational practice, it is not so. This is recommended as a fascinating possible avenue of further investigation.

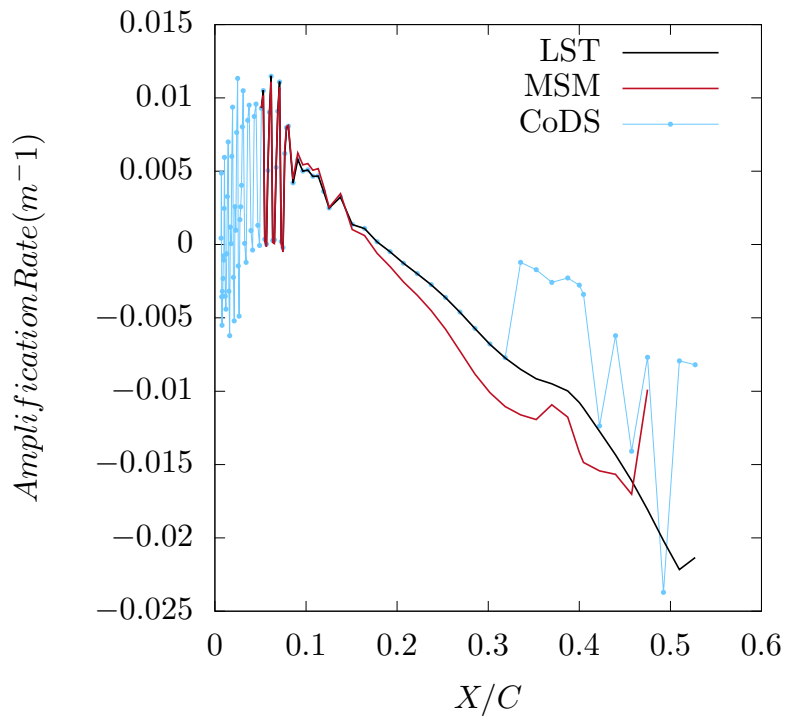


Figure 4.3: Amplification - RAE5243 30° sweep - 200 ms^{-1} at sea level, $F = 5.2kHz$, $SWN = 3500m^{-1}$, $Re_C = 13692140$

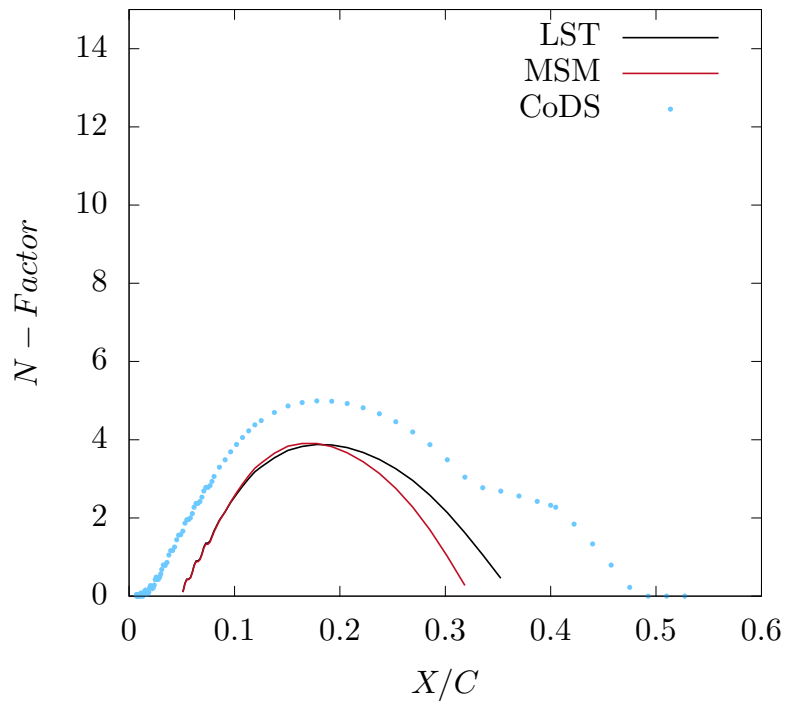


Figure 4.4: N-Factor - RAE5243 30° sweep - 200 ms^{-1} at sea level, $F = 5200Hz$, $SWN = 3500m^{-1}$, $Re_C = 13692140$

Chapter 5

Numerical Methods

The primary output from the present work is a code which implements the theory set out in Chapter 4. This chapter explores some of the numerical methods which could be used in the implementation, and highlights which are chosen.

5.1 Root finding

Often in engineering the governing equations are difficult or impossible to solve analytically. In such cases a numerical approach is adopted. Such approaches typically use an educated initial guess, then update that guess through many iterations with a root finding algorithm until a suitably accurate answer is found. Usually the algorithm attempts to find the location where a function of one or more variables is equal to zero.

5.1.1 The method of bisection

The method of bisection is a simple root finding algorithm which will always find a root, should one exist within a chosen interval. An interval must be specified; the function is then carried out and the outcome evaluated. The method begins by choosing the value in the centre of the interval, then the function whose root is sought is applied to the chosen value. Should the output be too large, the interval is split in half, retaining the lower half, and the process starts again. Should the output be too small, the upper half of the interval is retained. This process is continued until the root is found.

5.1.2 The Newton-Raphson method

This method is more complex than the method of bisection, and it is not always guaranteed to find a root, even if one exists. However, when the conditions are correct, it closes in with much greater speed. A guess must be made for the location of the root, then the function and its gradient are evaluated at that point. The point and gradient are then used to construct a straight line, whose root is easily obtained. This value is then used as the next guess. Formally, a single iteration is given by:

$$x_{n+1} = z_n - \frac{f(x_n)}{f'(x_n)} \quad (5.1)$$

This procedure should be continued until the root has been found.

5.2 Numerical solutions of ODEs

The governing equations in linear stability theory have the form of ordinary differential equations with boundary conditions at more than one boundary. These boundary value problems (BVPs) have two widely used solution methodologies; shooting methods, and matrix methods.

5.2.1 Shooting methods

A shooting method comprises an initial value problem (IVP) numerical integration scheme, and a root finding algorithm. The problem is initially treated as an IVP, specifying boundary conditions on one end of the computational domain, including guesses for unknown values. Integration is performed with those boundary conditions then the boundary conditions are checked on the other edge of the domain to determine if the guesses were sufficiently accurate. If not, new guesses are supplied according to a suitable root finding method. Typical integration schemes evaluate the function at some point using its values and derivatives at a previous point. The first method of this family was developed in 1768 by Euler [9].

5.2.1.1 The Euler method

If the problem is an IVP of the form: $u' = f(u)$ then Euler's method and the values of u and its derivatives are known at a point then the values at the next point are given by:

$$u_{n+1} = u_n + hu'_n \quad (5.2)$$

Where h is the distance between the points. By taking a Taylor expansion about the zeroth point, it can be shown that method has second order accuracy.

$$u(y_0 + h) = u(y_0) + hu'(y_0) + \frac{1}{2}h^2u''(y_0) + \dots \quad (5.3)$$

The error is given by:

$$\varepsilon = u(y_0 + h) - u_1 = \frac{1}{2}h^2 u''(y_0) + O(h^3) + \dots \quad (5.4)$$

5.2.1.2 The improved Euler method

Euler's method can be improved by treating it as only the first step and then applying a correction before moving on to the next point. The formulation is given by:

$$\begin{aligned} u_{n+1} &= u_n + \frac{h}{2} (\text{predictor} + \text{corrector}) \\ \text{predictor} &= f(u_n) \\ \text{corrector} &= f(u_n + h \times \text{predictor}) \end{aligned} \quad (5.5)$$

By taking the Taylor expansion exactly as for the basic Euler method it can be shown that the scheme has third order accuracy. Increased accuracy however, comes at a price. The additional step inevitably adds computation time.

5.2.1.3 Runge-Kutta (RK) methods

Runge-Kutta is the name given to a family of numerical integration schemes which extend the concept of the improved Euler method, seeking an ever more accurate estimate for the slope between the points at n and $n + 1$. The most common of these methods is the fourth order scheme (RK4), which uses four steps to estimate the slope in the interval between n and $n + 1$. The first step is the same as in Euler, but three other estimates are used as well:

$$\begin{aligned} k_1 &= f(u) \\ k_2 &= f\left(u + \frac{h}{2}k_1\right) \\ k_3 &= f\left(u + \frac{h}{2}k_2\right) \\ k_4 &= f(u + hk_3) \\ u_{n+1} &= u_n + \frac{h}{6}(k_1 + 2k_2 + 2k_3 + k_4) \end{aligned} \quad (5.6)$$

There are other RK schemes, but RK4 is the most commonly used. As with the improved Euler scheme, the benefit in accuracy is paid for in complexity, and computation time.

5.2.2 Matrix methods

Matrix methods are a completely different approach to solving differential equations. The differential operator is in some way approximated as a matrix, where boundary conditions can be imposed on both ends (or anywhere else). This makes these types of schemes very useful for solving BVPs.

5.2.2.1 Finite differences

The simplest of the matrix methods are the finite difference methods. In these schemes the gradient at a point is given by the values at nearby points. Some popular choices are:

$$u'_i = \frac{u_{i+1} - u_i}{h} \quad (5.7)$$

$$u'_i = \frac{u_{i+1} - u_{i-1}}{2h} \quad (5.8)$$

The order accuracy of this family of methods depends on how many points are used in the formulation. Although this makes it easy in theory to add accuracy, larger stencils reaching further away from i make implementation of boundary conditions more difficult, and often result in unwieldy matrices.

5.2.2.2 Compact differences

Compact differences [21] attempt to achieve greater accuracy with a smaller number of points. By limiting the scheme to two points, the matrix system should remain more manageable. However, the formulation requires a little more effort to understand. Consider a set of equations in the form:

$$A\hat{q} = \hat{q}' \quad (5.9)$$

The Euler-Maclaurin formula states[21]:

$$\hat{q}^k - \hat{q}^{k-1} = \frac{h}{2} \left(\frac{d}{dy} \hat{q}^k + \frac{d}{dy} \hat{q}^{k-1} \right) - \frac{h^2}{12} \left(\frac{d^2}{dy^2} \hat{q}^k - \frac{d^2}{dy^2} \hat{q}^{k-1} \right) + O(h^5) \quad (5.10)$$

By differentiation of equation (5.9):

$$\begin{aligned}
 A' \hat{q} + A \hat{q}' &= \hat{q}'' \\
 A' \hat{q} + A (A \hat{q}) &= \hat{q}'' \\
 (A' + A^2) \hat{q} &= \hat{q}''
 \end{aligned}
 \tag{5.11}$$

This can be substituted into equation (5.10) to give:

$$\hat{q}^k - \hat{q}^{k-1} = \frac{h}{2} (A \hat{q}^k + A \hat{q}^{k-1}) - \frac{h^2}{12} [(A' + A^2) \hat{q}^k - (A' + A^2) \hat{q}^{k-1}] + O(h^5)
 \tag{5.12}$$

For the full domain this results in a block bi-diagonal matrix multiplied by the eigenfunction equal to a zero vector on the right hand side. This is not a particularly useful form to solve; a square would be much more convenient.

5.2.2.3 Squaring a rectangular matrix

The matrix is block bi-diagonal, which means it is $n \times (n + m)$ in size, where n is the number of points and m is the number of equations. Since square matrices make solution much easier, m columns need to be removed. Fortunately this can be done by employing boundary conditions. Firstly a modified identity matrix B is constructed with additional rows so its size is $(n + m) \times n$. The additional rows contain only zeros so that by taking BA the result is a matrix whose size is $n \times n$, and whose coefficients are identical to A , apart from m missing columns. The removed coefficients are multiplied by the appropriate boundary condition and added to the right hand side vector. This leaves a system which can be solved with an appropriate matrix decomposition or inversion scheme.

5.3 Solution of linear systems

When the governing equations have been successfully expressed as a linear system, there are a number of methods by which they can then be solved. This is by a wide margin the most computationally intense part of the process, so the choice here is critical. In this section the linear

system is denoted by:

$$A\mathbf{x} = \mathbf{b} \tag{5.13}$$

5.3.1 Direct matrix inversion

The original method for solving these kinds of systems is matrix inversion, where the objective is to obtain A^{-1} such that:

$$AA^{-1} = A^{-1}A = I \tag{5.14}$$

This involves computing the determinant of A and its matrix of minors, for small matrices this is simple and can be done by hand, but as the matrix size increases this becomes burdensome. As a consequence this approach is never adopted for very large computations.

5.3.2 Gaussian elimination

An early form of matrix decomposition favoured by Alan Turing and his contemporaries, this method shows that if the matrix can be manipulated into a triangular form, then multiplying its inverse by a vector becomes simple. Typically it is useful to find either the upper triangle form, or the lower triangle form:

$$U = \begin{bmatrix} u_{11} & u_{12} & u_{13} \\ 0 & u_{22} & u_{23} \\ 0 & 0 & u_{33} \end{bmatrix}, L = \begin{bmatrix} l_{11} & 0 & 0 \\ l_{21} & l_{22} & 0 \\ l_{31} & l_{32} & l_{33} \end{bmatrix} \tag{5.15}$$

$$\tag{5.16}$$

These forms are found by adding multiples of rows to other rows, much as would be done for solutions of simultaneous equations which are not expressed with matrices. To ensure that the row operations are applied to the correct rows, the augmented matrix is formed:

$$\left[\begin{array}{ccc|c} x_{11} & x_{12} & x_{13} & b_1 \\ x_{21} & x_{22} & x_{23} & b_2 \\ x_{31} & x_{32} & x_{33} & b_3 \end{array} \right] \tag{5.17}$$

Once the system is in the correct form, it can be solved by working from top to bottom or vice versa substituting in the answers from the previous row. This method uses $O(n^2)$ operations to complete.

5.3.2.1 Pivoting

Occasionally, there will be a fortunate situation where a row already conforms to part of the triangular shape; it is useful to have a tool which would allow shuffling of entire rows around at will, leaving them in more optimum positions. The permutation matrix is just such a tool. When applied to another matrix it shuffles the rows. For example, this permutation matrix swaps the second and third rows of a three by three matrix:

$$P_{23} = \begin{bmatrix} 1 & 0 & 0 \\ 0 & 0 & 1 \\ 0 & 1 & 0 \end{bmatrix} \tag{5.18}$$

$$\tag{5.19}$$

Not only can this save a few operations, it also can increase the stability of the solution.

5.3.2.2 Gauss-Jordan elimination

Previously, applying Gaussian elimination to a vector provides a solution to a system of linear equations. By applying the same principal to the identity matrix, the original matrix can be reduced to identity, and in the process the identity on the right hand side of the dividing line is converted into the inverse.

$$\left[A \mid \begin{array}{ccc} 1 & 0 & 0 \\ 0 & 1 & 0 \\ 0 & 0 & 1 \end{array} \right] \rightarrow \left[\begin{array}{ccc} 1 & 0 & 0 \\ 0 & 1 & 0 \\ 0 & 0 & 1 \end{array} \mid A^{-1} \right] \tag{5.20}$$

$$\tag{5.21}$$

Although this requires more work than simply solving $A\mathbf{x} = \mathbf{b}$, the result is much more useful as A^{-1} can be used to find \mathbf{x} given any \mathbf{b} .

5.3.3 Matrix decompositions

Using Gauss-Jordan elimination is powerful, but it is also computationally intense, and difficult to implement for matrices of general dimension. Lower-upper (LU) decompositions, on the other hand, are much simpler. Instead of seeking to solve a linear system, or to find the inverse, it is possible to decompose a matrix into the product of an upper triangle and lower triangle. These can then be used together to solve the linear system for any \mathbf{b} .

5.3.3.1 Cholesky decomposition

For certain kinds of matrices (Hermitian, positive-definite) there exists a decomposition of the form:

$$A = LL^\dagger \quad (5.22)$$

Clearly this is an extremely useful form, as it only requires storage for one of the two matrices. Unfortunately however, the matrices which are most useful for describing stability problems cannot be guaranteed to be Hermitian.

5.3.3.2 Crout decomposition

The Crout decomposition exists for all non-singular square matrices. Since LU decompositions are not unique, some properties which are useful can be specified. Crout specifies that the upper matrix has ones on its leading diagonal:

$$A = LU = \begin{bmatrix} l_{11} & 0 & 0 \\ l_{21} & l_{22} & 0 \\ l_{31} & l_{32} & l_{33} \end{bmatrix} \begin{bmatrix} 1 & u_{12} & u_{13} \\ 0 & 1 & u_{23} \\ 0 & 0 & 1 \end{bmatrix} = \begin{bmatrix} a_{11} & a_{12} & a_{13} \\ a_{21} & a_{22} & a_{23} \\ a_{31} & a_{32} & a_{33} \end{bmatrix} \quad (5.23)$$

The unknown entries of L and U can be computed using the definition of the dot product used in matrix multiplication.

5.3.3.3 Doolittle decomposition

The Doolittle decomposition is formed in the exact same way as the Crout, except that instead of the ones making up the leading diagonal of U, they make up the leading diagonal of L:

$$A = LU = \begin{bmatrix} 1 & 0 & 0 \\ l_{21} & 1 & 0 \\ l_{31} & l_{32} & 1 \end{bmatrix} \begin{bmatrix} u_{11} & u_{12} & u_{13} \\ 0 & 1_{22} & u_{23} \\ 0 & 0 & u_{33} \end{bmatrix} = \begin{bmatrix} a_{11} & a_{12} & a_{13} \\ a_{21} & a_{22} & a_{23} \\ a_{31} & a_{32} & a_{33} \end{bmatrix} \quad (5.24)$$

5.4 Numerical methods used in the present analysis

There are plenty of numerical processes available. The code developed as part of the present work uses the compact difference scheme to discretise the primitive variable problem, and the rectangular matrix is squared off using the method suggested in § 5.2.2.3. This matrix system is inverted using a modified Doolittle decomposition implemented in the Eigen C++ library [17] which achieves greater efficiency by exploiting the sparsity of the system. The final boundary condition is checked using a Newton-Raphson scheme.

Chapter 6

Code Development

A code has been developed which implements the non-parallel approach which has been outlined. In order to do this, it of course must have the capability to solve linear stability problems and their adjoints. This chapter will discuss some of the challenges involved with developing such a code, and present the strategies used to overcome them.

6.1 Parameter space

To predict the onset of turbulence using linear stability, typically the growth rate of a particular wave is tracked as it develops downstream. When this reaches some critical value, that location is said to be the start of the transitional region or the turbulent region. Of course there are many waves all influencing the same boundary layer at the same time. This means they must all be tracked, or that those which are the most likely to cause transition must be identified and all of those must be tracked. If the problem under consideration involves only purely two-dimensional stability, a contour of amplification against frequency and chordwise position can be plotted:

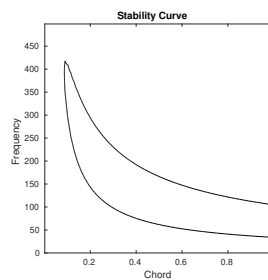


Figure 6.1: Parameter Space in 2D

If N-factors are calculated, these can all be superimposed together to show the maximum at each chordwise location.

However in three dimensions things get much more complex. Waves that may share a frequency but travel in different directions must be considered, and it may also be required to observe waves at different spanwise positions. This more complex parameter space is a grid of grids.

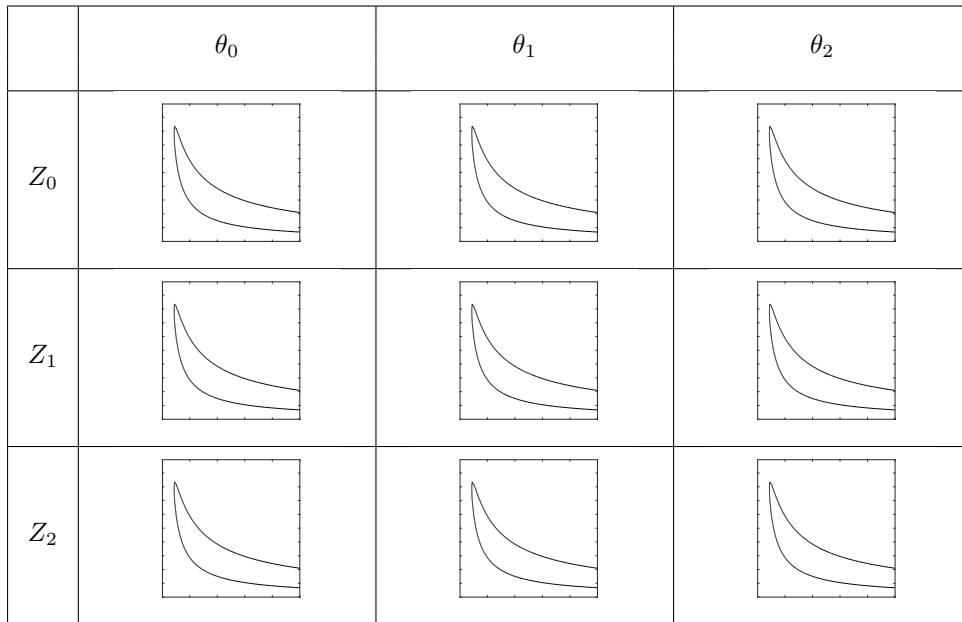


Figure 6.2: Parameter Space in full 3D

In practice however, the space is not fully explored. For each frequency there is a band of angles with likely transition candidates, and only these bands are analysed. Maximal N-factors are still superimposed as with the 2D case. The possibility of calculating stability at differing spanwise positions has been suggested in Chapter 7. Since corrected growth rates are of concern in the present work, at every point in this space where there is an eigenvalue, there is also a correction to consider.

6.2 Navigating the $Re - \omega$ plane

For certain numerical root-finding methods, convergence on the correct solution can be dependent on the choice of initial guess. Even if this radius of convergence is large, it is still beneficial to supply a guess that is close to the solution, since this will usually result in fewer iterations and therefore faster convergence. A particularly useful way of ensuring the guess is suitable, is to use the solution from a nearby point in the $Re - \omega$ plane. This is especially useful for similar flow boundary layers where the velocity profile can remain constant and only Re and ω change. A parametric space filling curve may prove useful by guaranteeing that each $Re - \omega$ pair is reasonably close to the previous one. Under the assumption that wavenumber is an analytical function of Reynolds number and frequency, this should mean that the previous solution is sufficiently good as an initial guess.

6.2.1 Space filling curves

A function is sought which will fill the entire $Re - \omega$ plane with data points in a useful pattern. The pattern should provide a sequence of points which fill the plane, in which each subsequent point is reasonably close (in the plane) to its neighbours in the sequence.

6.2.1.1 The Archimedean spiral

As a first approximation the Archimedean spiral (shown in fig. 6.3) was used. It has the parametric equation:

$$x = \theta \cos \theta \tag{6.1a}$$

$$y = \theta \sin \theta \tag{6.1b}$$

6.2.1.2 Squaring the spiral

A spiral such as this leaves large areas in the corners of the plane completely empty. A scaling function $f_s(\theta)$ is needed to stretch out the corners of the circle whilst leaving the edge midpoints

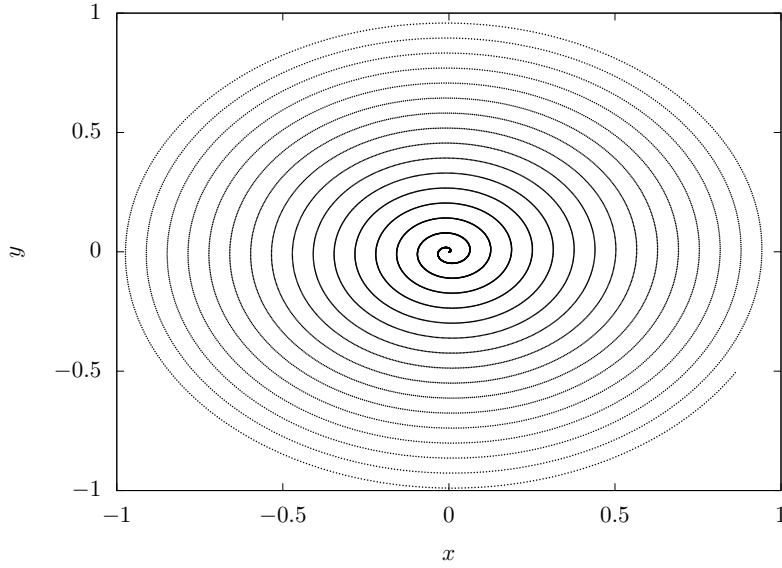


Figure 6.3: Archimedean spiral

as they are. This condition is described by:

$$\theta = \frac{n\pi}{2}, n \in \mathbb{Z} \rightarrow f_s = 1 \quad (6.2a)$$

$$\theta = \frac{n\pi}{2} + \frac{\pi}{4}, n \in \mathbb{Z} \rightarrow f_s = \sqrt{2} \quad (6.2b)$$

As long as these conditions are satisfied and the function is well behaved in between, it will suitably fill the corners of the plane. The following function which fits the criteria is deduced:

$$f_s(\theta) = \sqrt{1 + |\cos(2\theta)|} \quad (6.3)$$

Its curve is shown in fig. 6.4. Its points are shown in fig. 6.5: When applied to the Archimedean spiral, its equations become:

$$x = \frac{\theta}{f_s} \cos \theta, \quad y = \frac{\theta}{f_s} \sin \theta \quad (6.4)$$

6.2.1.3 Fitting the curve to the problem

The curve must now be rescaled to fit the stability plane, which might extend, for example, from 0 to 5000 on the horizontal (Reynolds number) axis and from 0 to 0.15 on the vertical (frequency)

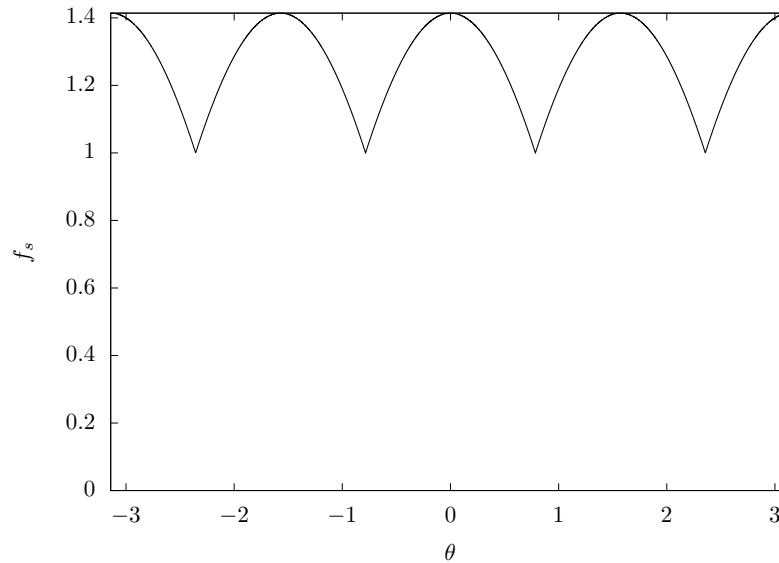


Figure 6.4: Corner scaling function

axis. The central value in fig. 6.6 marks a point whose eigenvalue should already be known, and could be used as a starting point.

6.2.1.4 Correcting the point distribution

Immediately it is clear from fig. 6.6 that this spiral unfairly selects too many points near the centre, and far fewer further away, this can be rectified by altering the distribution of θ , from linear to parabolic, which gives rise to the points shown in fig. 6.7. This new plot shows a more uniform point density along the spiral.

6.2.1.5 Correcting the spiral pitch

Finally it is clear that the distance between points along the curve is much smaller than the length of the spiral pitch, this can be corrected using a pitch scaling factor. This is chosen based on the total number of points in the plane. The scaling factor is most effective when the relation between the two is:

$$f_p = \pi\sqrt{N} \tag{6.5}$$

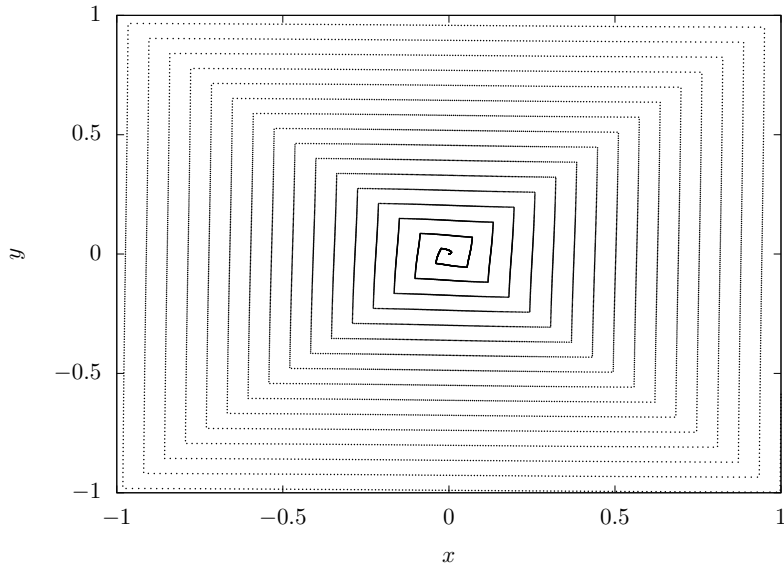


Figure 6.5: Squared spiral

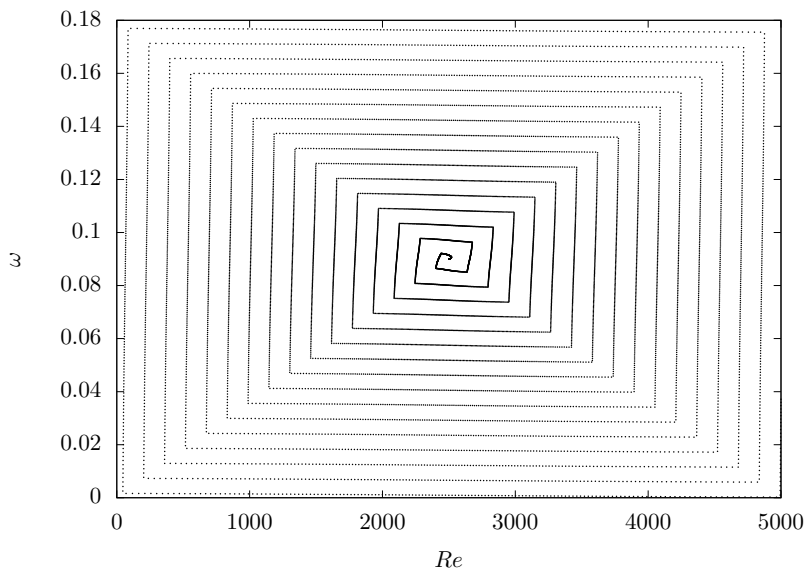


Figure 6.6: Rescaled squared spiral

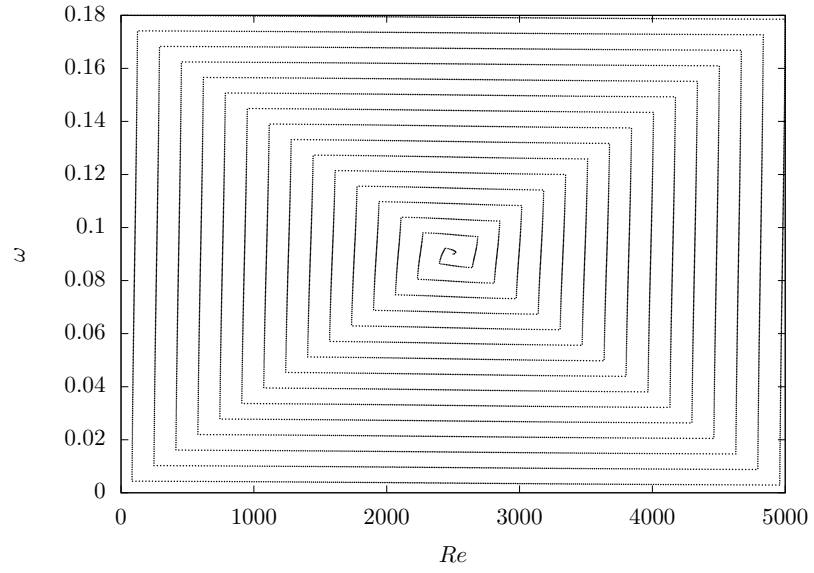


Figure 6.7: Rescaled squared spiral with corrected point distribution

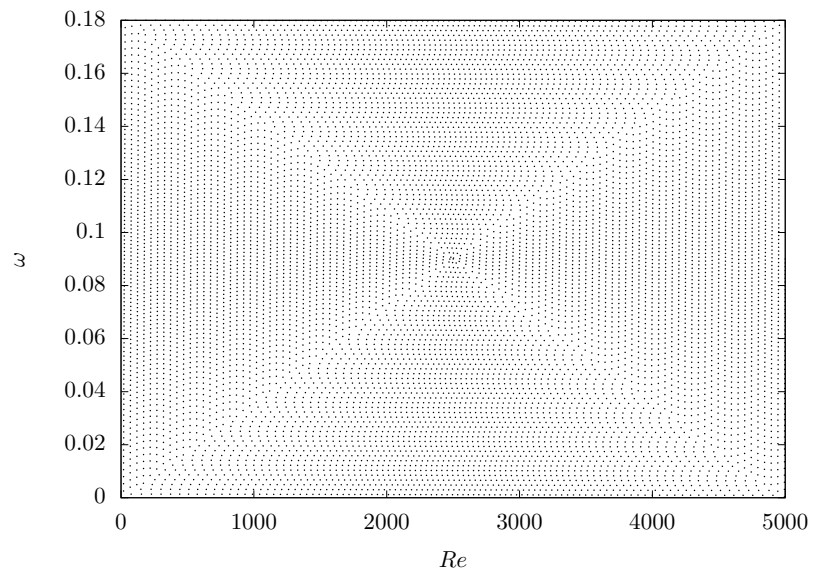


Figure 6.8: Rescaled squared spiral with corrected point distribution and corrected pitch

Now the structure of the spiral has become difficult to see, but the points are much more evenly distributed in the plane. A short MATLAB script which can be used to generate these points is:

```

1      %% SquareSpiral.m
2      % resolution and centre
3      n = 10000 ;
4      c = [2500, 0.09] ;
5
6      % pitch scaling factor
7      PSF = sqrt(n) * pi ;
8
9      % theta distribution
10     % t = linspace(0,2*pi,n)
11     t = zeros(n,1) ;
12     for i = 1:length(t) ;
13         t(i) = -1 + sqrt(i) ;
14     end
15     t = t / max([max(t), abs(min(t))]);
16
17     % Corner scaling factor
18     CSF = (1 + abs(cos(2 * PSF * t))).^(1/2);
19
20     % x and y coordinates
21     x = t .* cos(PSF * t) ./ CSF ;
22     x = x ./ max(abs(x)) * c(1) + c(1) ;
23     y = t .* sin(PSF * t) ./ CSF ;
24     y = y ./ max(abs(y)) * c(2) + c(2) ;

```

6.2.2 Intelligent navigation

The kind of shape filling curve described works extremely well when calculating stability curves for boundary layers with similarity solutions. However, for a real aerofoil with a varying pressure gradient this would mean also calculating a new base flow for every point. Clearly it would be beneficial to choose a smaller number of stations and calculate velocity profiles at these points, then use only these for stability calculations. A different scheme is employed that uses fixed chordwise locations, and fixed frequencies; starting at some point in the plane likely to have the most amplification, and working outwards in both directions from there.

6.2.2.1 Initial points

Assuming there are a predetermined number of stations, where the base flow velocity profiles and Reynolds numbers are known, these can be scanned and a suitable profile selected. Typically it

is of benefit to choose a profile for which a reasonable initial guess can be made with no prior calculations.

6.2.2.2 Subsequent points

After the initial eigenvalue is calculated, there is a choice to be made of where in the plane to attempt the next calculation; it is possible to move to a different frequency, or a different station. The present code will first move to another frequency, since the current point solution will likely be a better initial guess than if moving to a new station. Only after all frequencies have been exhausted at a particular station will it move to the next. The first frequency chosen at the new station is the one likely to be the most amplified. This is found by looking back at all the eigenvalues from the previous station.

6.3 Outside the $Re - \omega$ plane

Outside of the $Re - \omega$ plane, the navigation strategy is much simpler. The code begins with a wave angle of zero, and moves through the angles getting progressively larger. Every time a new angle is taken, a new stability curve can be drawn. The first point in each new curve is selected by identifying the most amplified point in the previous curve, and using the corresponding eigenvalue as the initial guess. As long as the step in angle isn't too large, this approach is quite successful.

The same kind of approach could be taken for spanwise position. Calculate everything for the previous set of curves, move to the next spanwise position and start again at angle zero. If the wing geometry at the new spanwise location is reasonably similar to the last, then this method is valid. A significant change in geometry however, would require either something more sophisticated, or for a new known value to be supplied.

6.4 Data structures

A number of classes have been developed, which are intended to make the code much more readable, and encourage proper encapsulation. Stability problems are complicated and involve a large amount of data, so this approach is vital.

6.4.1 Base flow data

6.4.1.1 A point in space

The smallest class employed is ‘D0’. It represents a point in space and contains information about how the base flow behaves. Specifically, velocities in each direction, their wall-normal derivatives, their wall-normal second derivatives, their chordwise derivatives, and their spanwise derivatives. It also contains the distance of the point from the wall.

6.4.1.2 A velocity profile

The class ‘D1’ represents a velocity profile, it’s most important component is an array containing many of ‘D0’. In addition it contains information which is specific to the particular velocity profile, Reynolds number, displacement thickness, distance from the leading edge, and other such quantities. Also included in this class is a method for interpolating the profile, should a different point distribution be desired.

6.4.1.3 A 2D boundary layer

The class ‘D2’ represents a sequence of velocity profiles. It consists of an array, storing many of ‘D1’, and all the data that is specific for a particular boundary layer, most notably: chord length, and the spanwise location of the layer.

6.4.1.4 A 3D boundary layer

The class ‘D3’ represents a sequence of 2D layers. It is constructed in the same way as ‘D2’ and includes information specific to a whole wing, most importantly, free stream velocity. This class

also reads data from external sources. It has access to all the smaller objects and can populate them with data.

6.4.2 Disturbance data

The class ‘Mode’ describes the behaviour of a wave. Its frequency and spanwise wavenumber are included, as are methods for converting these to and from non-dimensional form. This class also contains an array of ‘GrowthQuants’ which is discussed in § 6.4.7.

6.4.3 Linear stability

The class ‘LinearStability’ is where the first calculations are performed. It can read from ‘Mode’ and ‘D1’ to construct a stability problem. Then it solves this problem, retaining the eigenvalue, and eigenfunction if required.

6.4.4 Adjoint linear stability

The class ‘AdjointLinearStability’ constructs the adjoint problem in a similar way. However, the equations can be easily expressed as a modified version of those in ‘LinearStability’. By giving ‘AdjointLinearStability’ access to ‘LinearStability’, it can copy the equations directly, then make the modifications and solve the system. Once again, eigenvalues and eigenfunctions can be retained.

6.4.5 Non-parallel correction

The non-parallel correction is calculated by ‘MultipleScales’. It can access both ‘LinearStability’, and ‘AdjointLinearStability’, both of whose eigenfunctions are needed. There are a large number of possible ways to determine the value of the correction. All of these, or just a selection can be retained.

6.4.6 Interaction between classes

The class ‘Problem’ coordinates the interactions between the other classes. It reads ‘D3’ and determines which ‘D1’ should be sent to ‘LinearStability’, ‘AdjointLinearStability’, and ‘MultipleScales’.

It has a range of options for doing this including a single eigenvalue search, stability of a single wave across a boundary layer, or stability of many waves across a boundary layer. This class implements the appropriate $Re - \omega$ navigation strategies discussed in §6.2. methods are also included here for calculating N-factors, and N-factors which have been modified by the application of the non-parallel correction.

6.4.7 Growth rate data

The class ‘GrowthQuants’ stores all of the output data from every previously mentioned class. Many instantiations of this class are stored in one instantiation of ‘Mode’, so if there are many modes under examination, envelopes can easily be calculated. Even the eigenfunctions and adjoint eigenfunctions may be stored if they are needed for later calculations.

6.5 Safety

The multiple scales method is quite complex and depends upon many prerequisites. If any one of these fails then the correction methodology will at best be wrong, and at worst could crash the code. For each step there are safety procedures built into the code which will halt the process under circumstances which are likely to cause a crash, or spurious result.

6.5.1 Linear stability

The first step of the method is the linear stability calculation. For most cases a particular wave is selected and its growth is calculated at all points in the boundary layer. If the code is scanning upstream from the initial station and finds a station with very strong damping of the wave, or an unphysical result, the upstream scan will be halted in that direction. The same rule is applied scanning downstream. A flag is raised on any station without a valid LST result.

When calculating stability curves over multiple frequencies, the code starts at some middle frequency and scans in both directions. If a frequency is found with no growth at all, the scan is halted in the appropriate direction.

6.5.2 Adjoint linear stability

If a station has not been flagged as invalid, it will be permitted to calculate an adjoint eigenfunction there. A valid LST result is an indicator of a valid adjoint LST results, but not a guarantee. A check is performed here too, that the result is still physical, and also not too strongly damped. Another additional check is in place here to ensure the result matches LST. A different flag is raised indicating any station without a valid adjoint LST result.

6.5.3 Multiple scales

If a station has valid LST and adjoint LST results, then it will be permitted to calculate a multiple scales correction. This is once again checked for physicality and an invalid flag may be raised. Further calculations (N-factor and corrected N-factors for example) are only permitted if none of the associated invalid flags are raised.

6.5.4 Coding practices

The code is written in C++ and follows the object oriented paradigm. This is done to ensure proper data encapsulation. The ‘Problem’ class which coordinates all the others is often instantiated only once, but if the user wished to set up several distinct problems (For example, using different boundary layer data) then many of these can be created to ensure that no information from an earlier case can pollute a subsequent one. The same principal is applied to modes, each ‘Mode’ has a ‘GrowthQuants’ as part of its composition, this way no growth information can move between modes without express instruction to do so.

Chapter 7

Conclusions and

Recommendations for Further

Work

7.1 Objectives

At the outset, the goals of the present work were threefold:

1. Develop mathematics capable of driving a simulation tool using the multiple scale method in fully three-dimensional boundary layers
2. Develop the simulation tool itself
3. Demonstrate the capability of the tool

As the work progressed however, another goal became clear; to resolve certain difficulties in the literature and present it in a clear, succinct way. This would itself have two separate parts:

1. To explore the distinct meanings of overloaded terminology, particularly “adjoint”
2. To explore the historical disagreements in the field, and if possible, weigh in with new insights

7.2 Technical Outcomes

The mathematics necessary for the intended tool are outlined in Chapters 2 to 4. Some further details of the derivations are given in Appendix A. It has been shown for the LST case and the adjoint LST case that the present primitive variable formulations are compatible with the Orr-Sommerfeld/adjoint Orr-Sommerfeld approaches used by Gaster [10]. Analysis in Chapter 3 shows that the adjoint stream function has an exact analogue in primitive variables, which has been called the “adjoint pressure” in Chapter 3. This has enabled the creation of a simulation package capable of calculating and displaying:

- Eigenvalues of the linear stability problem in boundary layers
- Adjoint eigenfunctions
- Multiple scale corrections¹
- Traditional N-factors

All of these are available for swept non-similar BLs, and perturbations with a relative wave angle to the inviscid streamline. In most cases we have observed that the correction term is responsible for a slight destabilisation of the wave.

Good agreement is observed with LST results from Davey[13], Gaster[10], Atkin[2]. Eigenvalues for both temporal and spatial stability are given, along with eigenfunctions, and stability curves. Adjoint results, also from Gaster [10], show very close agreement as well. Good agreement is observed between the present analysis and existing multiple scales results due to Gaster [12] for the Blasius flow. Competing methods and results from other authors have been investigated, and where appropriate, comparisons made.

7.3 Insights into the field

7.3.1 Understanding adjoints

Adjoint problems have historically been used in a number of ways². One can think of the adjoint problem as a partner to the existing direct problem. If all that are sought are solutions to an eigenvalue

¹Calculated using integrated kinetic energy, but other options may be implemented.

²Even schoolchildren learning manual matrix inversion are taught that the adjoint is the transpose of the matrix of cofactors.

problem (i.e. eigenvalues), the adjoint formulation may be used. This is because both formulations share common eigenvalues. In some cases these can even be calculated at reduced computational effort.

The adjoint solutions find great utility as sensitivities. As discussed in §3.9 the adjoint forms part of the gradient, from which the drift in eigenvalue due to a change in the structure of the problem can be calculated. Again this can sometimes come with significant benefits in terms of computational overhead.

Finally, the multiple scales method is a reformulated version of the parallel stability problem. It takes a similar form to the non-parallel, with the addition of non-homogeneous terms. We know that the solution to this can only exist where the non-homogeneous terms are orthogonal to the adjoint solution, and this condition supplies an equation which can be solved to give modified solutions.

The adjoint operator/function itself is the same in all cases and always satisfies the definition given in §3.1. Occasionally, an alternate definition is given, and this can inspire some confusion. However, in each of these cases, equation (3.1) is a more generalised version of the given alternative. Once found, the adjoint can be used in any of the aforementioned ways. In §3.10 this concept has been discussed and a new scheme has been created showing the related classes of problems, including the categorisation of the multiple scales method.

7.3.2 Historical disagreements

In Chapter 4 we discuss some of the historical controversies in the field. There have been differing opinions on a range of issues, and chief among these is the metric for amplitude for the multiple scales correction. Firstly, a part of the eigenfunction to use as a proxy for amplitude must be chosen, of course a variety of choices can be found in the literature, and different choices yield different results. As each new option was published, it invariably cast doubt upon those which came before it. Kinetic energy was chosen in this case, simply for ease of comparison with the literature. Streamwise velocity may be easier to measure directly in a wind tunnel, so this parameter really should be left to each individual investigator to select. There should be no particular difficulty in the interpretation of results using either criterion, assuming that it has correctly noted.

Secondly, the method to collapse the wall-normal distribution to a single value must be chosen. Again there is no agreement in the literature. Here the wall-normal integral is chosen for comparison.

Thirdly, the normalisation of the eigenfunction has been questioned. Several different approaches exist in literature. It has been shown that with careful calculation of the eigenfunction gradients, this choice can be rendered completely inconsequential.

Finally, and most importantly, there has been controversy over whether or not it is necessary to include this metric at all. It has been shown in Chapter 4 that the inclusion of this term can indeed affect the result significantly, and in the author's opinion, the reasons given for its exclusion are found to be unconvincing.

7.4 Recommendations for further work

As with any theoretical or computational work, there would be great value in experimentation to validate the model. This would likely need to be conducted in a low turbulence wind tunnel with a carefully selected aerofoil, and artificially generated wave. Data on the development of the wave would be collected, but also highly resolved base flow data would be necessary as an input for the simulation. Other numerical techniques could be employed too. PSEs, bi/triglobal stability, and DNS may each be useful for comparison.

The suggestions for wall-normally distinct MSM corrections would especially benefit from comparisons, experimental or otherwise. It may be possible to identify new correlations and use these to better predict transition.

Curvature has been included, but as part of the linear problem. As discussed in §4.2, it would be appropriate to include this instead with the correction terms. The computational requirements to successfully do this require further investigation and development.

Presently the boundary layer data used was generated by the 'BL2D' package, which assumed a swept-tapered geometry which is similar in the spanwise direction. Output from a tool capable of producing a fully three-dimensional boundary layer could be used to generate a more accurate picture of the state of the flow across the entire wing. Perhaps rivets or even pylons could be included in the analysis.

As with any computational undertaking, there can always be improvements made in performance and user experience. The multiple scale method is fully local, which makes it a prime candidate for parallelisation. Gaster's rapid eigenvalue method [14] might provide another good starting point for better performance. It may also be possible to better define the safety features and edge case handling.

Finally, the methodology presented could be adapted for wider use. Building this into existing industrial analysis would allow greater accuracy in transition prediction, and benefits in wing aerodynamics could result.

Appendix A

Expanded Derivations

A.1 The method of multiple scales

In § 4.1.1 the governing equations of the method of multiple scales are derived. Presented here are the full derivations, including many intermediate steps. Each equation will be dealt with separately, starting with continuity, which is shown in equation (4.1a):

A.1.1 Continuity

From the Navier-Stokes equations:

$$\frac{\partial u}{\partial x} + \frac{\partial v}{\partial y} + \frac{\partial w}{\partial z} = 0$$

Decompose into base flow and perturbation using $u = U + \tilde{u}$ etc. (remember that V is small, so ϵV should be substituted, also base flow derivatives in x and z are small so $\partial\{U, V, W\}/\partial\{x, z\}$ should be substituted with $\partial\{\epsilon U, \epsilon V, \epsilon W\}/\partial\{x, z\}$):

$$\frac{\partial(\epsilon U + \tilde{u})}{\partial x} + \frac{\partial(\epsilon V + \tilde{v})}{\partial y} + \frac{\partial(\epsilon W + \tilde{w})}{\partial z} = 0$$

Expand the brackets:

$$\epsilon \frac{\partial U}{\partial x} + \frac{\partial \tilde{u}}{\partial x} + \epsilon \frac{\partial V}{\partial y} + \frac{\partial \tilde{v}}{\partial y} + \epsilon \frac{\partial W}{\partial z} + \frac{\partial \tilde{w}}{\partial z} = 0$$

Linearise in perturbations by subtracting the base flow solution:

$$\frac{\partial \tilde{u}}{\partial x} + \frac{\partial \tilde{v}}{\partial y} + \frac{\partial \tilde{w}}{\partial z} = 0$$

Expand $x = x_0 + \epsilon x_1 + \dots$ etc. for u, v, w, p, x , and z :

$$\left(\frac{\partial}{\partial x_0} + \epsilon \frac{\partial}{\partial x_1} \right) (u_0 + \epsilon u_1) + \frac{\partial}{\partial y} (v_0 + \epsilon v_1) + \left(\frac{\partial}{\partial z_0} + \epsilon \frac{\partial}{\partial z_1} \right) (w_0 + \epsilon w_1) = 0$$

Expand the brackets:

$$\frac{\partial \tilde{u}_0}{\partial x_0} + \epsilon \frac{\partial \tilde{u}_1}{\partial x_0} + \epsilon \frac{\partial \tilde{u}_0}{\partial x_1} + \frac{\partial \tilde{v}_0}{\partial y} + \epsilon \frac{\partial \tilde{v}_1}{\partial y} + \frac{\partial \tilde{w}_0}{\partial z_0} + \epsilon \frac{\partial \tilde{w}_1}{\partial z_0} + \epsilon \frac{\partial \tilde{w}_0}{\partial z_1} + \dots = 0$$

Split the equation using similar powers of ϵ , ignoring higher powers than 1:

$$\begin{aligned} \epsilon^0 \left\{ \frac{\partial \tilde{u}_0}{\partial x_0} + \frac{\partial \tilde{v}_0}{\partial y} + \frac{\partial \tilde{w}_0}{\partial z_0} = 0 \right. \\ \left. \epsilon^1 \left\{ \frac{\partial \tilde{u}_1}{\partial x_0} + \frac{\partial \tilde{v}_1}{\partial y} + \frac{\partial \tilde{w}_1}{\partial z_0} = -\frac{\partial \tilde{u}_0}{\partial x_1} - \frac{\partial \tilde{w}_0}{\partial z_1} \right. \right. \end{aligned}$$

Apply the assumption that the perturbation behaves as a wave when seen in the x , and z directions, but not in y ($[\tilde{u}, \tilde{v}, \tilde{w}, \tilde{p}](x, y, z, t) = [\hat{u}, \hat{v}, \hat{w}, \hat{p}](y)e^{i(\alpha x + \beta z - \omega t)}$):

$$\begin{aligned} \frac{\partial \hat{u}_0 e^{i(\alpha x + \beta z - \omega t)}}{\partial x_0} + \frac{\partial \hat{v}_0 e^{i(\alpha x + \beta z - \omega t)}}{\partial y} + \frac{\partial \hat{w}_0 e^{i(\alpha x + \beta z - \omega t)}}{\partial z_0} = 0 \\ \frac{\partial \hat{u}_1 e^{i(\alpha x + \beta z - \omega t)}}{\partial x_0} + \frac{\partial \hat{v}_1 e^{i(\alpha x + \beta z - \omega t)}}{\partial y} + \frac{\partial \hat{w}_1 e^{i(\alpha x + \beta z - \omega t)}}{\partial z_0} = -\frac{\partial \hat{u}_0 e^{i(\alpha x + \beta z - \omega t)}}{\partial x_1} - \frac{\partial \hat{w}_0 e^{i(\alpha x + \beta z - \omega t)}}{\partial z_1} \end{aligned}$$

Now certain derivatives can be separated. This will leave the equation with every term still having a common factor in $e^{i(\alpha x + \beta z - \omega t)}$. This can be divided through:

$$\begin{aligned} i\alpha \hat{u}_0 + \hat{v}'_0 + i\beta \hat{w}_0 = 0 \\ i\alpha \hat{u}_1 + \hat{v}'_1 + i\beta \hat{w}_1 = -\frac{\partial \hat{u}_0}{\partial x_1} - \frac{\partial \hat{w}_0}{\partial z_1} \end{aligned}$$

The following manipulations and derivatives will be needed later :

$$\hat{v}'_0 = -i\alpha \hat{u}_0 - i\beta \hat{w}_0 \quad (\text{A.1a})$$

$$\hat{v}''_0 = -i\alpha \hat{u}'_0 - i\beta \hat{w}'_0 \quad (\text{A.1b})$$

$$\hat{v}''_1 = -i\alpha \hat{u}'_1 - i\beta \hat{w}'_1 - \frac{\partial \hat{u}'_0}{\partial x_1} - \frac{\partial \hat{w}'_0}{\partial z_1} \quad (\text{A.1c})$$

A.1.2 Momentum (\mathbf{u})

From Navier-Stokes (equation (4.1b)):

$$\frac{\partial u}{\partial t} + u \frac{\partial u}{\partial x} + v \frac{\partial u}{\partial y} + w \frac{\partial u}{\partial z} = -\frac{\partial p}{\partial x} + \frac{1}{Re} \left(\frac{\partial^2 u}{\partial x^2} + \frac{\partial^2 u}{\partial y^2} + \frac{\partial^2 u}{\partial z^2} \right)$$

Decompose into base flow and perturbation using $u = U + \tilde{u}$ etc. (remember that V is small, so ϵV should be substituted, also base flow derivatives in x and z are small so $\partial\{U, V, W, P\}/\partial\{x, z\}$ should be substituted with $\partial\{\epsilon U, \epsilon V, \epsilon W, \epsilon P\}/\partial\{x, z\}$):

$$\begin{aligned} \frac{\partial(U + \tilde{u})}{\partial t} + (U + \tilde{u}) \frac{\partial(\epsilon U + \tilde{u})}{\partial x} + (\epsilon V + \tilde{v}) \frac{\partial(U + \tilde{u})}{\partial y} + (W + \tilde{w}) \frac{\partial(\epsilon U + \tilde{u})}{\partial z} = \\ -\frac{\partial(\epsilon P + \tilde{p})}{\partial x} + \frac{1}{Re} \left(\frac{\partial^2(\epsilon^2 U + \tilde{u})}{\partial x^2} + \frac{\partial^2(U + \tilde{u})}{\partial y^2} + \frac{\partial^2(\epsilon^2 U + \tilde{u})}{\partial z^2} \right) \end{aligned}$$

Expand the brackets:

$$\begin{aligned} \frac{\partial U}{\partial t} + \frac{\partial \tilde{u}}{\partial t} + \epsilon U \frac{\partial U}{\partial x} + \epsilon \tilde{u} \frac{\partial U}{\partial x} + U \frac{\partial \tilde{u}}{\partial x} + \tilde{u} \frac{\partial \tilde{u}}{\partial x} \\ + \epsilon V \frac{\partial U}{\partial y} + \epsilon \tilde{v} \frac{\partial U}{\partial y} + \epsilon V \frac{\partial \tilde{u}}{\partial y} + \tilde{v} \frac{\partial \tilde{u}}{\partial y} \\ + \epsilon W \frac{\partial U}{\partial z} + \epsilon \tilde{w} \frac{\partial U}{\partial z} + W \frac{\partial \tilde{u}}{\partial z} + \tilde{w} \frac{\partial \tilde{u}}{\partial z} = \\ -\epsilon \frac{\partial P}{\partial x} - \frac{\partial \tilde{p}}{\partial x} + \frac{1}{Re} \left(\epsilon^2 \frac{\partial^2 U}{\partial x^2} + \frac{\partial^2 \tilde{u}}{\partial x^2} + \frac{\partial^2 U}{\partial y^2} + \frac{\partial^2 \tilde{u}}{\partial y^2} + \epsilon^2 \frac{\partial^2 U}{\partial z^2} + \frac{\partial^2 \tilde{u}}{\partial z^2} \right) \end{aligned}$$

Linearise in perturbations by subtracting the base flow solution and neglecting products of two perturbations:

$$\frac{\partial \tilde{u}}{\partial t} + \epsilon \tilde{u} \frac{\partial U}{\partial x} + U \frac{\partial \tilde{u}}{\partial x} + \epsilon \tilde{v} \frac{\partial U}{\partial y} + \epsilon V \frac{\partial \tilde{u}}{\partial y} + \epsilon \tilde{w} \frac{\partial U}{\partial z} + W \frac{\partial \tilde{u}}{\partial z} = -\frac{\partial \tilde{p}}{\partial x} + \frac{1}{Re} \left(\frac{\partial^2 \tilde{u}}{\partial x^2} + \frac{\partial^2 \tilde{u}}{\partial y^2} + \frac{\partial^2 \tilde{u}}{\partial z^2} \right)$$

Expand $x = x_0 + \epsilon x_1 + \dots$ etc. for u, v, w, p, x , and z :

$$\begin{aligned}
& \frac{\partial(\tilde{u}_0 + \epsilon\tilde{u}_1)}{\partial t} + \epsilon(\tilde{u}_0 + \epsilon\tilde{u}_1) \left(\frac{\partial}{\partial x_0} + \epsilon \frac{\partial}{\partial x_1} \right) U + U \left(\frac{\partial}{\partial x_0} + \epsilon \frac{\partial}{\partial x_1} \right) (\tilde{u}_0 + \epsilon\tilde{u}_1) \\
& \quad + \epsilon(\tilde{v}_0 + \epsilon\tilde{v}_1) \frac{\partial}{\partial y} + \epsilon V \frac{\partial}{\partial y} (\tilde{u}_0 + \epsilon\tilde{u}_1) \\
& \quad + \epsilon(\tilde{w}_0 + \epsilon\tilde{w}_1) \left(\frac{\partial}{\partial z_0} + \epsilon \frac{\partial}{\partial z_1} \right) U + W \left(\frac{\partial}{\partial z_0} + \epsilon \frac{\partial}{\partial z_1} \right) (\tilde{u}_0 + \epsilon\tilde{u}_1) = \\
& - \left(\frac{\partial}{\partial x_0} + \epsilon \frac{\partial}{\partial x_1} \right) (p_0 + \epsilon p_1) + \frac{1}{Re} \left(\left(\frac{\partial}{\partial x_0} + \epsilon \frac{\partial}{\partial x_1} \right) \left(\frac{\partial}{\partial x_0} + \epsilon \frac{\partial}{\partial x_1} \right) (\tilde{u}_0 + \epsilon\tilde{u}_1) \right. \\
& \quad \left. + \frac{\partial^2}{\partial y^2} (\tilde{u}_0 + \epsilon\tilde{u}_1) + \left(\frac{\partial}{\partial x_0} + \epsilon \frac{\partial}{\partial x_1} \right) \left(\frac{\partial}{\partial x_0} + \epsilon \frac{\partial}{\partial x_1} \right) (\tilde{u}_0 + \epsilon\tilde{u}_1) \right)
\end{aligned}$$

Expand the brackets:

$$\begin{aligned}
& + \frac{\partial\tilde{u}_0}{\partial t} + \epsilon \frac{\partial\tilde{u}_1}{\partial t} + U \frac{\partial\tilde{u}_0}{\partial x_0} + \epsilon U \frac{\partial\tilde{u}_0}{\partial x_1} + \epsilon U \frac{\partial\tilde{u}_1}{\partial x_0} + \epsilon^2 U \frac{\partial\tilde{u}_1}{\partial x_1} \\
& \quad + \epsilon \frac{\partial U}{\partial x_0} \tilde{u}_0 + \epsilon^2 \frac{\partial U}{\partial x_1} \tilde{u}_0 + \epsilon^2 \frac{\partial U}{\partial x_0} \tilde{u}_1 + \epsilon^3 \frac{\partial U}{\partial x_1} \tilde{u}_1 \\
& \quad + \epsilon V \frac{\partial\tilde{u}_0}{\partial y} + \epsilon^2 V \frac{\partial\tilde{u}_1}{\partial y} + \frac{\partial U}{\partial y} \tilde{v}_0 + \epsilon \frac{\partial U}{\partial y} \tilde{v}_1 \\
& \quad + W \frac{\partial\tilde{u}_0}{\partial z_0} + \epsilon W \frac{\partial\tilde{u}_0}{\partial z_1} + \epsilon W \frac{\partial\tilde{u}_1}{\partial z_0} + \epsilon^2 W \frac{\partial\tilde{u}_1}{\partial z_1} \\
& \quad + \epsilon \frac{\partial U}{\partial z_0} \tilde{w}_0 + \epsilon^2 \frac{\partial U}{\partial z_1} \tilde{w}_0 + \epsilon^2 \frac{\partial U}{\partial z_0} \tilde{w}_1 + \epsilon^3 \frac{\partial U}{\partial z_1} \tilde{w}_1 \\
& \quad + \frac{\partial\tilde{p}_0}{\partial x_0} + \epsilon \frac{\partial\tilde{p}_0}{\partial x_1} + \epsilon \frac{\partial\tilde{p}_1}{\partial x_0} + \epsilon^2 \frac{\partial\tilde{p}_1}{\partial x_1} \\
& - \frac{1}{Re} \left(+ \frac{\partial^2\tilde{u}_0}{\partial x_0^2} + \epsilon \frac{\partial^2\tilde{u}_0}{\partial x_0\partial x_1} + \epsilon \frac{\partial^2\tilde{u}_1}{\partial x_0^2} + \epsilon^2 \frac{\partial^2\tilde{u}_1}{\partial x_0\partial x_1} + \epsilon \frac{\partial^2\tilde{u}_0}{\partial x_0\partial x_1} + \epsilon^2 \frac{\partial^2\tilde{u}_0}{\partial x_1^2} + \epsilon^2 \frac{\partial^2\tilde{u}_1}{\partial x_0\partial x_1} + \epsilon^3 \frac{\partial^2\tilde{u}_1}{\partial x_1^2} \right. \\
& \quad \left. + \frac{\partial^2\tilde{u}_0}{\partial y^2} + \epsilon \frac{\partial^2\tilde{u}_1}{\partial y^2} \right. \\
& \quad \left. + \frac{\partial^2\tilde{u}_0}{\partial z_0^2} + \epsilon \frac{\partial^2\tilde{u}_0}{\partial z_0\partial z_1} + \epsilon \frac{\partial^2\tilde{u}_1}{\partial z_0^2} + \epsilon^2 \frac{\partial^2\tilde{u}_1}{\partial z_0\partial z_1} + \epsilon \frac{\partial^2\tilde{u}_0}{\partial z_0\partial z_1} + \epsilon^2 \frac{\partial^2\tilde{u}_0}{\partial z_1^2} + \epsilon^2 \frac{\partial^2\tilde{u}_1}{\partial z_0\partial z_1} + \epsilon^3 \frac{\partial^2\tilde{u}_1}{\partial z_1^2} \right) = 0
\end{aligned}$$

Split the equation using similar powers of ϵ , ignoring higher powers than 1:

$$\begin{aligned}
\epsilon^0 : & \left\{ \frac{\partial\tilde{u}_0}{\partial t} + U \frac{\partial\tilde{u}_0}{\partial x_0} + \tilde{v}_0 \frac{\partial U}{\partial y} + W \frac{\partial\tilde{u}_0}{\partial z_0} + \frac{\partial\tilde{p}_0}{\partial x_0} - \frac{1}{Re} \left(\frac{\partial^2\tilde{u}_0}{\partial x_0^2} + \frac{\partial^2\tilde{u}_0}{\partial y^2} + \frac{\partial^2\tilde{u}_0}{\partial z_0^2} \right) \right\} = 0 \\
\epsilon^1 : & \left\{ \frac{\partial\tilde{u}_1}{\partial t} + U \frac{\partial\tilde{u}_1}{\partial x_0} + \tilde{v}_1 \frac{\partial U}{\partial y} + W \frac{\partial\tilde{u}_1}{\partial z_0} + \frac{\partial\tilde{p}_1}{\partial x_0} - \frac{1}{Re} \left(\frac{\partial^2\tilde{u}_1}{\partial x_0^2} + \frac{\partial^2\tilde{u}_1}{\partial y^2} + \frac{\partial^2\tilde{u}_1}{\partial z_0^2} \right) \right. \\
& \quad \left. + \frac{1}{Re} \left(2 \frac{\partial^2\tilde{u}_0}{\partial x_0\partial x_1} + 2 \frac{\partial^2\tilde{u}_0}{\partial z_0\partial z_1} \right) - U \frac{\partial\tilde{u}_0}{\partial x_1} - \tilde{u}_0 \frac{\partial U}{\partial x_0} - V \frac{\partial\tilde{u}_0}{\partial y} - W \frac{\partial\tilde{u}_0}{\partial z_1} - \tilde{w}_0 \frac{\partial U}{\partial z_0} - \frac{\partial\tilde{p}_0}{\partial x_1} \right\} = 0
\end{aligned}$$

Apply the assumption that the perturbation behaves as a wave when seen in the x , and z directions, but not in y ($[\tilde{u}, \tilde{v}, \tilde{w}, \tilde{p}](x, y, z, t) = [\hat{u}, \hat{v}, \hat{w}, \hat{p}](y)e^{i(\alpha x + \beta z - \omega t)}$):

$$\begin{aligned} & \frac{\partial \hat{u}_0 e^{i\phi}}{\partial t} + U \frac{\partial \hat{u}_0 e^{i\phi}}{\partial x_0} + \hat{v}_0 e^{i\phi} \frac{\partial U}{\partial y} + W \frac{\partial \hat{u}_0 e^{i\phi}}{\partial z_0} + \frac{\partial \hat{p}_0 e^{i\phi}}{\partial x_0} - \frac{1}{Re} \left(\frac{\partial^2 \hat{u}_0 e^{i\phi}}{\partial x_0^2} + \frac{\partial^2 \hat{u}_0 e^{i\phi}}{\partial y^2} + \frac{\partial^2 \hat{u}_0 e^{i\phi}}{\partial z_0^2} \right) = 0 \\ & \frac{\partial \hat{u}_1 e^{i\phi}}{\partial t} + U \frac{\partial \hat{u}_1 e^{i\phi}}{\partial x_0} + \hat{v}_1 e^{i\phi} \frac{\partial U}{\partial y} + W \frac{\partial \hat{u}_1 e^{i\phi}}{\partial z_0} + \frac{\partial \hat{p}_1 e^{i\phi}}{\partial x_0} - \frac{1}{Re} \left(\frac{\partial^2 \hat{u}_1 e^{i\phi}}{\partial x_0^2} + \frac{\partial^2 \hat{u}_1 e^{i\phi}}{\partial y^2} + \frac{\partial^2 \hat{u}_1 e^{i\phi}}{\partial z_0^2} \right) = \\ & \frac{1}{Re} \left(2 \frac{\partial^2 \hat{u}_0 e^{i\phi}}{\partial x_0 \partial x_1} + 2 \frac{\partial^2 \hat{u}_0 e^{i\phi}}{\partial z_0 \partial z_1} \right) - U \frac{\partial \hat{u}_0 e^{i\phi}}{\partial x_1} - \hat{u}_0 e^{i\phi} \frac{\partial U}{\partial x_0} - V \frac{\partial \hat{u}_0 e^{i\phi}}{\partial y} - W \frac{\partial \hat{u}_0 e^{i\phi}}{\partial z_1} - \hat{w}_0 e^{i\phi} \frac{\partial U}{\partial z_0} - \frac{\partial \hat{p}_0 e^{i\phi}}{\partial x_1} \end{aligned}$$

where $\phi = \alpha x + \beta z - \omega t$. Now certain derivatives can be separated. This will leave the equation with every term still having a common factor in $e^{i(\alpha x + \beta z - \omega t)}$. This can be divided through:

$$\begin{aligned} & -i\omega \hat{u}_0 + i\alpha U \hat{u}_0 + U' \hat{v}_0 + i\beta W \hat{u}_0 + i\alpha \hat{p}_0 - \frac{1}{Re} (-\alpha^2 \hat{u}_0 + \hat{u}_0'' - \beta^2 \hat{u}_0) = 0 \\ & -i\omega \hat{u}_1 + i\alpha U \hat{u}_1 + U' \hat{v}_1 + i\beta W \hat{u}_1 + i\alpha \hat{p}_1 - \frac{1}{Re} (-\alpha^2 \hat{u}_1 + \hat{u}_1'' - \beta^2 \hat{u}_1) = \\ & \frac{1}{Re} \left(2i\alpha \frac{\partial \hat{u}_0}{\partial x_1} + 2i\beta \frac{\partial \hat{u}_0}{\partial z_1} \right) - U \frac{\partial \hat{u}_0}{\partial x_1} - \frac{\partial U}{\partial x_0} \hat{u}_0 - V \hat{u}_0' - W \frac{\partial \hat{u}_0}{\partial x_1} - \frac{\partial U}{\partial z_0} \hat{w}_0 - \frac{\partial \hat{p}_0}{\partial x_1} \end{aligned}$$

A.1.3 Momentum (v)

From Navier-Stokes(equation (4.1c)):

$$\frac{\partial v}{\partial t} + u \frac{\partial v}{\partial x} + v \frac{\partial v}{\partial y} + w \frac{\partial v}{\partial z} = -\frac{\partial p}{\partial y} + \frac{1}{Re} \left(\frac{\partial^2 v}{\partial x^2} + \frac{\partial^2 v}{\partial y^2} + \frac{\partial^2 v}{\partial z^2} \right)$$

Decompose into base flow and perturbation using $u = U + \tilde{u}$ etc. (remember that V is small, so ϵV should be substituted, also base flow derivatives in x and z are small so $\partial\{U, V, W, P\}/\partial\{x, z\}$ should be substituted with $\partial\{\epsilon U, \epsilon V, \epsilon W, \epsilon P\}/\partial\{x, z\}$):

$$\begin{aligned} \frac{\partial(\epsilon V + \tilde{v})}{\partial t} + (U + \tilde{u}) \frac{\partial(\epsilon^2 V + \tilde{v})}{\partial x} + (\epsilon V + \tilde{v}) \frac{\partial(\epsilon V + \tilde{v})}{\partial y} + (W + \tilde{w}) \frac{\partial(\epsilon^2 V + \tilde{v})}{\partial z} = \\ -\frac{\partial(\epsilon P + \tilde{p})}{\partial y} + \frac{1}{Re} \left(\frac{\partial^2(\epsilon^3 V + \tilde{v})}{\partial x^2} + \frac{\partial^2(\epsilon V + \tilde{v})}{\partial y^2} + \frac{\partial^2(\epsilon^3 V + \tilde{v})}{\partial z^2} \right) \end{aligned}$$

Expand the brackets:

$$\begin{aligned} \epsilon \frac{\partial V}{\partial t} + \frac{\partial \tilde{v}}{\partial t} + \epsilon^2 U \frac{\partial V}{\partial x} + U \frac{\partial \tilde{v}}{\partial x} + \epsilon^2 \tilde{u} \frac{\partial V}{\partial x} + \tilde{u} \frac{\partial v}{\partial x} \\ + \epsilon^2 V \frac{\partial V}{\partial y} + \epsilon V \frac{\partial \tilde{v}}{\partial y} + \epsilon \tilde{v} \frac{\partial V}{\partial y} + \tilde{v} \frac{\partial v}{\partial y} + \epsilon^2 W \frac{\partial V}{\partial z} + W \frac{\partial \tilde{v}}{\partial z} + \epsilon^2 \tilde{w} \frac{\partial V}{\partial z} + \tilde{w} \frac{\partial v}{\partial z} = \\ + \epsilon \frac{\partial P}{\partial y} + \frac{\partial \tilde{p}}{\partial y} + \frac{1}{Re} \left(\epsilon^3 \frac{\partial^2 V}{\partial x^2} + \frac{\partial \tilde{v}}{\partial x} + \epsilon \frac{\partial^2 V}{\partial y^2} + \frac{\partial \tilde{v}}{\partial y} + \epsilon^3 \frac{\partial^2 V}{\partial z^2} + \frac{\partial \tilde{v}}{\partial z} \right) \end{aligned}$$

Linearise in perturbations by subtracting the base flow solution and neglecting products of perturbations:

$$\frac{\partial \tilde{v}}{\partial t} + U \frac{\partial \tilde{v}}{\partial x} + \epsilon^2 \tilde{u} \frac{\partial V}{\partial x} + \epsilon V \frac{\partial \tilde{v}}{\partial y} + \epsilon \tilde{v} \frac{\partial V}{\partial y} + W \frac{\partial \tilde{v}}{\partial z} + \epsilon^2 \tilde{w} \frac{\partial V}{\partial z} = + \frac{\partial \tilde{p}}{\partial y} + \frac{1}{Re} \left(+ \frac{\partial \tilde{v}}{\partial x} + \frac{\partial \tilde{v}}{\partial y} + \frac{\partial \tilde{v}}{\partial z} \right)$$

Expand $x = x_0 + \epsilon x_1 + \dots$ etc. for u, v, w, p, x , and z :

$$\begin{aligned}
& \frac{\partial(\tilde{v}_0 + \epsilon\tilde{v}_1)}{\partial t} + U \left(\frac{\partial}{\partial x_0} + \epsilon \frac{\partial}{\partial x_1} \right) (\tilde{v}_0 + \epsilon\tilde{v}_1) + \epsilon^2 (\tilde{u}_0 + \epsilon\tilde{u}_1) \frac{\partial V}{\partial x} \\
& \quad + \epsilon V \frac{\partial}{\partial y} (\tilde{v}_0 + \epsilon\tilde{v}_1) + \epsilon (\tilde{v}_0 + \epsilon\tilde{v}_1) \frac{\partial V}{\partial y} \\
& \quad + W \left(\frac{\partial}{\partial z_0} + \epsilon \frac{\partial}{\partial z_1} \right) (\tilde{v}_0 + \epsilon\tilde{v}_1) + \epsilon^2 (\tilde{w}_0 + \epsilon\tilde{w}_1) \frac{\partial V}{\partial z} = \\
& + \frac{\partial(\tilde{p}_0 + \epsilon\tilde{p}_1)}{\partial y} + \frac{1}{Re} \left(\left(\frac{\partial}{\partial x_0} + \epsilon \frac{\partial}{\partial x_1} \right) \left(\frac{\partial}{\partial x_0} + \epsilon \frac{\partial}{\partial x_1} \right) (v_0 + \epsilon v_1) \right. \\
& \quad \left. + \frac{\partial^2}{\partial y^2} (v_0 + \epsilon v_1) + \left(\frac{\partial}{\partial z_0} + \epsilon \frac{\partial}{\partial z_1} \right) \left(\frac{\partial}{\partial z_0} + \epsilon \frac{\partial}{\partial z_1} \right) (v_0 + \epsilon v_1) \right)
\end{aligned}$$

Expand the brackets:

$$\begin{aligned}
& + \frac{\partial\tilde{v}_0}{\partial t} + \epsilon \frac{\partial\tilde{v}_1}{\partial t} + U \frac{\partial\tilde{v}_0}{\partial x_0} + \epsilon U \frac{\partial\tilde{v}_0}{\partial x_1} + \epsilon U \frac{\partial\tilde{v}_1}{\partial x_0} + \epsilon^2 U \frac{\partial\tilde{v}_1}{\partial x_1} \\
& \quad + \epsilon^2 \frac{\partial V}{\partial x_0} \tilde{u}_0 + \epsilon^3 \frac{\partial V}{\partial x_1} \tilde{u}_1 \\
& \quad + \epsilon V \frac{\partial\tilde{v}_0}{\partial y} + \epsilon^2 V \frac{\partial\tilde{v}_1}{\partial y} + \epsilon \frac{\partial V}{\partial y} \tilde{v}_0 + \epsilon^2 \frac{\partial V}{\partial y} \tilde{v}_1 \\
& + W \frac{\partial\tilde{v}_0}{\partial z_0} + \epsilon W \frac{\partial\tilde{v}_0}{\partial z_1} + \epsilon W \frac{\partial\tilde{v}_1}{\partial z_0} + \epsilon^2 W \frac{\partial\tilde{v}_1}{\partial z_1} + \epsilon^2 \frac{\partial V}{\partial z_0} \tilde{w}_0 + \epsilon^3 \frac{\partial V}{\partial z_1} \tilde{w}_1 \\
& \quad + \frac{\partial\tilde{p}_0}{\partial y} + \epsilon \frac{\partial\tilde{p}_1}{\partial y} \\
& - \frac{1}{Re} \left(+ \frac{\partial^2\tilde{v}_0}{\partial x_0^2} + \epsilon \frac{\partial^2\tilde{v}_0}{\partial x_0\partial x_1} + \epsilon \frac{\partial^2\tilde{v}_1}{\partial x_0^2} + \epsilon^2 \frac{\partial^2\tilde{v}_1}{\partial x_0\partial x_1} + \epsilon \frac{\partial^2\tilde{v}_0}{\partial x_0\partial x_1} + \epsilon^2 \frac{\partial^2\tilde{v}_0}{\partial x_1^2} + \epsilon^2 \frac{\partial^2\tilde{v}_1}{\partial x_0\partial x_1} + \epsilon^3 \frac{\partial^2\tilde{v}_1}{\partial x_1^2} \right. \\
& \quad \left. + \frac{\partial^2\tilde{v}_0}{\partial y^2} + \epsilon \frac{\partial^2\tilde{v}_1}{\partial y^2} \right. \\
& \quad \left. + \frac{\partial^2\tilde{v}_0}{\partial z_0^2} + \epsilon \frac{\partial^2\tilde{v}_0}{\partial z_0\partial z_1} + \epsilon \frac{\partial^2\tilde{v}_1}{\partial z_0^2} + \epsilon^2 \frac{\partial^2\tilde{v}_1}{\partial z_0\partial z_1} + \epsilon \frac{\partial^2\tilde{v}_0}{\partial z_0\partial z_1} + \epsilon^2 \frac{\partial^2\tilde{v}_0}{\partial z_1^2} + \epsilon^2 \frac{\partial^2\tilde{v}_1}{\partial z_0\partial z_1} + \epsilon^3 \frac{\partial^2\tilde{v}_1}{\partial z_1^2} \right) = 0
\end{aligned}$$

Split the equation using similar powers of ϵ , ignoring higher powers than 1:

$$\begin{aligned}
\epsilon^0 : & \left\{ \frac{\partial\tilde{v}_0}{\partial t} + U \frac{\partial\tilde{v}_0}{\partial x_0} + W \frac{\partial\tilde{v}_0}{\partial z_0} + \frac{\partial\tilde{p}_0}{\partial y} - \frac{1}{Re} \left(\frac{\partial^2\tilde{v}_0}{\partial x_0^2} + \frac{\partial^2\tilde{v}_0}{\partial y^2} + \frac{\partial^2\tilde{v}_0}{\partial z_0^2} \right) \right\} = 0 \\
\epsilon^1 : & \left\{ \frac{\partial\tilde{v}_0}{\partial t} + U \frac{\partial\tilde{v}_0}{\partial x_0} + W \frac{\partial\tilde{v}_0}{\partial z_0} + \frac{\partial\tilde{p}_0}{\partial y} - \frac{1}{Re} \left(\frac{\partial^2\tilde{v}_0}{\partial x_0^2} + \frac{\partial^2\tilde{v}_0}{\partial y^2} + \frac{\partial^2\tilde{v}_0}{\partial z_0^2} \right) \right. \\
& \quad \left. + \frac{1}{Re} \left(2 \frac{\partial^2\tilde{v}_0}{\partial x_0\partial x_1} + 2 \frac{\partial^2\tilde{v}_0}{\partial z_0\partial z_1} \right) - U \frac{\partial\tilde{v}_0}{\partial x_1} - v_0 \frac{\partial V}{\partial y} - V \frac{\partial\tilde{v}_0}{\partial y} - W \frac{\partial\tilde{v}_0}{\partial z_1} \right\} = 0
\end{aligned}$$

Apply the assumption that the perturbation behaves as a wave when seen in the x , and z directions, but not in y ($[\tilde{u}, \tilde{v}, \tilde{w}, \tilde{p}](x, y, z, t) = [\hat{u}, \hat{v}, \hat{w}, \hat{p}](y)e^{i(\alpha x + \beta z - \omega t)}$):

$$\begin{aligned} \frac{\partial \hat{v}_0 e^{i\phi}}{\partial t} + U \frac{\partial \hat{v}_0 e^{i\phi}}{\partial x_0} + W \frac{\partial \hat{v}_0 e^{i\phi}}{\partial z_0} + \frac{\partial \hat{p}_0 e^{i\phi}}{\partial y} - \frac{1}{Re} \left(\frac{\partial^2 \hat{v}_0 e^{i\phi}}{\partial x_0^2} + \frac{\partial^2 \hat{v}_0 e^{i\phi}}{\partial y^2} + \frac{\partial^2 \hat{v}_0 e^{i\phi}}{\partial z_0^2} \right) &= 0 \\ \frac{\partial \hat{v}_0 e^{i\phi}}{\partial t} + U \frac{\partial \hat{v}_0 e^{i\phi}}{\partial x_0} + W \frac{\partial \hat{v}_0 e^{i\phi}}{\partial z_0} + \frac{\partial \hat{p}_0 e^{i\phi}}{\partial y} - \frac{1}{Re} \left(\frac{\partial^2 \hat{v}_0 e^{i\phi}}{\partial x_0^2} + \frac{\partial^2 \hat{v}_0 e^{i\phi}}{\partial y^2} + \frac{\partial^2 \hat{v}_0 e^{i\phi}}{\partial z_0^2} \right) &= \\ \frac{1}{Re} \left(2 \frac{\partial^2 \hat{v}_0 e^{i\phi}}{\partial x_0 \partial x_1} + 2 \frac{\partial^2 \hat{v}_0 e^{i\phi}}{\partial z_0 \partial z_1} \right) - U \frac{\partial \hat{v}_0 e^{i\phi}}{\partial x_1} - v_0 e^{i\phi} \frac{\partial V}{\partial y} - V \frac{\partial \hat{v}_0 e^{i\phi}}{\partial y} - W \frac{\partial \hat{v}_0 e^{i\phi}}{\partial z_1} & \end{aligned}$$

where $\alpha x + \beta z - \omega t = \phi$. Now certain derivatives can be separated. This will leave the equation with every term still having a common factor in $e^{i\phi}$. This can be divided through:

$$\begin{aligned} -i\omega \hat{v}_0 + i\alpha U \hat{v}_0 + i\beta W \hat{v}_0 + \hat{p}'_0 - \frac{1}{Re} (-\alpha^2 \hat{v}_0 + \hat{v}_0'' - \beta^2 \hat{v}_0) &= 0 \\ -i\omega \hat{v}_1 + i\alpha U \hat{v}_1 + i\beta W \hat{v}_1 + \hat{p}'_1 - \frac{1}{Re} (-\alpha^2 \hat{v}_1 + \hat{v}_1'' - \beta^2 \hat{v}_1) &= \\ \frac{1}{Re} \left(2i\alpha \frac{\partial \hat{v}_0}{\partial x_1} + 2i\beta \frac{\partial \hat{v}_0}{\partial z_1} \right) - U \frac{\partial \hat{v}_0}{\partial x_1} - W \frac{\partial \hat{v}_0}{\partial z_1} - V' \hat{v}_0 - V \hat{v}'_0 & \end{aligned}$$

Although this is the v momentum equation, in the system of first order equations which will be constructed, the derivative variable will in fact be pressure. In order to achieve this, equation (A.1a), equation (A.1b), and equation (A.1c) are substituted where appropriate, and using $\hat{u}' = \hat{\tau}_u$, and $\hat{w}' = \hat{\tau}_w$:

$$\begin{aligned} -i\omega \hat{v}_0 + i\alpha U \hat{v}_0 + i\beta W \hat{v}_0 + \hat{p}'_0 - \frac{1}{Re} (-\alpha^2 \hat{v}_0 - i\alpha \hat{\tau}_{u0} - i\beta \hat{\tau}_{w0} - \beta^2 \hat{v}_0) &= 0 \\ -i\omega \hat{v}_1 + i\alpha U \hat{v}_1 + i\beta W \hat{v}_1 + \hat{p}'_1 - \frac{1}{Re} (-\alpha^2 \hat{v}_1 - i\alpha \hat{\tau}_{u1} - i\beta \hat{\tau}_{w1} - \beta^2 \hat{v}_1) &= \\ \frac{1}{Re} \left(2i\alpha \frac{\partial \hat{v}_0}{\partial x_1} + 2i\beta \frac{\partial \hat{v}_0}{\partial z_1} + \frac{\partial \hat{u}_0}{\partial x_1} + \frac{\partial \hat{w}_0}{\partial z_1} \right) - U \frac{\partial \hat{v}_0}{\partial x_1} - W \frac{\partial \hat{v}_0}{\partial z_1} - V' \hat{v}_0 + i\alpha V u_0 + i\beta V w_0 & \end{aligned}$$

A.1.4 Momentum (w)

From Navier-Stokes (equation (4.1d)):

$$\frac{\partial w}{\partial t} + u \frac{\partial w}{\partial x} + v \frac{\partial w}{\partial y} + w \frac{\partial w}{\partial z} = -\frac{\partial p}{\partial z} + \frac{1}{Re} \left(\frac{\partial^2 w}{\partial x^2} + \frac{\partial^2 w}{\partial y^2} + \frac{\partial^2 w}{\partial z^2} \right)$$

Decompose into base flow and perturbation using $u = U + \tilde{u}$ etc. (remember that V is small, so ϵV should be substituted, also base flow derivatives in x and z are small so $\partial\{U, V, W, P\}/\partial\{x, z\}$ should be substituted with $\partial\{\epsilon U, \epsilon V, \epsilon W, \epsilon P\}/\partial\{x, z\}$):

$$\begin{aligned} \frac{\partial(W + \tilde{w})}{\partial t} + (U + \tilde{u}) \frac{\partial(\epsilon W + \tilde{w})}{\partial x} + (\epsilon V + \tilde{v}) \frac{\partial(W + \tilde{w})}{\partial y} + (W + \tilde{w}) \frac{\partial(\epsilon W + \tilde{w})}{\partial z} = \\ -\frac{\partial(\epsilon P + \tilde{p})}{\partial z} + \frac{1}{Re} \left(\frac{\partial^2(\epsilon^2 W + \tilde{w})}{\partial x^2} + \frac{\partial^2(W + \tilde{w})}{\partial y^2} + \frac{\partial^2(\epsilon^2 W + \tilde{w})}{\partial z^2} \right) \end{aligned}$$

Expand the brackets:

$$\begin{aligned} \frac{\partial W}{\partial t} + \frac{\partial \tilde{w}}{\partial t} + \epsilon U \frac{\partial W}{\partial x} + \epsilon \tilde{u} \frac{\partial W}{\partial x} + U \frac{\partial \tilde{w}}{\partial x} + \tilde{u} \frac{\partial \tilde{w}}{\partial x} \\ + \epsilon V \frac{\partial W}{\partial y} + \epsilon \tilde{v} \frac{\partial W}{\partial y} + \epsilon V \frac{\partial \tilde{w}}{\partial y} + \tilde{v} \frac{\partial \tilde{w}}{\partial y} \\ + \epsilon W \frac{\partial W}{\partial z} + \epsilon \tilde{w} \frac{\partial W}{\partial z} + W \frac{\partial \tilde{w}}{\partial z} + \tilde{w} \frac{\partial \tilde{w}}{\partial z} = \\ -\epsilon \frac{\partial P}{\partial x} - \frac{\partial \tilde{p}}{\partial z} + \frac{1}{Re} \left(\epsilon^2 \frac{\partial^2 W}{\partial x^2} + \frac{\partial^2 \tilde{w}}{\partial x^2} + \frac{\partial^2 W}{\partial y^2} + \frac{\partial^2 \tilde{w}}{\partial y^2} + \epsilon^2 \frac{\partial^2 W}{\partial z^2} + \frac{\partial^2 \tilde{w}}{\partial z^2} \right) \end{aligned}$$

Linearise in perturbations by subtracting the base flow solution and neglecting products of perturbations:

$$\frac{\partial \tilde{w}}{\partial t} + \epsilon \tilde{u} \frac{\partial W}{\partial x} + U \frac{\partial \tilde{w}}{\partial x} + \epsilon \tilde{v} \frac{\partial W}{\partial y} + \epsilon V \frac{\partial \tilde{w}}{\partial y} + \epsilon \tilde{w} \frac{\partial W}{\partial z} + W \frac{\partial \tilde{w}}{\partial z} = -\frac{\partial \tilde{p}}{\partial z} + \frac{1}{Re} \left(\frac{\partial^2 \tilde{w}}{\partial x^2} + \frac{\partial^2 \tilde{w}}{\partial y^2} + \frac{\partial^2 \tilde{w}}{\partial z^2} \right)$$

Expand $x = x_0 + \epsilon x_1 + \dots$ etc. for u, v, w, p, x , and z :

$$\begin{aligned}
& \frac{\partial(\tilde{w}_0 + \epsilon\tilde{w}_1)}{\partial t} + \epsilon(\tilde{u}_0 + \epsilon\tilde{u}_1) \left(\frac{\partial}{\partial x_0} + \epsilon \frac{\partial}{\partial x_1} \right) W + U \left(\frac{\partial}{\partial x_0} + \epsilon \frac{\partial}{\partial x_1} \right) (\tilde{w}_0 + \epsilon\tilde{w}_1) \\
& \quad + \epsilon(\tilde{v}_0 + \epsilon\tilde{v}_1) \frac{\partial}{\partial y} + \epsilon V \frac{\partial}{\partial y} (\tilde{w}_0 + \epsilon\tilde{w}_1) \\
& \quad + \epsilon(\tilde{w}_0 + \epsilon\tilde{w}_1) \left(\frac{\partial}{\partial z_0} + \epsilon \frac{\partial}{\partial z_1} \right) W + W \left(\frac{\partial}{\partial z_0} + \epsilon \frac{\partial}{\partial z_1} \right) (\tilde{w}_0 + \epsilon\tilde{w}_1) = \\
& - \left(\frac{\partial}{\partial z_0} + \epsilon \frac{\partial}{\partial z_1} \right) (\tilde{p}_0 + \epsilon\tilde{p}_1) + \frac{1}{Re} \left(\left(\frac{\partial}{\partial x_0} + \epsilon \frac{\partial}{\partial x_1} \right) \left(\frac{\partial}{\partial x_0} + \epsilon \frac{\partial}{\partial x_1} \right) (\tilde{u}_0 + \epsilon\tilde{u}_1) \right. \\
& \quad \left. + \frac{\partial^2}{\partial y^2} (\tilde{u}_0 + \epsilon\tilde{u}_1) + \left(\frac{\partial}{\partial x_0} + \epsilon \frac{\partial}{\partial x_1} \right) \left(\frac{\partial}{\partial x_0} + \epsilon \frac{\partial}{\partial x_1} \right) (\tilde{u}_0 + \epsilon\tilde{u}_1) \right)
\end{aligned}$$

Expand the brackets:

$$\begin{aligned}
& \frac{\partial\tilde{w}_0}{\partial t} + \epsilon \frac{\partial\tilde{w}_1}{\partial t} + U \frac{\partial\tilde{w}_0}{\partial x_0} + \epsilon U \frac{\partial\tilde{w}_0}{\partial x_1} + \epsilon U \frac{\partial\tilde{w}_1}{\partial x_0} + \epsilon^2 U \frac{\partial\tilde{w}_1}{\partial x_1} \\
& \quad + \epsilon u_0 \frac{\partial W}{\partial x_0} + \epsilon^2 u_0 \frac{\partial W}{\partial x_1} + \epsilon^2 u_1 \frac{\partial W}{\partial x_0} + \epsilon^3 u_1 \frac{\partial W}{\partial x_1} \\
& \quad + \epsilon V \frac{\partial\tilde{w}_0}{\partial y} + \epsilon^2 V \frac{\partial\tilde{w}_1}{\partial y} + v_0 \frac{\partial W}{\partial y} + \epsilon v_1 \frac{\partial W}{\partial y} \\
& \quad + W \frac{\partial\tilde{w}_0}{\partial z_0} + \epsilon W \frac{\partial\tilde{w}_0}{\partial z_1} + \epsilon W \frac{\partial\tilde{w}_1}{\partial z_0} + \epsilon^2 W \frac{\partial\tilde{w}_1}{\partial z_1} \\
& \quad + \epsilon w_0 \frac{\partial W}{\partial z_0} + \epsilon^2 w_0 \frac{\partial W}{\partial z_1} + \epsilon^2 w_1 \frac{\partial W}{\partial z_0} + \epsilon^3 w_1 \frac{\partial W}{\partial z_1} \\
& \quad + \frac{\partial\tilde{p}_0}{\partial z_0} + \epsilon \frac{\partial\tilde{p}_0}{\partial z_1} + \epsilon \frac{\partial\tilde{p}_1}{\partial z_0} + \epsilon^2 \frac{\partial\tilde{p}_1}{\partial z_1} \\
& - \frac{1}{Re} \left(\frac{\partial^2\tilde{w}_0}{\partial x_0^2} + \epsilon \frac{\partial^2\tilde{w}_0}{\partial x_0\partial x_1} + \epsilon \frac{\partial^2\tilde{w}_1}{\partial x_0^2} + \epsilon^2 \frac{\partial^2\tilde{w}_1}{\partial x_0\partial x_1} + \epsilon \frac{\partial^2\tilde{w}_0}{\partial x_0\partial x_1} + \epsilon^2 \frac{\partial^2\tilde{w}_0}{\partial x_1^2} + \epsilon^2 \frac{\partial^2\tilde{w}_1}{\partial x_0\partial x_1} + \epsilon^3 \frac{\partial^2\tilde{w}_1}{\partial x_1^2} \right. \\
& \quad \left. + \frac{\partial^2\tilde{w}_0}{\partial y^2} + \epsilon \frac{\partial^2\tilde{w}_1}{\partial y^2} \right) \\
& + \frac{\partial^2\tilde{w}_0}{\partial z_0^2} + \epsilon \frac{\partial^2\tilde{w}_0}{\partial z_0\partial z_1} + \epsilon \frac{\partial^2\tilde{w}_1}{\partial z_0^2} + \epsilon^2 \frac{\partial^2\tilde{w}_1}{\partial z_0\partial z_1} + \epsilon \frac{\partial^2\tilde{w}_0}{\partial z_0\partial z_1} + \epsilon^2 \frac{\partial^2\tilde{w}_0}{\partial z_1^2} + \epsilon^2 \frac{\partial^2\tilde{w}_1}{\partial z_0\partial z_1} + \epsilon^3 \frac{\partial^2\tilde{w}_1}{\partial z_1^2} \Big) = 0
\end{aligned}$$

Split the equation using similar powers of ϵ , ignoring higher powers than 1:

$$\begin{aligned}
\epsilon^0 : & \left\{ \frac{\partial\tilde{w}_0}{\partial t} + U \frac{\partial\tilde{w}_0}{\partial x_0} + \tilde{v}_0 \frac{\partial W}{\partial y} + W \frac{\partial\tilde{w}_0}{\partial z_0} + \frac{\partial\tilde{p}_0}{\partial z_0} - \frac{1}{Re} \left(\frac{\partial^2\tilde{w}_0}{\partial x_0^2} + \frac{\partial^2\tilde{w}_0}{\partial y^2} + \frac{\partial^2\tilde{w}_0}{\partial z_0^2} \right) \right\} = 0 \\
\epsilon^1 : & \left\{ \frac{\partial\tilde{w}_1}{\partial t} + U \frac{\partial\tilde{w}_1}{\partial x_0} + \tilde{v}_1 \frac{\partial W}{\partial y} + W \frac{\partial\tilde{w}_1}{\partial z_0} + \frac{\partial\tilde{p}_1}{\partial z_0} - \frac{1}{Re} \left(\frac{\partial^2\tilde{w}_1}{\partial x_0^2} + \frac{\partial^2\tilde{w}_1}{\partial y^2} + \frac{\partial^2\tilde{w}_1}{\partial z_0^2} \right) \right. \\
& \left. \left[\frac{1}{Re} \left(2 \frac{\partial^2\tilde{w}_0}{\partial x_0\partial x_1} + 2 \frac{\partial^2\tilde{w}_0}{\partial z_0\partial z_1} \right) - U \frac{\partial\tilde{w}_0}{\partial x_1} - \tilde{u}_0 \frac{\partial W}{\partial x_0} - V \frac{\partial\tilde{w}_0}{\partial y} - W \frac{\partial\tilde{w}_0}{\partial z_1} - \tilde{w}_0 \frac{\partial W}{\partial z_0} - \frac{\partial\tilde{p}_0}{\partial z_1} \right] \right\} = 0
\end{aligned}$$

Apply the assumption that the perturbation behaves as a wave when seen in the x , and z directions, but not in y ($[\tilde{u}, \tilde{v}, \tilde{w}, \tilde{p}](x, y, z, t) = [\hat{u}, \hat{v}, \hat{w}, \hat{p}](y)e^{i(\alpha x + \beta z - \omega t)}$):

$$\begin{aligned} & \frac{\partial \hat{w}_0 e^{i\phi}}{\partial t} + U \frac{\partial \hat{w}_0 e^{i\phi}}{\partial x_0} + \hat{v}_0 e^{i\phi} \frac{\partial W}{\partial y} + W \frac{\partial \hat{w}_0 e^{i\phi}}{\partial z_0} + \frac{\partial \hat{p}_0 e^{i\phi}}{\partial z_0} - \frac{1}{Re} \left(\frac{\partial^2 \hat{w}_0 e^{i\phi}}{\partial x_0^2} + \frac{\partial^2 \hat{w}_0 e^{i\phi}}{\partial y^2} + \frac{\partial^2 \hat{w}_0 e^{i\phi}}{\partial z_0^2} \right) = 0 \\ & \frac{\partial \hat{w}_1 e^{i\phi}}{\partial t} + U \frac{\partial \hat{w}_1 e^{i\phi}}{\partial x_0} + \hat{v}_1 e^{i\phi} \frac{\partial W}{\partial y} + W \frac{\partial \hat{w}_1 e^{i\phi}}{\partial z_0} + \frac{\partial \hat{p}_1 e^{i\phi}}{\partial z_0} - \frac{1}{Re} \left(\frac{\partial^2 \hat{w}_1 e^{i\phi}}{\partial x_0^2} + \frac{\partial^2 \hat{w}_1 e^{i\phi}}{\partial y^2} + \frac{\partial^2 \hat{w}_1 e^{i\phi}}{\partial z_0^2} \right) = \\ & \frac{1}{Re} \left(2 \frac{\partial^2 \hat{w}_0 e^{i\phi}}{\partial x_0 \partial x_1} + 2 \frac{\partial^2 \hat{w}_0 e^{i\phi}}{\partial z_0 \partial z_1} \right) - U \frac{\partial \hat{w}_0 e^{i\phi}}{\partial x_1} - \hat{u}_0 e^{i\phi} \frac{\partial W}{\partial x_0} - V \frac{\partial \hat{w}_0 e^{i\phi}}{\partial y} - W \frac{\partial \hat{w}_0 e^{i\phi}}{\partial z_1} - \hat{w}_0 e^{i\phi} \frac{\partial W}{\partial z_0} - \frac{\partial \hat{p}_0 e^{i\phi}}{\partial z_1} \end{aligned}$$

where $\alpha x + \beta z - \omega t = \phi$. Now certain derivatives can be separated. This will leave the equation with every term still having a common factor in $e^{i(\alpha x + \beta z - \omega t)}$. This can be divided through:

$$\begin{aligned} & -i\omega \hat{w}_0 + i\alpha U \hat{w}_0 + W' \hat{v}_0 + i\beta W \hat{w}_0 + i\beta \hat{p}_0 - \frac{1}{Re} (-\alpha^2 \hat{w}_0 + \hat{w}_0'' - \beta^2 \hat{w}_0) = 0 \\ & -i\omega \hat{w}_1 + i\alpha U \hat{w}_1 + W' \hat{v}_1 + i\beta W \hat{w}_1 + i\beta \hat{p}_1 - \frac{1}{Re} (-\alpha^2 \hat{w}_1 + \hat{w}_1'' - \beta^2 \hat{w}_1) = \\ & \frac{1}{Re} \left(2i\alpha \frac{\partial \hat{w}_0}{\partial x_1} + 2i\beta \frac{\partial \hat{w}_0}{\partial z_1} \right) - U \frac{\partial \hat{w}_0}{\partial x_1} - \frac{\partial W}{\partial x_0} \hat{u}_0 - V \hat{w}_0' - W \frac{\partial \hat{w}_0}{\partial x_1} - \frac{\partial W}{\partial z_0} \hat{w}_0 - \frac{\partial \hat{p}_0}{\partial z_1} \end{aligned}$$

Bibliography

- [1] ACHENBACH, E., AND HEINECKE, E. On vortex shedding from smooth and rough cylinders in the range of reynolds numbers 6×10^3 to 5×10^6 . *Journal of Fluid Mechanics* 109 (Sep 1980), 239–251.
- [2] ATKIN, C. J. CoDS boundary layer stability analysis. Report, Qinetiq, 1993.
- [3] ATKIN, C. J. CoDS user guide. Software user manual, Qinetiq, 2014.
- [4] BACKER DIRKS, T. *On the controlability of saturating crossflow vortices*. PhD thesis, City, Univesity of London, 2019.
- [5] BIPPES, H. Basic experiments on transition in three-dimensional boundary layers dominated by crossflow instability. *Progress in Aerospace Sciences* 35 (1999), 363–412.
- [6] BOUTHER, M. Series representation of the eigenvalues of the Orr-Sommerfeld equation. *Journal Mecanique* 11 (1972), 599.
- [7] DEYHLE, H., AND BIPPES, H. Disturbance growth in an unstable three-dimensional boundary layer and its dependence on environmental conditions. *Journal of Fluid Mechanics* 316 (Dec 1995), 73–113.
- [8] EL HADY, N. M. Nonparallel instability of supersonic and hypersonic boundary layers. *Physics of Fluids A* 3 (Jan 1991), 2164–2178.
- [9] EULER, L. *Institutionum Calculi Integralis*. Impensis Academiae Imperialis Scientiarum, 1768.
- [10] GASTER, M. Personal communication.
- [11] GASTER, M. A note on the relation between temporally-increasing and spatially-increasing disturbances in hydrodynamic stability. *Journal of Fluid Mechanics* 14 (Oct 1962), 222–224.

- [12] GASTER, M. On the effects of boundary-layer growth on flow stability. *Journal of Fluid Mechanics* 66 (Jan 1974), 465–480.
- [13] GASTER, M. Series representation of the eigenvalues of the Orr-Sommerfeld equation. *Journal of Computational Physics* 28 (Jul 1977), 147–162.
- [14] GASTER, M. A rapid method of calculating N-factors for estimating transition position. Tech. rep., NATO, 2004.
- [15] HERBERT, T. Parabolized stability equations. *Annual Reviews: Fluid Mechanics* 29 (1997), 245–283.
- [16] IATA. Economic performance of the airline industry, Dec 2017.
- [17] JACOB, B., AND GUENNEBAUD, G. Eigen. <http://eigen.tuxfamily.org/>, 2009-2020.
- [18] JUNIPER, M. Applications of receptivity and sensitivity analysis to thermoacoustics. In *Progress in Flow Instability Analysis and Laminar-Turbulent Transition Modeling* (2014).
- [19] LUCHINI, P., AND BOTTARO, A. An introduction to adjoint problems. *Annual Review of Fluid Mechanics* 46 (Oct 2013), 493–517.
- [20] MACK, L. M. Boundary layer linear stability theory. In *AGARD-R-709* (1984).
- [21] MALIK, M. R. Numerical methods for hypersonic boundary layer stability. HTC Report 88-6, HTC, 1988.
- [22] MORKOVIN, M. V. On the many faces of transition. In *Viscous Drag Reduction* (1969).
- [23] MORKOVIN, M. V. Recent insights into instability and transition of turbulence in open-flow systems. ICASE report 88-44, NASA, 1988.
- [24] NAYFEH, A. H. *Perturbation Methods*, 1 ed. Wiley VCH, Weinheim, 1973.
- [25] ORR, W. M. The stability or instability of the steady motions of a perfect liquid and of a viscous liquid. *Proceedings of the Royal Irish Academy: Section A* 27 (Mar 1907), 9–68.
- [26] PRANDTL, L. Bemerkungen über die entstehung der turbulenz. *Zeitschrift für Angewandte Mathematik und Mechanik* 1 (Mar 1921), 431–436.
- [27] RAYLEIGH, L. On the stability, or instability, of certain fluid motions. *Proceedings of the London Mathematical Society* s1-11 (1879), 57–72.

- [28] REYNOLDS, O. An experimental investigation of the circumstances which determine whether the motion of water shall be direct or sinuous, and of the law of resistance in parallel channels. *Philosophical Transactions of the Royal Society of London* 35 (Mar 1883), 84–99.
- [29] ROSENHEAD, L. *Laminar Boundary Layers*. Oxford University Press, 1963.
- [30] SARIC, W. S., AND NAYFEH, A. H. Nonparallel stability of boundary-layer flows. *The Physics of Fluids* 18 (Aug 1975), 945–950.
- [31] SCHLICHTING, H. Zur entstehung der turbulenz bei der plattenströmung. *Abhandlungen der Deutschen Akademie der Wissenschaften zu Berlin, Klasse für Mathematik, Physik und Technik* (1933), 181–208.
- [32] SCHLICHTING, H. *Boundary Layer Theory*. McGraw-Hill, 1955.
- [33] SCHMID, P. J., AND HENNINGSON, D. S. *Stability and Transition of Shear Flows*, 1 ed. Springer, New York, 2001.
- [34] SCHUBAUER, G. B., AND SKRAMSTAD, H. K. Laminar boundary-layer oscillations and transition on a flat plate. *Journal of Research of the National Bureau of Standards* 38 (Feb 1947), 251–292.
- [35] SMITH, A., AND GAMBERONI, N. Transition, pressure gradient and stability theory. Report ES26388, Douglas, 1956.
- [36] SOMMERFELD, A. Ein beitrag zur hydrodynamische erklärang der turbulenten flüssigkeitsbewegungen. In *Proceedings of the 4th International Congress of Mathematicians* (1908).
- [37] SQUIRE, H. B. On the stability for three-dimensional disturbances of viscous fluid flow between parallel walls. *Proceedings of the Royal Society A* 142 (1933), 621–628.
- [38] TAYLOR, G. I. Eddy motion in the atmosphere. *Philosophical Transactions of the Royal Society of London* 215 (May 1915), 1–26.
- [39] TOLLMIEEN, W. The production of turbulence. Technical Memorandum 609, NACA, 1929.
- [40] VAN INGEN, J. A suggested semi-empirical method for the calculation of the boundary layer transition region. VTH Report 74, Technische Hogeschool Vliegtuigbouwkunde, 1956.